SCIENTIFIC NOTE BOOK # 317
Subsurface Electrical Conductivity Mapping of Fortymile Wash and the Amargosa Desert

by

David A. Farrell

Southwest Research Institute
Center for Nuclear Waste Regulatory Analyses
San Antonio, Texas

Date of Issue: March 18, 1999
Valid Dates: March 18, 1999 to February 28, 2000

Table of Contents **Page #**

List of Figures **Page #**

List of Tables **Page #**

1. INITIAL ENTRIES

Scientific Note Book: # 317

Issued to: David A. Farrell

Issue Date: March 18, 1999

Printing Period: February 28, 2000 (final printout)

Project Title: **Subsurface Electrical Conductivity Mapping of Fortymile Wash and the Amargosa Desert**

(USFIC KTI)

Project Staff: David A. Farrell and Peter La Femina (CNWRA, SWRI), Stewart Sandberg and Noel Rogers (Geophysical Solutions)

By agreement with the CNWRA QA, this notebook is to be printed at approximate quarterly intervals. This computerized Scientific Notebook is intended to address the criteria of CNWRA QAP-001.

[David A. Farrell, June 6, 19991

1.1. Objectives

Within the Amargosa Desert and Fortymile Wash regions adjacent to Yucca Mountain, Nevada, vast areas exist along the projected radionuclide flow path for which little hydrogeologic and geologic data are unavailable. As a result groundwater flow and mass transport models are poorly constrained within this region. One cost effective, non-invasive approach for improving our knowledge of the hydrogeology and geology of this region involves the use of surface geophysics. Several non-invasive geophysical methods are available for inferring subsurface structure, e.g., gravity methods, seismic methods, magnetic methods, electromagnetic methods and electrical methods. Of these methods, electromagnetic and electric methods are commonly used in hydrogeological studies aimed at identification of watertables and plume delineation due in part to the sensitivity of subsurface electrical conductivity to soil moisture content and pore-water chemistry.

The objectives of this study are to use electromagnetic, induced polarization and standard depth sounding resistivity methods to map subsurface resistivity distributions within the Amargosa Desert and Fortymile Wash with the ultimate goals being identification of the watertable, the tuff-alluvium contact and the zone where the watertable transitions from the tuff units into the alluvial valley fill deposits of Fortymile Wash. In addition to collecting and interpreting the data sets independently, a joint inversion of the data sets will be performed.

This notebook documents aspects of the work performed by CNWRA staff and consultants on this project. Some of the details regarding the field work are not described in this notebook. A detailed description of field procedures an experiences are included in the field notebooks of Stewart Sandberg and Noel Rogers (Geophysical Solutions) and Peter La Femina. (CNWRA). Sandberg's notebook deals specifically with geophysical data collection, while La Femina's notebook deals with aspects of geolocation. Copies of these notebooks are currently being acquired and will be attached as appendices to hard copies of this electronic notebook.

1.2. Computers, Computer Codes, and Data Files

The computer codes used in the data analyses were based on a suite of codes developed by Stewart Sandberg and purchased by CNWRA. Version 6 of this suite dated August 7, 1998, includes ZONGE, READZONG, T47INPUT, READ, SLUMBER, RAMPRES3 and EINVRT6. These codes are discussed in the software users manual "Inverse Modeling Software for Resistivity, Induced Polarization (IP), and Transient Electromagnetic (TEM, TDEM) Soundings" written by Stewart Sandberg and dated August 7, 1998 (Appendix 1). The data analyses were carried out using computer systems running either DOS 6.0, or Windows 95 or higher (Geophysical Solutions). Processed and unprocessed data files will be included on floppy disk with the hard copy of this report.

2. Introduction

The geophysical survey which this report discusses was an extension of the May 1998 geophysical survey performed by Charles Connor in Fortymile Wash and the northern portion of the Amargosa Desert, southern Nevada. Connor's work may be best described as a scoping exercise designed to investigate whether electromagnetic geophysical methods could be used to map geological structure and watertable elevation along the projected groundwater flow path from Yucca Mountain (YM) to regions located further south. At the time of Connor's survey, limited hydrogeological data existed within the survey area.

The geophysical survey discussed in this report was performed during the period January 13-24, 1999. The survey differed from the that performed by Connor in several aspects. First, in addition to the timedomain electromagnetic (TEM) technique which was used by Connor, timedomain induced polarization (TDIP) and Schlumberger resistivity depth profiling **(SR)** were also applied. The joint inversion of these data sets is expected to improve the resolution of subsurface features. Second, changes to the design of the TEM technique employed by Connor have been made. The changes relate to the dimensions of the survey loop and the current frequencies used. These changes should improve the method's depth of penetration and resolution. Third, wherever possible, survey lines started and ended at borehole elevations where hydrogeologic and geologic information were available. This design provides constraints for the proposed models.

3. **Theory** (May **24,** 1999)

The TEM, TDIP and SR techniques were employed during the January, 1999 field survey. The following provides a brief summary of these methods.

3.1 Time-Domain IP (TDIP) Method

The theory behind the timedomain IP method is documented in Telford et al. (1976), Sharma (1997) and Parasnis (1986). The following provides a cursory discussion of the technique. Consider an electrode spread along the ground surface shown in Figure 1, where **A** and B represent current electrodes, and N and M represent voltage or potential electrodes. Further, assume that the subsurface has a finite resistivity. If the current applied across A and B is interrupted, the voltage across M and N will decrease to zero in a finite amount of time as shown in Figure 2. This relaxation in voltage, starts from some initial value less than the applied voltage, and may last from seconds to minutes. This decay in voltage is due to the process of induced polarization and essentially represents the time it takes for the system to return to its original state. When the voltage decay is measured as a function of time following application of a DC pulse, the technique is termed "time-domain IP".

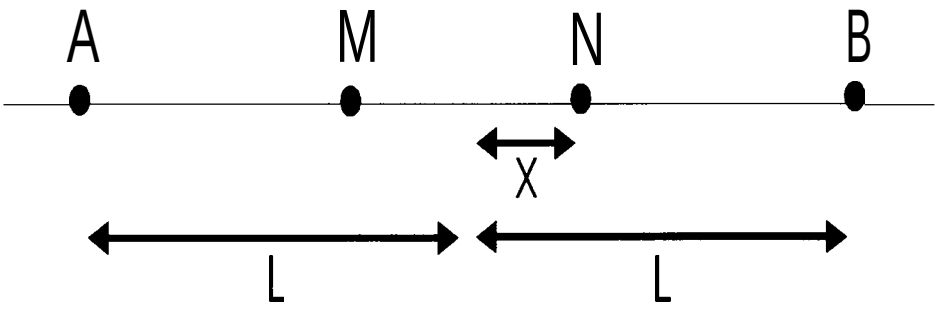

Figure 1: Schematic of TDIP electrode array

IP effects may due to either membrane polarization or electrode polarization. Membrane polarization results from ion flow in pore fluids under an induced voltage. This process is enhanced by the presence charged mineral and soil grains such as clay particles. When an electric current is forced through such a system, the motion of negative ions may be inhibited by the presence of the negatively charged particles within the porous medium. This results in localized regions of negative ion accumulation. Interruption of the applied voltage produces an observed voltage decay as the ions diffuse back to an equilibrium state. Membrane polarization is generally enhanced by the presence of clay minerals scattered throughout the matrix.

Electrode polarization is due to the presence of metallic minerals in the subsurface. Where this occurs, subsurface current flow results from the combination of electronic and electrolytic processes. This may be demonstrated by considering a metallic mineral in the subsurface. Under an applied voltage, the opposite faces of the mineral grain will develop opposite charges and a localized electrolysis cell will develop. This results in a pile up of ions along the faces of the mineral grain. When the applied voltage is interrupted, the residual voltage decays as the ions diffuse back to their equilibrium state.

Induced polarization is frequently measured in terms of chargeability *(M)*,
where *V(t)* represents the residual voltage after the current is interrupted, V_c represents the steady voltage measured at the potential electrodes (Figure 2), and t, and t_n represent the first and last measuring times. The

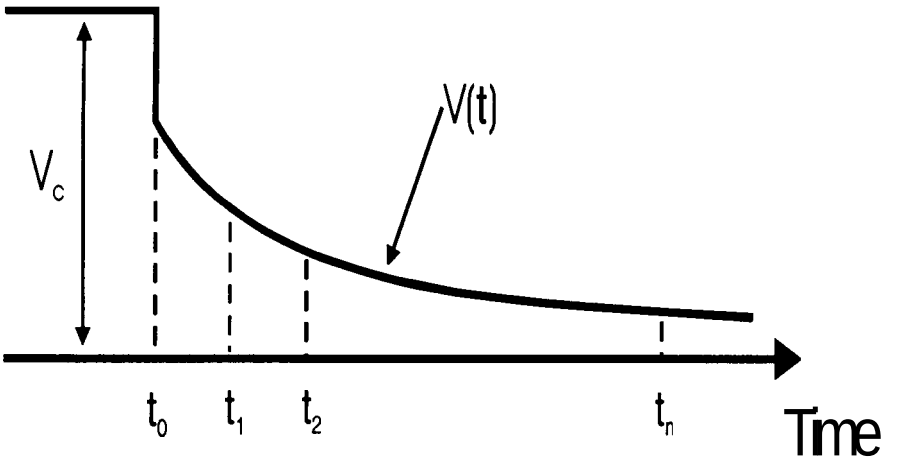

Figure 2: Observed voltage decay due to IP effects.

units of chargeability are mVs/V (millivoltsecond per volt).

$$M = \frac{1}{V_c}\int_{t_1}^{t_n} V(t)\,dt$$

An advantage of IP is that it provides a means for distinguishing between clay layers and other low resistivity **strata.**

3.2 Schlumberger Resistivity (SR) Method

The theory behind the SR method is well documented in Telford et al. (1976), Sharma (1997) and Parasnis (1986). Subsurface electrical resistivities may be determined by passing a current through the subsurface and measuring the voltage difference across a pair of electrodes inserted into the subsurface. The resisitivity measured in this way, the apparent resistivity, is a function of the combined resistivities of the subsurface porous medium and pore fluids present. A shortcoming of electrical methods such as the Schlumberger method, is their sensitivity to minor variations in electrical conductivity near the surface (Telford et al., 1976).

The SR approach is one of the more commonly applied resistivity surveying methods. The electrode array used is identical to that described in Figure 1. Here the current electrodes are A and B while the potential

electrodes are represented by M and N. Apparent resistivities @,)for this array are computed using the following expression:

$$\rho_a = \frac{\pi L^2}{2x}\frac{\mathrm{Av}}{I}$$

where [represents the applied current, L represents the distance from the mid-point of the array to the current electrodes, x represents the distance from the mid-point of the array to the potential electrodes, and ***Av*** represents the measured voltage across the voltage electrodes. In depth sounding mode, the voltage electrodes are ideally kept fixed while the current electrodes are expanded symmetrically about the mid-point of the array.

The equipment and field procedures used for the SR soundings are quite similar to those used for the TDIP with the exception that a direct current is applied to the current electrodes and voltages across the potential electrodes are measured during the current on-time.

3.3 Time-Domain Electromagnetic (TEM) Methods

TEM methods are based on electromagnetic induction theory, whereby a changing magnetic field, which may be due to an electromagnetic source, induces an electromotive force (emf) in a nearby conductor. Associated with these induced or secondary emfs, is a magnetic field, the secondary magnetic field. This secondary magnetic field may then induce emfs in nearby conductors which may be recorded. This approach is commonly applied in geophysics to map subsurface resistivities.

TEM methods in geophysics generally involve laying out a large square wire loop on the ground surface which is connected to a transmitter. The dimensions of the transmitter loop can vary from tens of meters to hundreds of meters depending on the depth of penetration required. At the center of the transmitter loop is placed a smaller circular receiver loop. This configuration is termed the central loop configuration. Application of symmetrical square wave current to the transmitter coil produces a constant magnetic flux in the subsurface. When the applied current rapidly falls to zero during the off-cycle, the changing magnetic flux in the subsurface induces secondary time varying emf in conductive layers. The vertical component of the changing secondary magnetic field associated with these emfs induce emfs in the receiver coil present at the surface. The induced emf in the receiver is recorded and later analyzed. Corrections to the raw field data may be applied to account for the finite turn-off time of commonly used transmitters (Sandberg, **1998).**

In the central loop configuration, measurement of the decaying field at the loop center is equivalent to measurement of resistivity as a function of depth (Sharma, **1997).** Sharma **(1997)** describes the depth of investigation as a function of delay time of the decaying secondary field which is independent of the transmitter-receiver separation.

Advantages of the timedomain system over frequencydomain systems include greater depth of penetration (Sharma, **1997).** The data scatter frequently observed in d.c. resistivity and magnetotelluric soundings are

often due to lateral variations in resistivity and measurement of the electric field. The scatter is reduced in central loop TDEM soundings mainly because of short source-receiverseparation and measurement of time derivatives of the magnetic field.

4. Equipment and Field Procedures

As pointed out earlier, the field survey was conducted between January 13-24, 1999 and utilized the techniques described above. The following provides a summary of the equipment used.

4.1 Time-Domain IP (TDIP) Method

Equipment:
Timedomain IP soundings were performed using the PHOENIX **V-5** multipurpose receiver and the PHOENIX T-3 transmitter. The instruments were on temporary loan from the University of Southern Maine. The transmitter was used to supply current to the current electrodes **A** and B while the receiver was used to record the potential difference across the potential electrodes M and N. The transmitter was powered by a portable generator. Steel stakes were used for the current electrodes while porous cups containing a copper sulphate solution were used for the potential electrodes.

Field Procedures:
Data acquisition procedures used during this survey conformed to standard operating procedures as outlined in the operations manuals of the equipment, and standard field procedures described in literature. In addition, Dr. Sandberg gave all members of the survey team a brief demonstration of the safe operation of the equipment. Note that Dr. Sandberg and Noel Rogers operated the IP instruments in all cases, and used their professional judgement to suggest modifications to the survey, i.e., array design etc.

The field procedures used may be summarized as follows:

(i) Figure 1 shows a schematic of the field layout. The separation of the potential electrodes was generally kept fixed while the separation of the current electrodes was expanded outward in a symmetric manner about the center point of the array. Note that for the cases where the measured potential at the potential electrodes were low and undiscernable from background noise, the potential electrodes were expanded outward from the center point. (S. Sandberg and N. Rogers)

(ii) The electrode grid was mapped using both GPS and a measuring tape.(D. Farrell and P. La Femina)

(iii) The transmitter is connected to the portable generator and the transmitter is powered up and tested. During this phase, output from the transmitter to the current electrodes was turned off. (S. Sandberg and N. Rogers, monitored by D. Farrell)

(iv) Next, the current electrodes are inserted into the ground surface and the area around them is saturated with a saltwater solution to ensure good electrical coupling. Porous cups containing a copper sulphate solution are used for the potential electrodes. The area beneath these electrodes is also saturated with saltwater to ensure good electrical coupling. Note that current to the electrodes is turned off while the electrodes are moved. (R. Klar and B. Strye under the supervision of S. Sandberg, monitored by D. Farrell)

(v) Next, the receiver is connected to the potential electrodes. (S. Sandberg and N. Rogers, monitored by D. Farrell)

(vi) The transmitter is then connected to the current electrodes and a periodic square wave of known frequency and amplitude (see Figure 3) is passed through the system. (S. Sandberg and N. Rogers, monitored by D. Farrell)

(vii) The current in the system is adjusted until the observed IP response (the voltage recorded at the receiver) is above background. Data for the different time gates at the receiver are then stacked. The stacked voltage at each time gate is then recorded along with the applied current, current electrode spacing and potential electrode spacing. The current in the system is verified using a voltmeter. (S. Sandberg and N. Rogers, monitored by D. Farrell ... data stored in the field notebooks of S. Sandberg and N. Rogers Appendix 2)

(viii) Current to the system is then switched off (S. Sandberg) and the current electrode spacing expanded (R. Klar and B. Strye, monitored by D. Farrell).

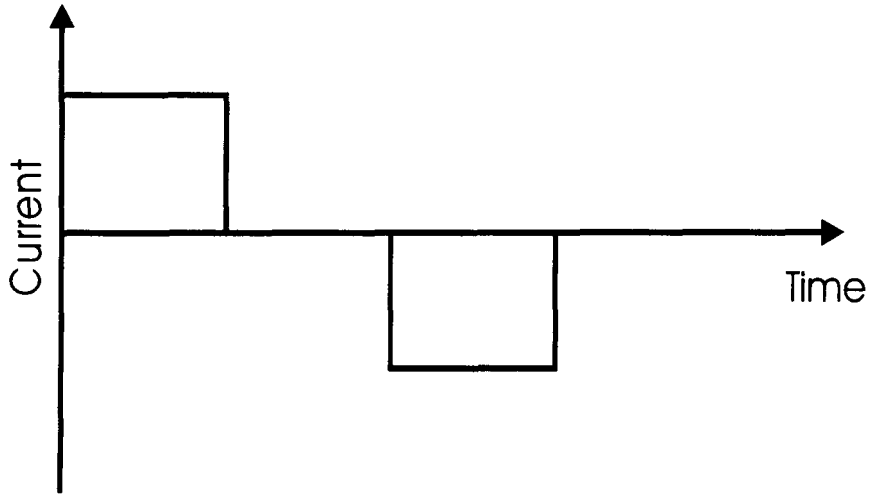

Figure 3: Input signal to current electrodes.

4.2 Schlumberger Resistivity (SR) Method

The equipment and field procedures used for the SR soundings were quite similar to those used for the TDIP with the exception that a direct current was applied to the current electrodes and voltages across the potential electrodes were measured during the current on-time. These measurements were performed simultaneously with the TDIP.

4.1 Time-Domain Electromagnetic (TEM) Method

Equipment:
The equipment used for the TEM survey was the GEONICS PROTEM TEM system. This system consists of a transmitter and a receiver. Two transmitters were used in this survey: the PROTEM 57-MK2 transmitter and the PROTEM 47/S transmitter. The PROTEM 57-MK2 transmitter was rented from TerraPlus in Littleton, Colorado while the PROTEM 47/S transmitter was obtained on a temporary loan from the University of Southern Maine. The former is used for large loops *(> 100m x 100m)* and is powered by a battery pack or a portable motor generator, while the latter is used for loop sizes on the order of *(≤ 100m x 100m)*. In the field survey, the PROTEM 57-MK2 transmitter was used with a portable generator. A PROTEM Digital receiver was used to store the received signal. Two receivers coils were also employed with this receiver. For the larger transmitter loop dimensions, a low frequency (bandwidth 60 kHz) air-cored coil 1.0 m in diameter was employed whereas for the smaller transmitter loop dimensions, a higher frequency (bandwidth 850 kHz) air-cored coil 0.63 m was employed. The smaller loop was obtained on a temporary loan from the University of Southern Maine while the larger was rented from TerraPlus in Littleton, Colorado.

Field Procedures:
Data acquisition procedures used during this survey conformed to the Center for Nuclear Waste Regulatory Analyses Quality Assurance Procedures, standard operating procedures as outlined in the operations manuals of the equipment, and standard field procedures described in literature. Note that Dr. Sandberg and Noel Rogers operated the IP instruments in all cases, and used their professional judgement to modifying aspects of the survey approach.

The general field procedures used may be summarized as follows:

(i) For the TEM soundings the circular receiver coil was located at the center of the larger square transmitter loop. In most cases, the transmitter loop was oriented N-S and E-W. The comers of the loop were established using GPS (D. Farrell and P. La Femina). In addition to the UTM coordinates of the comers of the transmitter loop, the UTM coordinates and the elevation of the center of the loop were also recorded in most cases. (Note that elevation data was not initially collected due to some initial confusion regarding its use ... some of this data was later collected ... some elevation data could not be collected due to logistic problems, e.g., rover packs unable to see the base station)

(ii) The transmitter loop was laid out and an electric current passed through the loop to test its integrity. This was particularly important for the large loop which was constructed by splicing, three 400 m cables (loop layout and integrity were supervised by S. Sandberg, monitored by D. Farrell).

(iii) Receiver set up: Several steps were required to set up the receiver prior to data acquisition. These included (i) auto-testing and auto-calibration of the receive; (ii) crystal clock synchronization between the transmitter and the receiver when the two instruments were not physically connected during the sounding; (iii) selection of the appropriate receiver coil; (iv) selection of the desired component of the magnetic field to be read; (v) selection of the appropriate "turn-on/turn-off times"; (vi) selection of the transmitter instrument type and the transmitter loop dimensions; (vii) selection of the transmission frequency; (viii) creation of a new data file; (ix) assessment of

background noise; (x) gain adjustment. (Receiver setup, synchronization and internal calibration performed by S. Sandberg, monitored by D. Farrell)

(iv) On completion of the steps listed in *(3.)* the receiver and the receiver coil are both moved to the center of the transmitter loop and connected together (S. Sandberg). The transmitter is then connected to the transmitter loop (N. Rogers). Note that for small loops a physical connection is maintained between the transmitter and the receiver.

(v) The system is power-up and data recorder at several frequencies, currents and gains (S. Sandberg and N. Rogers (under the supervision of S. Sandberg, monitored by D. Farrell)).

(vi) At the end of the recording session, the data is stored on a data logger in the receiver, the systems is powereddown, and the equipment collected (S. Sandberg).

5. Field Work (June 7, **1999)**

This section summarizes various field aspects of this work. Field work began on January **14, 1999** and terminated on January 24, **1999.** Parameter values used at each measuring station during this period were recorded in the field notebooks of Stewart Sandberg, Noel Rogers and Peter La Femina and are not reproduced here. However, copies of, or excerpts from, these notebooks will be placed in appendices at the end of this report.

Day 1 (Thursday, January 14, 1999):

Equipment collection in Las Vegas, NV. Rolls of cable necessary to perform the TEM survey did not amve but are expected to arrive on Friday. Visited the Badging Office at Mercury to make sure that the badges were available. Site familiarization.

Day 2 (Friday, January 15, 1999):

TDIP survey at station TEM 1 (IP **1).** Located east of the Lathrop Wells Cinder Cone (Cind-R-Lite). At this location two TDIP surveys were performed perpendicular to each other as a means of estimating any subsurfacedip. TDIP data reported in S. Sandberg's notebook (Appendix 2). La Femina and Connor returned to Las Vegas to collect the rolls of wire for the TEM.

Day 3 (Saturday, January 16, 1999):

TEM survey at the site of the previous TDIP. Recorded as TEM 1 **...** large loop used *(300* m *x 300* m). Second TEM survey performed further east **...** recorded as TEM 2. TEM instrument settings recorded in S. Sandberg's notebook (Appendix 2).

Day 4 (Sunday, January 17, 1999):

TEM and TDIP survey performed adjacent to Nye County well NC-EWDP-2D. Two transmitter loop sizes used for the TEM survey **...** TEM *3 (300* m *x 300* m) and TEM 3A **(40** m **x 40** m). North trending IP survey performed (recorded at TDIP 2) along the western edge of the large loop. TEM instrument settings recorded in S. Sandberg's notebook (Appendix 2). TDIP data reported in S. Sandberg's notebook (Appendix 2).

Connor returned to San Antonio.

Day 5 (Monday, January 18, 1999):

Small loop TEM survey performed immediately west of the Lathrop Wells Cinder Cone. Recorded as (TEM **4 (40** m **x 40** m)). Aim of this survey was to investigate the possible characteristic signal of the tuff-alluvium contact. A short distance away from this site, the tuff can be observed dipping beneath the alluvium. TEM instrument settings recorded in S. Sandberg's notebook (Appendix **2).**

Large loop surveys **(300** m **x 300** m) performed east of TEM **3** location. Recorded as TEM 5, TEM 6 and TEM 7. Note that TEM 5 is located adjacent to an excavated area. TEM 7 is the farthest east. TEM instrument settings recorded in S. Sandberg's notebook (Appendix 2).

Day 6 (Tuesday, January 19, 1999):
Survey moved to the NTS. Daily check-in at the Mercury gate and FOC.

Small loop TEM survey **(40** m **x 40** m) performed on the eastside of the Fortymile Wash, south of Busted Butte and JF-3, near gravel road **...** recorded as TEM **8.** Small cables located further to the east following the survey **...** these could cause some problems with the interpretation **...** note these cable were located more than 75 m from the closest edge of the survey line. Recognizance located additional cables in the region making it difficult to find suitable survey stations. TEM instrument settings recorded in S. Sandberg's notebook (Appendix **2).**

Large loop TEM survey **(300** m **x 300** m) performed southwest of TEM **8** adjacent to the Fortymile Wash. Recognizance indicates no cables present. Sounding recorded as TEM 9. Small loop **(40** m **x 40** m) also recorded at this site **...** recorded as TEM **10.** Additional small loop **(40** m **x 40** m) also nearby in Fortymile Wash **...** recorded as TEM **11.** TEM instrument settings recorded in S. Sandberg's notebook (Appendix **2).**

Recognizance performed on the west side of the wash revealed no cables. Decision made to perform the surveys on the west side of the wash to avoid complications related to the presence of cables.

Day 7 (Wednesday, January 20, 1999):
Returned to **NTS.** Daily check-in at the Mercury gate and FOC.

New site located on the west side of Fortymile Wash, along the east-west gravel road located south of Busted Butte. Tuff can be seen dipping beneath the alluvium about 500 to 1000 m further west. Large loop TEM survey performed **(300** m **x 300** m) **...** recorded as TEM **12.** Small loop survey **(40** m **x 40** m) was also performed at this location **...** recorded as TEM **13.** Stewart was surprised by the TEM **13** data so an additional small loop TEM survey **(40** m **x 40** m) was performed further south. This is reported as TEM **14.** An IP survey was also performed parallel to the road at this location. Recorded as TDIP **3.** TEM instrument settings recorded in S. Sandberg's notebook (Appendix **2).** TDIP data reported in S. Sandberg's notebook (Appendix 2).

Large loop TEM survey **(300** m **x 300** m) performed east of TEM **12** adjacent to Fortymile Wash. Recorded as TEM **15.** TEM instrument settings recorded in S. Sandberg's notebook (Appendix **2).**

Day 8 (Thursday, January 21, 1999):

Returned to NTS. Daily check-in at the Mercury gate and FOC.

Large loop TEM survey **(300** m **x 300** m) performed south of TEM 15 along the west side of Fortymile Wash. Recorded as TEM 16. At the same site a small loop TEM survey **(40** m **x 40** m) was also performed **...** recorded as TEM 17. TEM instrument settings recorded in S. Sandberg's notebook (Appendix 2).

Large loop TEM survey **(300** m **x 300** m) performed further south. Recorded as TEM 18. Small loop TEM survey **(40** m **x 40** m) also performed **...** recorded as TEM 19. TEM instrument settings recorded in S. Sandberg's notebook (Appendix 2).

Day 9 (Friday, January 22, *1999):*
Returned to NTS. Daily check-in at the Mercury gate and FOC.

Large loop TEM survey **(300** m **x 300** m) performed further south of TEM 18. Recorded as TEM 20. Small loop survey also performed at this location **...** recorded as TEM 21. TEM instrument settings recorded in S. Sandberg's notebook (Appendix 2).

To map the tuff-alluvium contact beneath the west side of Fortymile Wash, an east-west, small loop **(40** m **x 40** m) survey was performed. The western end of the survey approached the tuff out-crops along the southern margins of the wash. The station locations for this survey are recorded as TEM 22 through TEM 26. TEM instrument settings recorded in S. Sandberg's notebook (Appendix 2).

Surveys on the NTS now complete.

Day 10 (Saturday, January 23, *1999):*
Surveys on this day performed in the Amargosa Desert south of Lathrop Wells cinder cone. Survey designed to map both deep and shallow structures beneath Fortymile Wash. Survey line projects southeast from well at Lathrop Wells cinder cone to the Amargosa Town C well.

Large loop TEM survey **(300** m **x 300** m) performed **...** recorded as **TEM** 27. Small loop survey **(40** m **x 40** m) survey also performed at this location **...** recorded as **TEM** 28. South-east of this location an additional large loop **(300** m **x 300** m) and small loop survey **(40** m **x 40** m) performed **...** recorded as TEM 29 and **30.** TEM instrument settings recorded in S. Sandberg's notebook (Appendix 2). At the second location, a TDIP survey was performed **...** data for this survey recorded in S. Sandberg's field note book. Note that the TDIP survey was terminated prematurely due to declining weather conditions (sand-storm).

Day 11 (Sunday, January 24, *1999):*
Surveys on this day performed in the Amargosa Desert southeast of the previous day's locations. Large loop TEM survey **(300** m **x 300** m) performed **...** recorded as TEM 31. Small loop survey **(40** m **x 40** m) survey also performed at this location **...** recorded as TEM **32.** Southeast of this location an additional large loop **(300** m **x 300** m) and small loop survey **(40** m **x 40** m) performed **...** recorded as TEM **33** and **34.** TEM instrument settings recorded in S. Sandberg's notebook (Appendix 2). Note that the field work ended early due to S. Sandberg's declining health.

Day 12 (Monday, January 25, 1999):
Equipment shipped from Las Vegas back to rental companies. Returned to San Antonio.

6. **Analyses and Results:** (June 8, 1999)
The survey can be broken up into three zones. Zone 1 occupies the lower section of Fortymile Wash, and extends from the Lathrop Wells Cinder Cone to the town of Amargosa Valley; Zone 2 occupies the Fortymile Wash region of the NTS; and Zone 3 occupies the Amargosa Desert region between the Lathrop Wells Cinder Cone and the town of Amargosa Farms. The following provides a summary of the data collected within each zone.

Station Number	UTM_East (m)	UTM_North (m)	Zone	Sounding Type
1	544736	4059006	1	TDIP; SR; TEM 1
2	546700	4058850	1	TEM 1
3	548050	4057600	1	TEM 1; TEM 2; TDIP; SR
4	543130	4060860	1	TEM 2
5	550075	4057275	1	TEM 1
6	551189	4057024	1	TEM 1
7	552500	4056750	1	TEM 1
8	554820	4065605	2	TEM 2
9	553218	4064962	2	TEM 1
10	553068	4065112	2	TEM 2
11	552868	4065324	2	TEM 2
12	552910	4068390	2	TEM 1
13	552769	4068528	2	TDIP; SR; TEM 2
14	552790	4068239	2	TEM 2
15	553650	4068400	2	TEM 1
16	553500	4067360	2	TEM 1

17	553390	4067470	2	TEM 2
18	552690	4066170	2	TEM 2
19	552580	4066280	2	TEM 1
20	552130	4064850	2	TEM 1
21	551980	4065000	2	TEM 2
22	551680	4065000	2	TEM 2
23	551380	4065000	2	TEM2
24	551080	4065000	2	TEM 2
25	552346	4064956	2	TEM 2
26	552504	4064927	2	TEM 2
27	544753	4056625	3	TEM 1
28	544623	4056746	3	TEM 2
29	545100	4055732	3	TEM 1
30	544977	4055862	3	TDIP; SR; TEM 2
31	547220	4052850	3	TEM 1
32	547175	4052666	3	TEM 2
33	547446	4050363	3	TEM 1
34	547316	4050233	3	TEM 2

TEM 1: **300m x 300m** TEM transmitter loop
TEM 2: **40m x** 40m TEM transmitter loop
SR: Schlumberger resistivity sounding
TDIP: Timedomain IP

Interim reports have been received from Geophysical Solutions.

Interim Report 1: The first of these reports is dated February 10, 1999. This report presented the results of analyses on the data collected at station TEM 1. The data included the TEM survey data, the IP data and the SR data. Simultaneous inversion of these data was performed and a model of the results presented. A possible watertable at elevation 770 m was identified. A copy of the interim report is attached as Appendix 3.

June 7, 1999

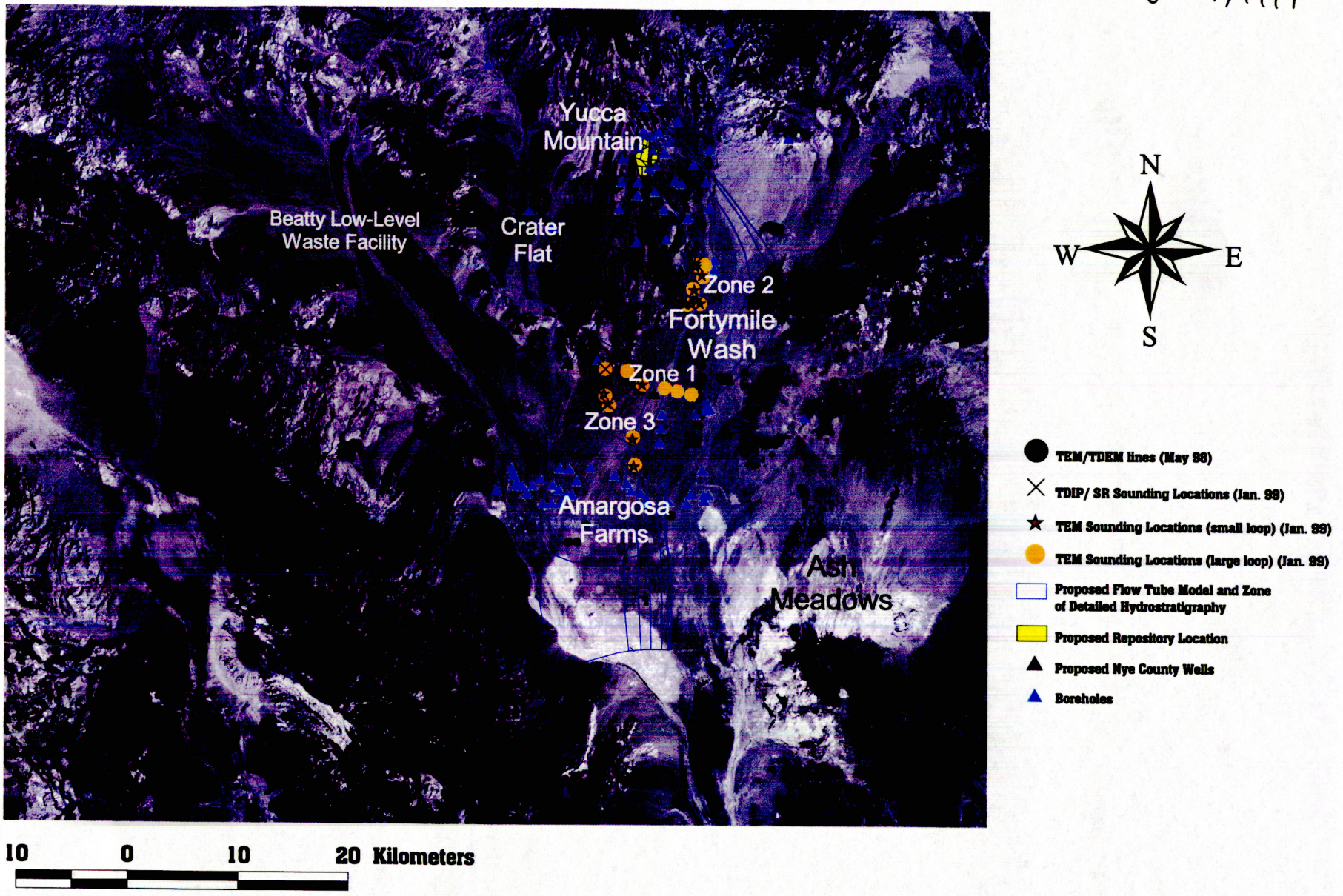

Figure 4a: Map of geophysical survey locations in Yucca Mountain and Amargosa Desert regions.

D.A.F.
June 7, 1999

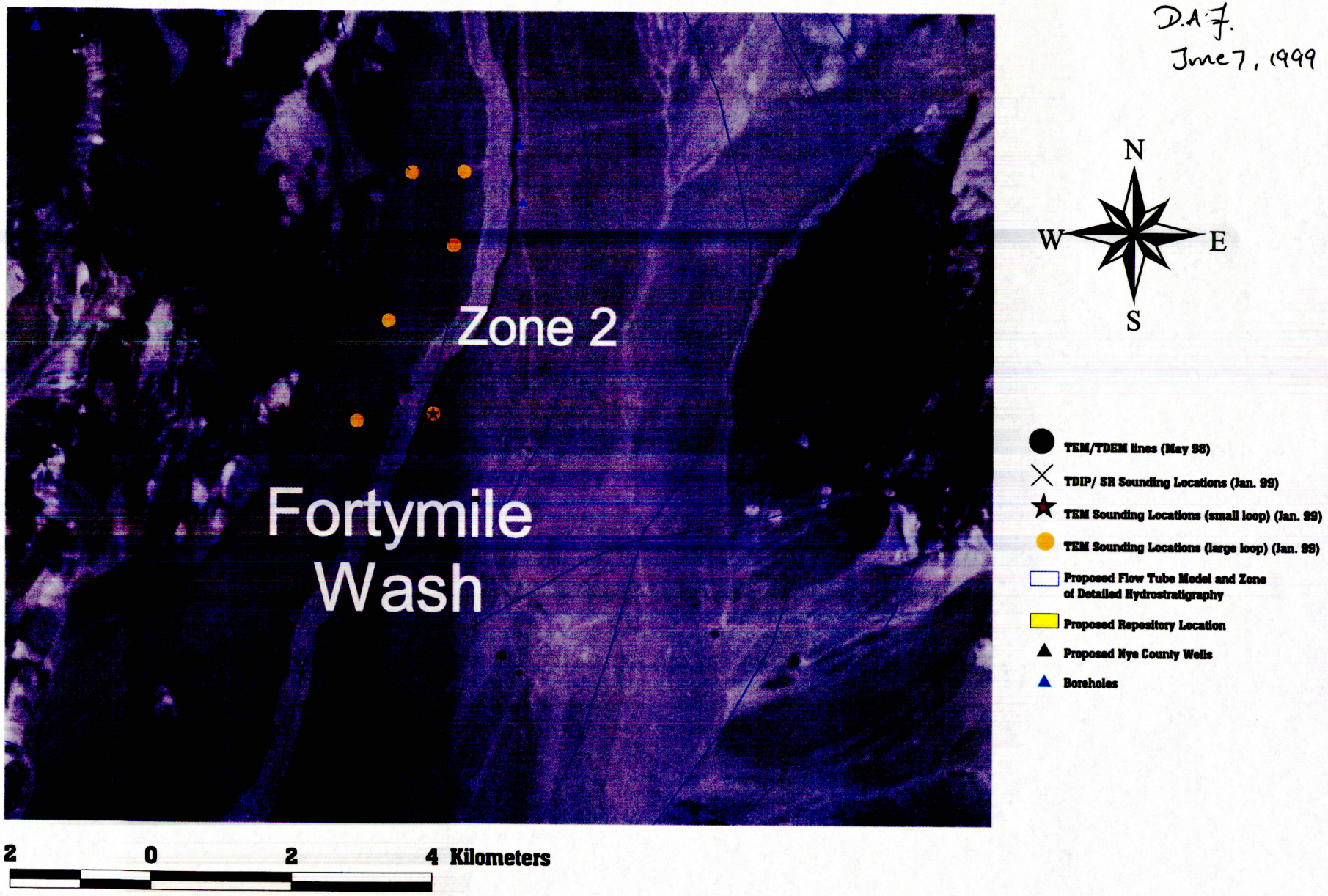

Figure 4b: Expanded view of geophysical survey locations the Fortymile Wash area of the NTS

D.A.7.
June 7, 1999

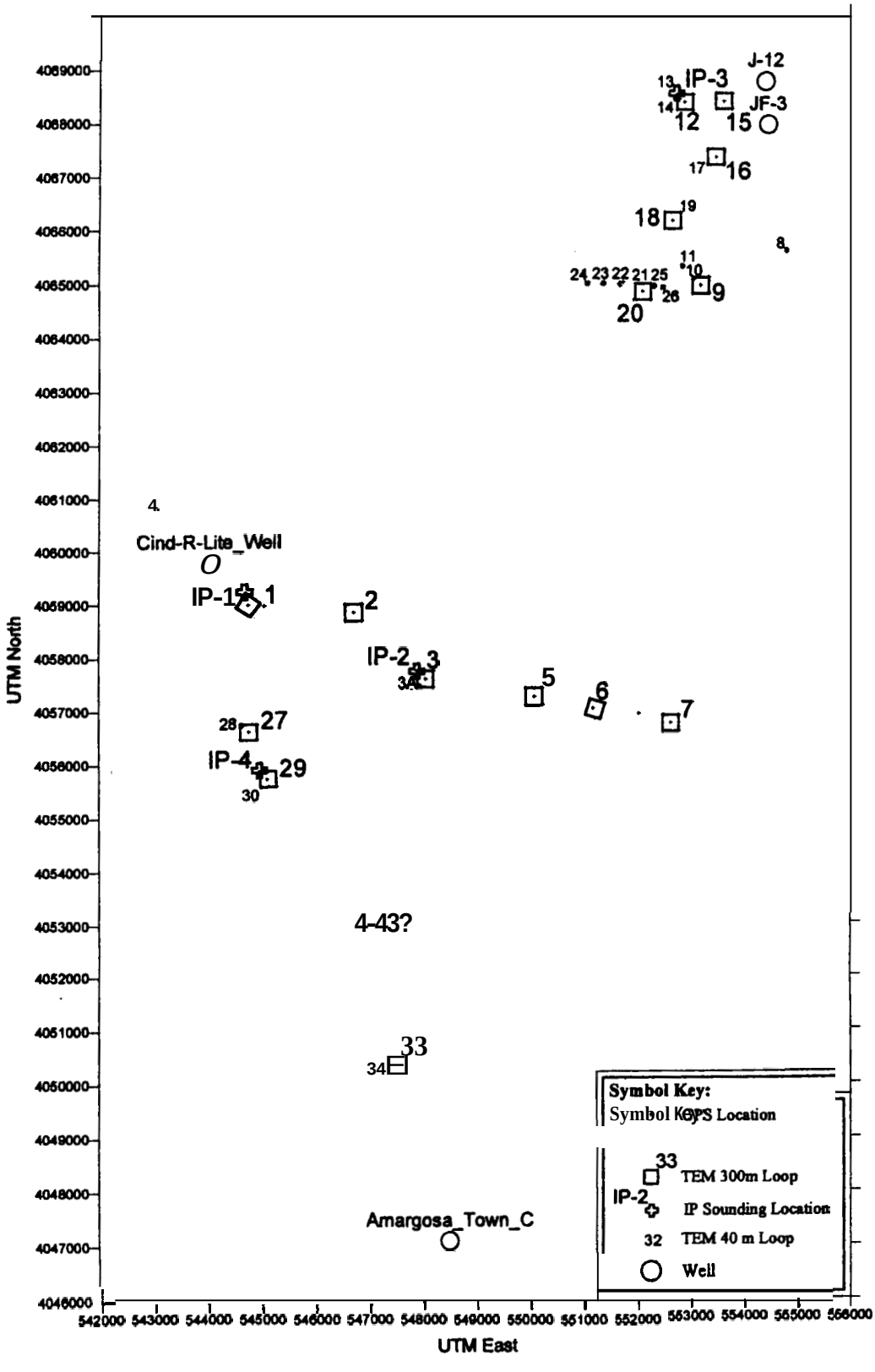

Figure 4C: Geophysical data locations corresponding to Table 1

Interim Report 2: The second interim report is dated March 25, 1999 and contained in Appendix **4.** This report presented a more extensive discussion of the results of analyses on data collected at stations within Zone 1. Included in the report are plots of the processed data and models fitted to the data. Where relevant (e.g., TEM 1 and TEM 3) simultaneous inversion results are presented. An important aspect of this report in the resistivity cross-section model presented for the data in Zone 1. The watertable as indicated by the cross-section model shows reasonably good agreement with observed waterlevel data recorded at Nye County wells NC-EWDP-2D and NC-EWDP-Washburn 1X. Discrepencies observed appeared to be due to poor surface elevation control ... elevations were inferred and not measured at some of the stations located in Zone 1. Elevations will be recorded for these locations in the near future. A correlation of the modeled resistivities to well bore data from NC-EWDP-2D will also be performed in the near future.

Entries into Scientific Notebook No. 371 for the period March 18,1999 to July 28,1999 have been made by David A. Farrell

No original text entered into this Scientific Notebook has been removed.

Data Analysis Update (October 13, 1999)
Stewart Sandberg forwarded a contour map of a processed cross-section for an east-west line (B-B') located on the NTS, south of Busted Butte. This line include sounding locations TEM-24, TEM-23, TEM-22, TEM-21, TEM-25, TEM-26, TEM-11, TEM-10, and TEM-8 (Figure 4). The line shows a high resistivity anomaly at depth along the western edge of the profile. This high resistivity is believed to be an expression of the tuff units which can be observed (visually) dipping beneath the alluvium west of TEM-24. The fault located along the western section of the line requires further investigation since it has not been identified in any of the previous literature (personal communication, D. Sims). The low resistivity zone beneath Fortymile Wash is interesting and requires further investigation since it may represent infiltration water (note this is speculation at this point in time).

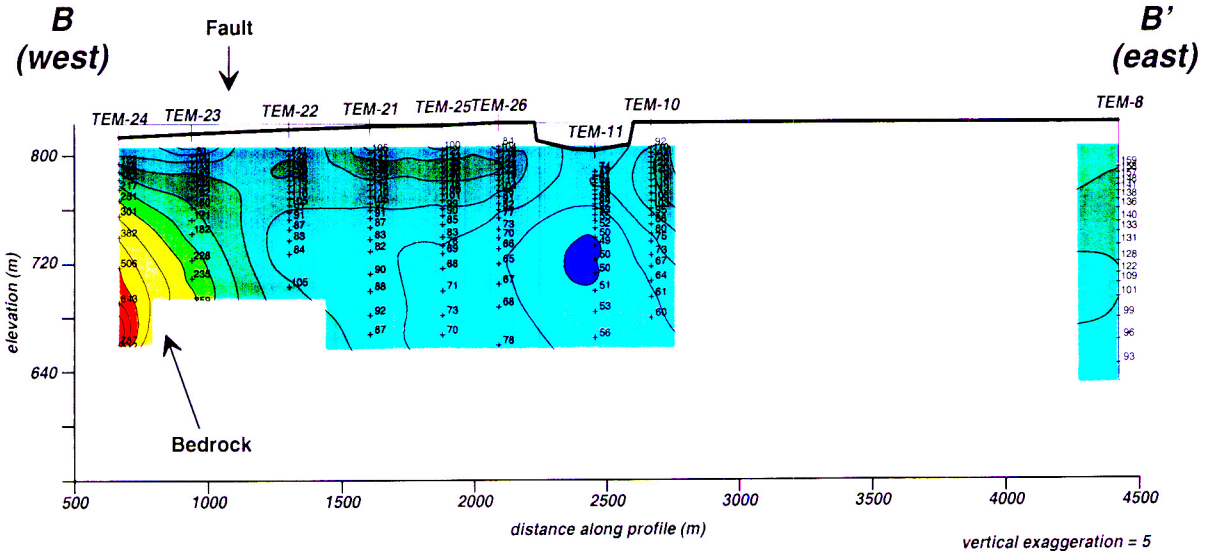

Figure 5: Approximate depth section for B-B' showing resistivity versus depth.

Data Analysis Update (October 21, 1999)
Resistivity depth section forwarded from Stewart Sandberg for work performed on the NTS along the north-east trending line DD'. This includes sounding locations TEM-20, TEM-18, TEM-16, and TEM-15. I've forwarded a comment to Stewart Sandberg concerning the low resistivities at TEM-20. Figure 5 shows the depth section.

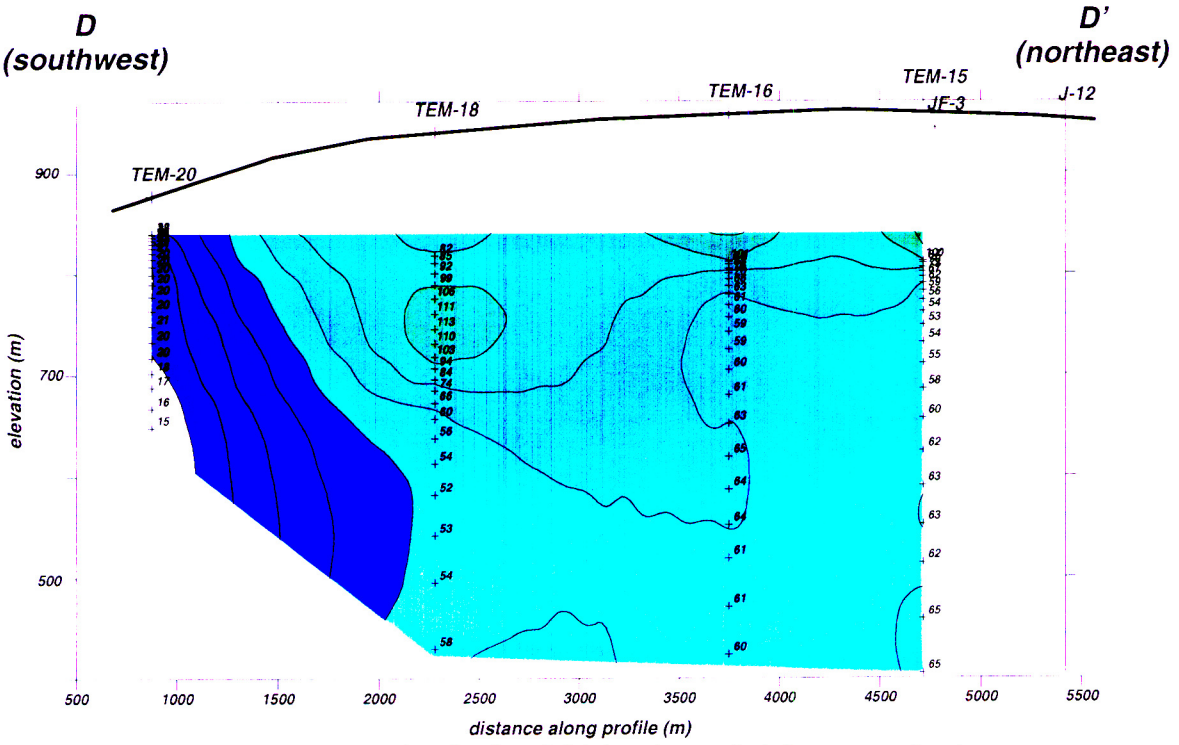

Figure 6: Approximate depth section for line DD'showing resistivity versus depth.

Data Analysis Update (October 22, 1999)
Depth section for line DD' forwarded from Stewart Sandberg. The section shows the interpreted water table based on observed data at wells JF-3 and 5-12.

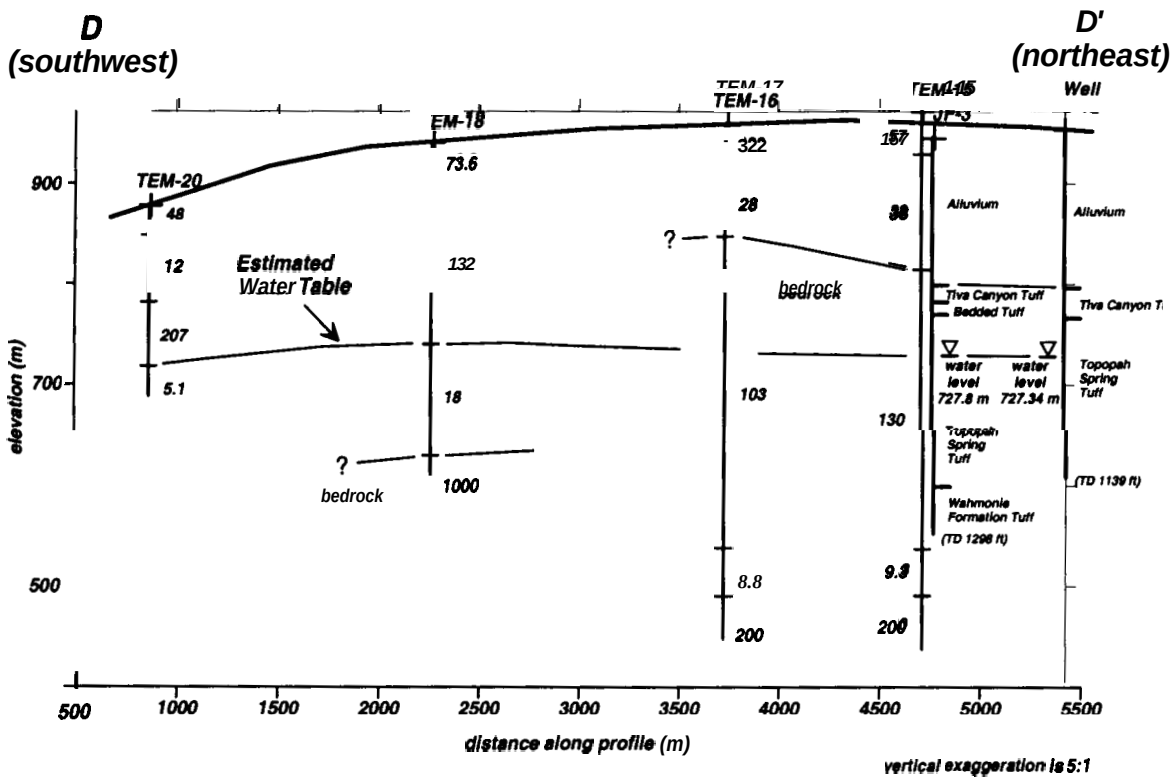

Figure 7: Interpreted resistivity cross-section for line D-D' (resistivities shown adjacent to sounding stations are given in ohm-m).

Entries into Scientific Notebook No. 371 for the period July 29, 1999 to October 24. 1999 have been made by David A. Farrell

No original text entered into this Scientific Notebook has been removed.

Data Analysis Update (November 10, 1999)

This update summarizes a reevaluation of the cross-section presented for line D-D' and presents the electrical resistivity cross-section for lines B-B' and A-A'. The results are being incorporated in a proceeding manuscript for the SAGEEP 2000 Conference.

The modified electrical cross-section for line D-D' is based in part on a comparison with existing aeromagnetic data for the region. Note this aeromagnetic data does not include the most recent data being collected by Nye County. In the reanalysis it has been assumed that the low resistivity unit observed at depth between TEM-17 and TEM-15 represents a continuous unit between these two sounding stations. Possible continuation of this unit to the west may be reflected by the 18 ohm-m resistivity unit observed at TEM-18 and the 5.1 ohm-m resistivity unit observed at TEM-20. However, this interpretation does pose some problems since the watertable is assumed to be co-incident with the surface connecting the low resistivity units at TEM-20 and TEM-18. This would suggest a steep watertable gradient between TEM-17 and TEM-18, and would indicate a possible watertable depth at TEM-15 and TEM-17 that is grossly inconsistent with the watertable elevations present at 5-12 and JF-3. The reason for the high resistivities below these units is

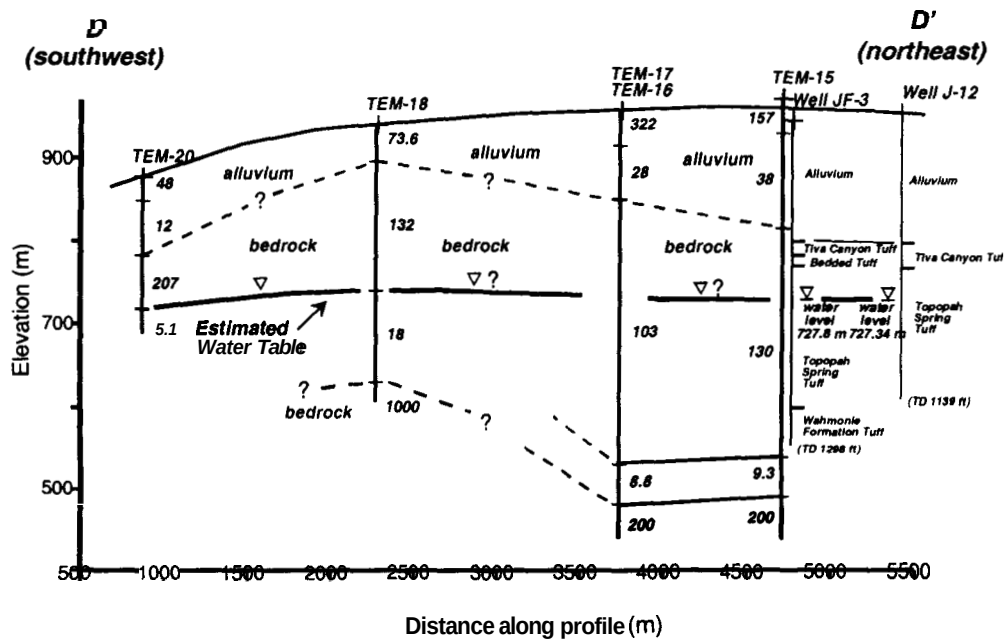

Figure 8: Modified resistivity cross-section for line D-D'. (resistivities shown adjacent to sounding stations are given in ohm-m)

currently unclear, but it is possible that these units may represent low porosity, tighly welded units. If this is the case then electrical conduction in these units would be restricted exclusively to the matrix and may explain the higher resistivities observed.

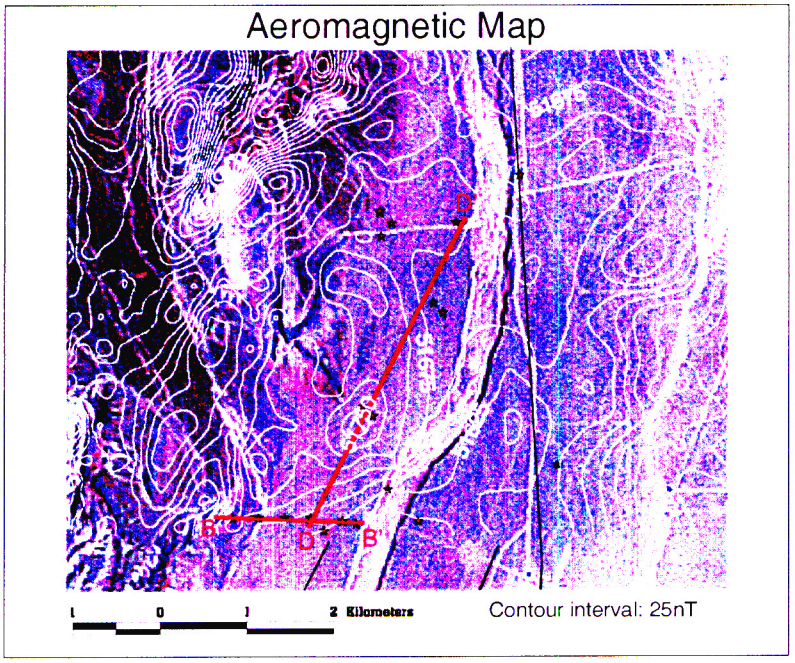

Figure 9: Aeromagnetic map for the region surrounding line D-D'.

Figure 9 (inset) shows that the topographic high observed in the vicinity of TEM-18 is supported by available aeromagnetic data. The areomagnetic data shows a local high in the vicinity of TEM-18 and therefore lends some support to the TEM data interpretation in this region.

An electrical cross-section for the line B-B' has also been supplied by Geophysical Solutions. A modified version of this model is contained in Figure 10. The modification added is the dashed line along the western end of the model. The model essentially shows a the tuff-alluvium contact along the western end of the survey line as a eastwardly dipping interface, with the resistivity of the tuff unit (the Tiva Canyon Tuff) being considerably higher than that of the overlying alluvial (valley-fill) material. The decreasing bed-rock elevation shown in the electrical cross-section appears consistent with the decreasing magnitude of the total magnetic field from west to east as shown in Figure 9. Within the alluvial unit three resistivity zones are observed: a shallow surficial unit of low resistivity (layer 1) overlying a zone of much higher resistivity (layer 2), which in turn overlies a a deeper unit of lower resistivity, $30 \leq \rho \leq 70$ ohm-m (layer 3). Layer 3 can represent either a perched watertable overlying the Tiva Canyon Tuff or an electrically conductive unit. This unit is too shallow to represent the region watertable. Layer 2 may represent either a zone of low moisture content or low clay content while layer 1 may represent either a layer of higher moisture content or increased clay content. More definitive answers may be obtained from TDIP surveys.

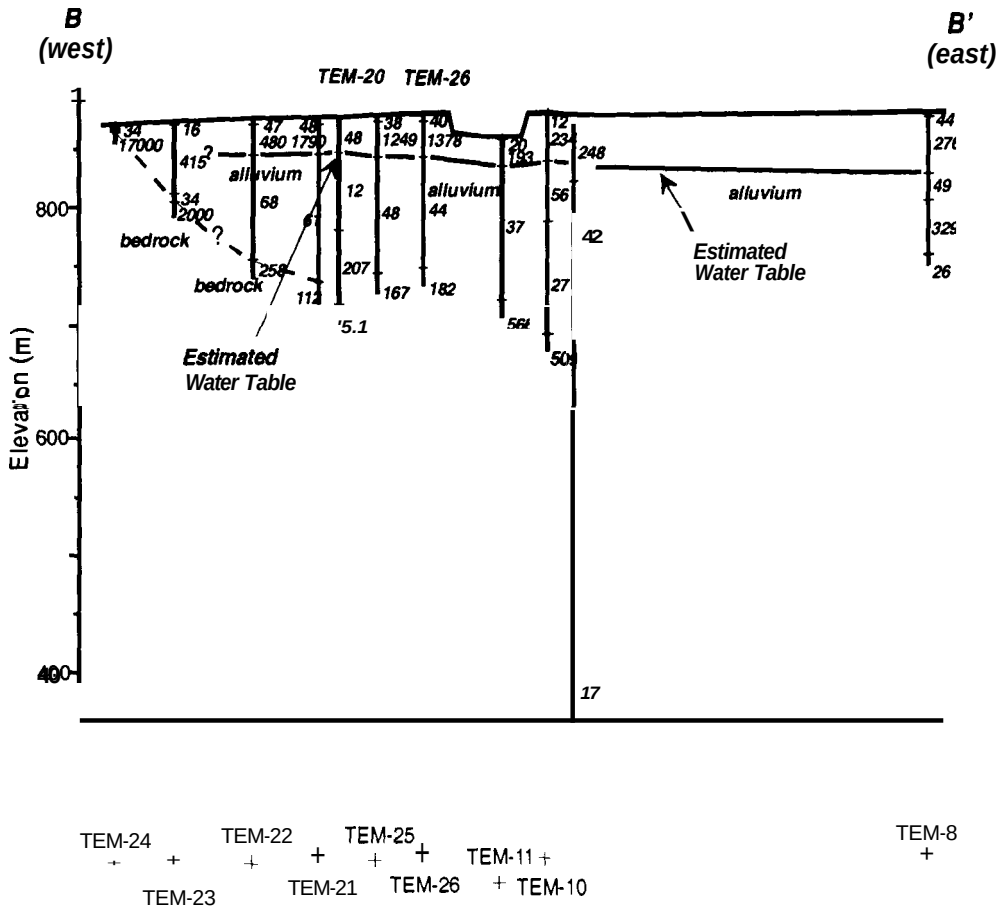

Figure 10: Interpreted resistivity cross-section for line B-B' (resistivities shown adjacent to sounding stations are given in ohm-m).

Data Analysis Update (January 22, 2000)
Final report received from Geophysical Solutions (Appendix 5). The report contains detailed electrical cross-sections for the survey lines traversed.

An electrical cross-section for the survey line C-C' (E-E' in Geophysical Solutions report, Figure 69) appears to clearly delineate the watertable. The model does show a possible watertable mound beneath the Amargosa Desert. In the region of the mound, the model is constrained not as well constrained as at other sounding locations. This may explain the slight mound observed. Interestingly, however is the fact that the watertable topography in the region of the mound appears to follow the ground elevation. The hydraulic gradients due to this mounding appears to be rather small. However, it does suggest possible diverging flow beneath the Amargosa Desert. This needs to be further investigated. The IP results along the cross-section indicates the presence of various clay units. The presence of clay units within the valley-fill deposits is also illustrated by IP sounding along A-A'. The presence of clay within the valley-fill deposits within Fortymile Wash and the Amargosa Desert is not surprising based on drilling logs for the region obtained from NC-EWDP wells.

The final survey line worth discussing is an east-west line consisting of two sounding stations, TEM-12/IP-3 and TEM-15, located on the NTS and referred to as C-C' in the report submitted by Geophysical Solutions (Plate 1, and Figure 57). TEM surveys conducted at both locations were based on 300 m **x** 300 m loop geometries. The results for the sounding at TEM-12/IP-3 show the presence several clay units with varying IP signatures. In the absence of IP data these clay units may be easily misinterpreted as shallow perched units. The watertable observed along this line appears to occur around 720 m and correlates well with the watertable elevation observed at 5-12. The models for the data collected at TEM-15 are not as well constrained as those collected at TEM-12/IP-3. As a result, correlating structures across the line is much more difficult. This is especially true for near-surface features ... no small-loop data collected for this location. Estimation of the watertable along this line is quite difficult.

Close-out of Electronic Notebook **317**

No further entries will be made to this electronic note book after February 28, 2000. Any further work on this project will be done in the form of journal articles or CNWRA/NRC publications.

Entries into Scientific Notebook No. 371 for the period October 24. 1999 to February 28, 2000 have been made by David A. Farrell

Apart from a modification to the caption of Figure 7 (February 28, 2000), no original text entered into this Scientific Notebook has been removed.

7. References

Parasnis, D.S. 1986. Principles of Applied Geophysics. **4"** Edition. New York: Chapman and Hall.

Sandberg, S.K. 1998. Inverse Modeling Software for Resistivity, Induced Polarization (IP), and Transient Electromagnetic (TEM) Soundings.

Sharma, P.V. 1997. Environmental and Engineering Geophysics. Cambridge University Press, UK.

Telford, W.M., L.P. Geldart, R.E. Sheriff, and D.A. Keys. 1976. Applied Geophysics. Cambridge University Press, USA.

Appendix 1

INVERSE MODELING SOFTWARE FOR RESISTIVITY, INDUCED POLARIZATION (IP), AND TRANSIENT ELECTROMAGNETIC (TEM, TDEM) SOUNDINGS

Manual
for
Computer Programs:

ZONGE
READZONG
T47INPUT
READ
SLUMBER
RAMPRES3
EINVRT6

MS-DOS Version ***6.0***
August 7, 1998

Written *by:*
Stewart K. **Sandberg,** Ph.D., P.G.
Noel Rogers

Geophysical Solutions

Geophysical Contracting & Consulting
1308 Narcisco **Court** NE
Albuquerque, NM 87112
(505)299-6878 e-mail: geophysh@aol.com
http://members.aol.com/geophysh/index.html

TABLE OF CONTENTS

INTRODUCTION

This manual describes the theory and use of geophysical modeling software for interpreting geoelectrical sounding data. Specifically, this includes resistivity data fiom the Schlumberger or Wenner arrays, or the dipole-dipole array when one takes care in selecting a diagonal representative of a layered-earth; conventional induced polarization (IP) data fiom the Schlumberger or Wenner arrays; and transient electromagnetic (TEM or TDEM) data from the central loop configuration (in-loop).

Earlier versions of some of this software were made available by the New Jersey Geological Survey (Sandberg, 1988, 1990). Changes since then include correction for previous TEM pulses (run-on effect), and enabling data fiom the Zonge TEM and NANOTEM systems to be interpreted.

EQUIPMENT REQUIREMENTS

Hardware reauirements

This software was written for an IBM-compatible computer with at least 512 KB of memory, and one disk drive (a hard disk is preferable). Version 6.0 is a DOS-based program which runs in Windows 95 within a DOS window. Screen graphics is incorporated into the code using the IBM Graphics Development Toolkit version 1.12, but there is an option to operate without graphics if the graphics drivers are not available. The IBM Graphics Toolkit drivers for the VGA, EGA and CGA cards and monitors are appropriate. The programming languages used are the IBM BASICA interpreter (or GWBASIC) for the TEM and resistivity/IP data input routines (T47INPUT and SLUMBER, respectively), and IBM Professional FORTRAN for the remainder of the code (ZONGE, READZONG, READ, RAMPRES3, and EINVRT6).

Screen graphics

For the screen graphics to operate, the appropriate driver name must be added to the CONFIG.SYS file after which the computer must be re-booted. Prior to running software requiring graphics (the EINVRT6 program), the INIT_VDI.EXE program must be executed.

Field eauiument

The TEM receivers for which the software was designed are the Geonics PROTEM receiver (either the analog or the fully digital version) or the Phoenix V-5 receiver with the FASTEM option. The Zonge TEM and NANOTEM systems are supported. Transmitters supported are the Geonics EM-37, EM-47, and EM-57, and the Phoenix (with appropriate card) transmitters. If the Geonics EM-37-3 receiver is used, the TEMINPUT.BAS code in Sandberg (1988) must be used to account for the instrument channel gains. Any of the transmitted base frequencies available on the PROTEM receiver can be used (3, 7.5, 30, 75, and 315 [285] Hz). The linear ramp shutoff time obtained from the Geonics-type transmitter is used in the algorithms.

The resistivity/IP equipment for which the software was designed is the Huntec M4 time-domain system, or the Phoenix V-5, which collects data according to the same protocol. However, any basic IP equipment could be used if the IP data are scaled to the same order of magnitude as the sum of the 10 time windows of the Huntec as read on the receiver display. (For more information pertaining to IP scaling and its importance, see the section on IP under Forward model algorithms.)

Resistivity-alone data obtained from any standard resistivity equipment can be interpreted with this software. Data points required include the transmitter current, the receiver voltage, and the electrode array parameters (AB/2 and MN for Schlumberger, a-spacing and n-value for dipole-dipole). However, the software can accept resistance and current from the ABEM receiver in place of the voltage and current.

INTRODUCTION TO INVERSE MODELING

Modern surface electrical geophysical investigations in which soundings are applied to solve geologic mapping problems almost always employ mathematical inversion of field measurements to obtain a geoelectric model. The use of forward modeling alone for data interpretation has become almost as outdated as its predecessor, curve matching. Inversion has a second advantage besides being one step closer to the elusive automatic interpretation, and that is its ability to produce quantitative resolution information. It is an analysis of resolution which has led to a better understanding of the capabilities of various geophysical methods.

There are two approaches to one-dimensional (layered-earth) modeling: 1) direct, or approximate analysis, or imaging, and 2) discrete layer modeling. In effect, these approaches are appropriate for multidimensional modeling also, but the software described in this manual applies only to one-dimensional modeling, Direct, or approximate modeling employs a simplification in order to solve for a continuous function of resistivity versus depth. Meju (1998) presents an example representative of this first approach.

The approach to one-dimensional modeling used in this software is discrete layer modeling. In this approach, the local subsurface is modeled as a finite number of layers. Often, when no other information is available, a minimum number of layers are used which can describe an observed data set to a specific degree of accuracy. When other information is available, layers are assigned based on this other information.

INTRODUCTION TO SIMULTANEOUS INVERSE MODELING

In the past few years, simultaneous inverse modeling techniques, where data are obtained from two different electrical geophysical methods, have been shown to improve resolution. Examples include Vozoff and Jupp (1975), Raiche and others (1985), Gustafson and McEuen (1987), and Sandberg (1993). The software described in this manual has the capability to model resistivity and IP data simultaneously, to model resistivity and TEM data simultaneously, and to model resistivity, IP, and TEM data simultaneously.

INVERSE MODELING TECHNIQUE

Inverse modeling, like many other endeavors, requires a certain amount of experience. The software in this manual is designed to facilitate a better understanding of this process.

Simultaneous inverse modeling is an art. A knowledge of several geophysical method responses is required; moreover fitting only one geologic model to more than one of these responses is tricky business. Because there are usually several local squared-error minima in geoelectrical inverse problems, it is important to obtain an initial guess of parameters which provides a close fit to the field data. Therefore, repeated modeling attempts varying the initial guess coupled with substantial geologic input are crucial to making good interpretations.

Much in modeling depends upon the complexity of the model. For only 3 to 4 layers and one geophysical technique, such as Schlumberger resistivity, initial guesses *can* be quite poor and the algorithm will find a reasonable solution. In this case the important factor is the number of layers in the model. If an insufficient number of layers is specified, the model commonly will not provide a close fit. Trial and error often provides a good "feel" for the situation.

When using depth rather than thickness as a parameter, the algorithm approximation is only correct for small changes. The code prevents an interface moving past another one, but the sensitivity of the depth is often incorrect when the initial *guess* is not good.

PRACTICE

Suggested interpretation process

The interpretation process described in this section is designed to minimize the amount of time required to interpret field data. The programs are sufficient to process resistivity, IP, and TEM sounding data in an organized manner. The data input routines are straightforward.

First, field data must be put into standard data files. This procedure amounts to running the T47INPUT or READ, or ZONGE, and SLUMBER programs for TEM and resistivity (or resistivity/IP) data, respectively. Next, the output plot file of reduced field data generated by SLUMBER should be plotted so that initial guesses for the resistivity and IP layer parameters *can* be made. For TEM data, the program RAMPRES3 should be run in order to generate reduced data and plots. Plotting can be done using the program PPLOT (Sandberg, 1990), a program which is able to read this file (such as EXCEL, LOTUS, GRAPHER, or Harvard Graphics), or by hand on log-log graph paper.

Initial *guess* layer parameters *can* be obtained by curve-matching, forward modeling, geologic information, or by experienced guessing. However these are obtained, they are needed to execute the EINVRT6 program.

The next step is running EINVRT6 in two stages. Through the prompting process (stage 1), an input file is created (when using data from the PROTEM or V-5, or when interpreting data obtained using the Zonge system, the program READZONG is used). When this is complete, the question "go on? (yes=1, no=0)" is output from EINVRT6 to the screen. Respond "no" and edit the input file with a text editor program (such as MS-DOS EDIT, the IBM Professional Editor, MS Word, Wordperfect, Wordstar, or other ASCII-type

text editor). Errors in parameter initial guesses and the number of iterations can be corrected at this point. Noisy data which will prevent the algorithm from finding a good fit can be deleted from the input file at this stage. Do not forget to change mr, mc, and mt on line 2 after deleting data. Note that decreasing mc (number of IP values) without deleting entire data lines is acceptable. Usable resistivity data from large electrode spacings, corresponding to low voltage levels at the receiver, could easily coincide with very noisy, and hence unusable IP data. The program has no provision to weight data points; either a data point is good, or it is not. Save this modified input file.

Stage 2 is to re-execute the EINVRT6 program. The prompts are minimized now that an input file exists. By observing the inversion screen graphics (or by carefully watching output on the screen when screen graphics is not available), one can determine how well the model is fitting the data. Adjustments can be made to the input file for subsequent runs of the program. Several runs are usually made in interpreting field data.

Tips on how to speed up the modeling process

Because the TEM forward algorithm used in EINVRT6 is fairly slow, and due to added complexity in incorporating additional methods, when doing simultaneous modeling it is advisable to interpret the resistivity data first. Next, interpret both the resistivity and IP data together, and finally, interpret all the data (resistivity/IP/TEM) together. This procedure will speed up the modeling process.

Specifying either ifwd=0 (for forward modeling) to tighten up initial guess parameters, or ifwd=3 (a small number) iterations is recommended to test whether the program can find a solution. Once things are going well, edit the input file and replace the old initial guess parameters with new ones found by previous program runs, or by other geologic ideas.

Often, fixing parameters dictated by geologic information can be very useful because run times are directly related to how many parameters are free to vary. Fixing parameters amounts to reparameterization, which can also aid in improving the resolution of remaining free parameters.

In addition, one might use only every other time channel in the TEM data for initial runs. This simple procedure can cut the run time in half.

One useful method of obtaining a good starting model (and thereby reducing the time needed to interpret the data set) is to run the inversion program only long enough to see how good the input guess is, after which type an S when the program pauses after a plot. This will halt the program and return you to an MS-DOS prompt. Then, the input file is edited, parameters are changed, and the inversion program is executed again with the altered input file.

How to tell when a model is adeauate

One difficult task for the unexperienced interpreter is to determine when a model is adequate. Hohmann and Raiche (1988, p. 488) describe how to quantitatively evaluate the confidence that *can* be placed in inversion results. Their procedure is summarized in this manual in the section on Parameter Resolution Statistics. It involves looking at the estimated standard error (here called RCSQ), and the noise-to-signal ratio (NSR). Confidence intervals often are swamped by high parameter correlations, but sometimes are meaningful.

Qualitatively, one *can* examine plots of field versus model-derived data to determine visually whether the model fits the data. Experience, and a knowledge of how precise parameters have to be for the specific application, help determine when data have been fit well enough for a reasonable geologic interpretation.

One empirical method which appears to work in determining whether enough iterations have been performed is to look at the parameter increments (displayed in log space). If increments on any of the parameters in the last iteration are > 0.1, then more iterations should be performed. Edit the input file, put the parameters from the final iteration in as the initial guess, and run the inversion again.

DATA HANDLING AND *APPARENT* RESISTIVITY SOFTWARE

This section describes software developed specifically to improve resolution in electrical geophysical surveys. The software incorporates many features useful to the practicing geophysicist to save time in the interpretation process. In addition, features useful to the geophysicist for understanding the subtle features of the inversion method applied to each specific case have been incorporated.

Electrical geophysical methods alone and in combination, addressed by this software include the following one-dimensional (sounding-type) techniques: 1) Schlumberger array resistivity, 2) simultaneous Schlumberger resistivity and induced polarization (IP), 3) transient electromagnetic (TEM, or TDEM) central loop, or in-loop array soundings, 4) simultaneous TEM and Schlumberger resistivity soundings, 5) simultaneous TEM and dipole-dipole array resistivity soundings, and 6) simultaneous TEM, Schlumberger resistivity, and IP soundings. Also, owing to the way that the resistivity forward solution is calculated, Wenner array resistivity and/or IP soundings can be substituted in the above categories where Schlumberger array is listed. Half-Schlumberger array resistivity and IP data can be interpreted also.

FIELD DATA REDUCTION AND STORAGE

TEM field notebook data must be reduced for receiver coil amplifier gain and the receiver coil's effective area (area of coil multiplied by number of turns). In addition, a standardized data format is necessary. Data obtained with the Zonge systems (files sometimes referred-to as Z files) are read using the program READZONG, producing intermediate files similar to the NJGS format described below. These files are directly read by the program ZONGE to produce input files for inversion.

The BASIC program T47INPUT creates standardized data files by keying-in data values displayed on the PROTEM receiver datalogger screen. Alternatively, the FORTRAN program READ translates the file created by the Geonics transfer program GSPx7 (Geonics, Dec. 1988), and creates one output file for each TEM sounding. However, as stated in the previous section, the BASIC program TEMINPUT in Sandberg (1988) must be used to account for the instrument channel gains when reducing data obtained with the Geonics EM-37-3 receiver.

Resistivity and IP sounding field data require a standardized format, not for data reduction, but for storage. These data initially need to be reduced to apparent resistivity versus current electrode separation and plotted to determine data quality and allow determination of an initial guess for the inversion. A program for resistivity data input and generation of a plot file of apparent resistivity versus current electrode half-separation is included as the BASIC program SLUMBER.

TEM data-file format

The TEM data-file format was described by Sandberg (1988) as the NJGS (New Jersey Geological Survey) Standard TEM Data Format. Software presented in Sandberg (1988) and in this manual require input files in

this format (except for Zonge-type data). TEM data values in the NJGS Standard TEM Data Format are produced by both data input routines T47INPUT and READ.

BASIC program T47INPUT

This program creates a data file for each TEM sounding through the interactive process of keying-in data values from the PROTEM receiver data-logger display. *Note* that ***entering a duplicate file name to a pre-existing file will cause the pre-existing file to be overwritten.***

Input. The program prompts for a file name in which the reduced data will be stored. Next, the following variables are entered:

code gain ai toff tx

where

code = Number corresponding to the transmitted base frequency and receiver coil type. Allowable values are:

1 (for 3 Hz or LO receiver setting)

2 (for 7.5 Hz or MD)

3 (for 30 Hz or HI setting with the low frequency coil and the EM-57 or EM-37 transmitter)

4 (for 30 Hz or HI with the low frequency coil and the EM-47 transmitter)

5 (for 30 Hz or HI with the high frequency coil and the EM-47 transmitter)

6 (for 75 Hz or VH)

7 (for 315 Hz or UH)

gain = The amplifier gain from the receiver expressed as a power of 2.

ai = The transmitter current in amperes.

toff = The transmitter current pulse *turnoff* time in microseconds. This value is obtained from a meter on the transmitter (Geonics), or during data processing (Phoenix).

tx = The transmitter loop side dimension (Figure 1.1) in meters.

Finally, 20 channels of data are requested. At the end, provision is made to enter another data file while the program is running.

Output. The output is a data file in free format consisting of 21 lines. The top line shows code, gain, ai, toff, and tx as defined above.

The remaining 20 lines are the calculated dB/dt in microvolts per square meter ($\mu V/m^2$) at the receiver coil at each of the 20 time windows of the receiver. The formula used in the calculation (Geonics Limited, 1988, p. 17) is:

$$\frac{dB}{dt} = \frac{19.2 \times v \times 2^{-gain}}{A_R}$$

where v (in mV) is the reading at the receiver and A_R is the effective area of the receiver coil (in m^2). This output format is the NJGS Standard TEM Data Format. All programs requiring TEM data input are read assuming this format. The inversion program EINVRT6 has an option to produce an output file in this format. Such a file is useful as a forward modeling result for either an arbitrary theoretical model, or as a final theoretical model which matches a set of field data. Other than this output file, the only forward modeling results are latestage asymptotic TEM apparent resistivity values.

FORTRAN program READ

This program reads the data file created by the Geonics GSPx7 Transient EM Data Handling & Modeling program (Geonics Limited, 1988). Data are uploaded from the PROTEM receiver data logger to the microcomputer using this manufacturer-suppliedsoftware. These data are then reduced and translated by the FORTRAN program READ into individual sounding files in the NJGS Standard TEM Data Format as described for T47INPUT in the previous section. This is an interactive process which is specific to the PROTEM receiver data logger; it has not been designed for data from the EM37 data logger. No account for differing channel gains has been made as in the program TEMINPUT (Sandberg, 1988).

FORTRAN program READZONG

This program reads the Zonge GDP Data Block file (sometimes called the Z file). Both TEM and NANOTEM files can be read. Selected data blocks of data can be read, selected by record number, two parameters sometimes used as northing and easting, or all data blocks can be read. Output consists of 5 parameters tfreq, rmom, curr, ramp, and txx. These correspond to the transmitter frequency, the receiver moment, the transmitted current, and the transmitter square loop side dimension. Following this line, a series of data values are listed, one per line, consisting of the gate time (seconds), and the dB/dt in microvolts per square meter ($\mu V/m^2$). This file is similar to the NJGS Standard TEM Data Format described above, except for the added column of gate times, and the use of the first and second parameter fields in the first line for transmitter frequency and receiver moment.

Resistivity/IP data-file format

The resistivity/IP data-file format is defined as the NJGS Standard Resistivity/IP Data Format. Details of this syntax are explained below in the Output section of the SLUMBER program description. Data are required in this format to be entered into the inversion program EINVRT6.

BASIC program SLUMBER

This program is a data-input routine which creates two output files: a data file for storage of resistivity/IP data in the NJGS Standard Resistivity/IP Data Format, and a plot file for initial inspection of field data. A separate data file is created for each resistivity/IP sounding. Note that entering a duplicate file name to a pre-existing file causes the preexisting file to be overwritten.

Input. Data are entered interactively in response to screen prompts. Input data consist of the current electrode half-separation (AB/2) in meters, potential electrode separation (MN) in meters, and the transmitted current (I) in amperes. Depending upon whether the data were collected with the ABEM Terrameter or a regular receiver (e.g. the Huntec M4, Phoenix V5, or Bison 2390), one is either prompted for the resistance (R) in ohms (for the ABEM), or the voltage (V) in volts. If IP data were also collected, one is then prompted to enter the chargeability in milliseconds. One enters a zero value for AB/2 to exit the program.

Output. Output consists of two files. A plot file of apparent resistivity versus current electrode half-separation (AB/2) is created for initial inspection of field data. In addition, a data file of electrode geometry and readings is created.

The plot file consists of three columns of numbers in free format. These columns are AB/2, apparent resistivity, and a plot-symbol number. The plot-symbol numbers correspond to plotting symbols as interpreted by NJGS plotting programs such as PLOT (Sandberg, 1988). This format has been referred to as the NJGS Standard Plot Format (Sandberg, 1988).

The data file consists of five columns of numbers in free format. These columns are AB/2, MN, received voltage, transmitted current, and chargeability. This is defined as the NJGS Standard Resistivity/IP Data Format because of its common use in various modeling and data-reduction programs at the New Jersey Geological Survey. If IP data are not collected, a "1" is placed in the chargeability column. If data were collected by the ABEM Terrameter, voltages are calculated based on the current readings and resistance readings.

TEM APPARENT RESISTIVITY

Background

Adequate near-surface interpretation, necessary for groundwater investigations, is difficult using TEM soundings. To understand how to improve the shallow resolution of TEM soundings, one must begin with one of the simplest concepts, that of apparent resistivity.

Reduction of field data to apparent resistivity is often used as a first step toward interpretation. This reduction is commonly used as a data compression scheme for preliminary data inspection. Receiver coil voltages can vary over 7 orders of magnitude, but the corresponding apparent resistivity may only vary by 2 orders of magnitude. In addition, TEM apparent resistivity curves, like those derived for resistivity and magnetotellurics, can indicate layering and show some information about the resistivities of the layers.

One popular concept of apparent resistivity is that it is the resistivity of an equivalent homogeneous halfspace which would yield the observed receiver coil voltage at its specific measurement time. This concept will be used to develop TEM apparent resistivity in this chapter.

Theory

The central loop (or in-loop) TEM sounding configuration consists of a large square transmitting wire with a vertical dipole receiver located at the center as in Figure 1. A common transmitter waveform, shown in Figure 2a, consists of a series of positive and negative current pulses, each terminated by a linear ramp. The receiver samples the secondary magnetic field while the transmitter is off during the "measurement time" shown in the figure. (Actually, the receiver measures the voltage in a receiver coil which is the time derivative of the secondary magnetic field.) Data obtained from many transmitter cycles are averaged (or stacked) in order to cancel random noise.

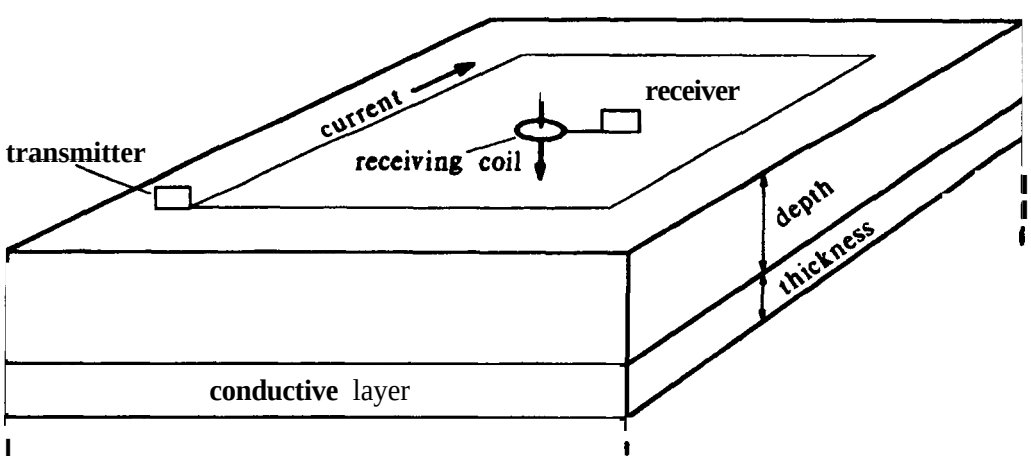

Figure 1. TEM sounding field layout showing **the central-loop sounding configuration** *using a* **large** *square* **transmitting loop.**

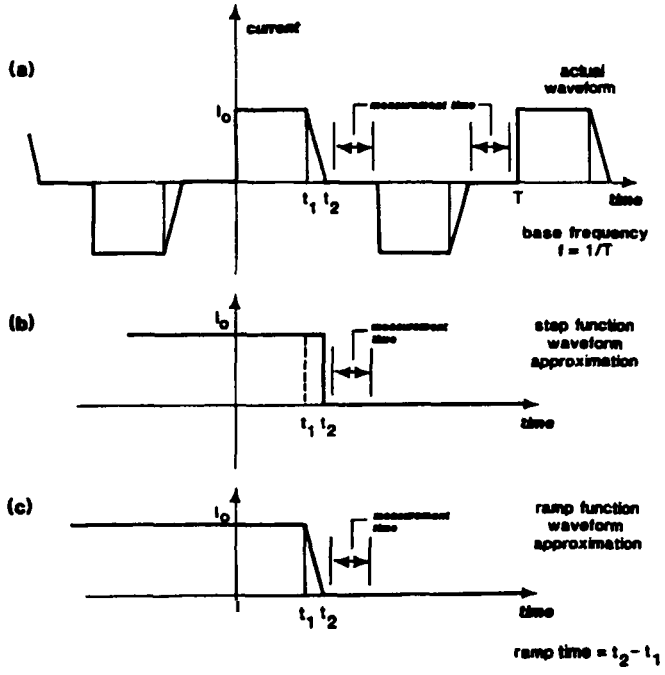

Figure 2. TEM transmitter current waveforms. (a) Idealized waveform (not depicting the actual exponential rise times), (b) step function waveform approximation, and (c) ramp function waveform approximation.

Because the current pulses by design are long enough to create a steady-state magnetic field in the ground, and the ramp time is usually very short, each cycle of this waveform can be approximated by a step function, as shown in Figure 2b. Raab and Frischknecht (1983) published computer programs for reducing field data to apparent resistivity based upon this step function approximation.

This section addresses calculating apparent resistivity using the approximation of the transmitted waveform with a ramp-terminated step function as shown in Figure 2c

From Raiche (1984) the mutual impedance, $Z(\rho,t)$, between a circular transmitting loop of area A_T, and a concentric receiving loop of area A_R, can be written as:

$$Z(\rho,t) = \frac{\pi\mu a}{2\delta} \times \frac{A_R}{A_T} \int_0^\infty G(\xi^2\tau, P) J_1(\xi) \xi d\xi \qquad (1)$$

where a is the circular transmitter loop radius, τ is the ramp length, J_1 is a Bessel function of order 1, P incorporates layer thicknesses and resistivities, μ is the magnetic permeability, and ξ is the integration variable for the inverse Hankel transform. In addition,

$$G(\xi^2\tau, P) = F(\xi^2\tau') - F(\xi^2\tau) \qquad (2)$$

where

$$\tau' = \frac{t}{\sigma\mu a^2}$$

$$\tau = \frac{t+\delta}{\sigma\mu a^2}$$

and, for the homogeneous half-space case:

$$F(\xi^2\tau) = \frac{2}{\sqrt{\pi}}\left[(1/2 + \xi^2\tau)\sqrt{\pi}\,erfc(\xi\sqrt{\tau}) - \xi\sqrt{\tau}e^{-\xi^2\tau}\right] \quad (3)$$

In these expressions, σ is the half-space conductivity, ρ is the half-space resistivity ($1/\sigma$), and *erfc* is the complementary error function. In this convention, the measurement time, t, is zero at the end of the ramp.

We can expand $J_1(\xi)$ from (1) in a power series

$$J_1(\xi) = \frac{1}{2}\sum_{k=0}^{\infty}\frac{(-1)^k\xi^{2k+2}}{4^k k!(k+1)!} \quad (4)$$

substitute it into (1) along with the analytic G function, obtained by substituting (3) into (2), and integrate the sum term-by-term.

After some algebraic simplification, the half-space mutual impedance result becomes

$$Z(\sigma,t) = \frac{\sqrt{\pi}\mu a}{2\delta} \times \frac{A_R}{A_T}\sum_{n=0}^{\infty}\frac{(-1)^n}{4^n n!(2n+3)(2n+5)} \times \left[\frac{1}{\tau'^{n+3/2}} - \frac{1}{\tau^{n+3/2}}\right] \quad (5)$$

In the processing of field data, it is assumed that a square transmitting loop is equivalent to a circular transmitting loop of equal area. Raiche (1987) showed this to be generally valid for the central loop configuration.

Apparent resistivity analysis

The next step involves a comparison of the mutual impedance derived from (5) with the step function response (Raab and Frischknecht, 1983) for various half-space resistivities. Figure 3a is a plot of mutual impedance versus half-space resistivity at 0.109 ms after transmitter shutoff, assuming a realistic ramp time of 180 μs, a square transmitter loop 300 m on a side, and a receiver coil with an effective area of 100 m^2. Also shown in the figure are the asymptotic "early" and "late" stage step function values based on the following relations (modified from Spies and Eggers, 1986):

$$Z_{early\ step}(\rho,t) = \frac{3A_R\rho}{a^3} \tag{6}$$

$$Z_{late\ step}(\rho,t) = \frac{a^2 A_R \mu^{5/2}}{20\pi^{1/2} t^{5/2} \rho^{3/2}} \tag{7}$$

Figures 3b and 3c show the response at 0.28 and 1.40 ms after transmitter shutoff, respectively. To describe these curves, the following terminology is used. The left-hand branch of the curve, corresponding to low resistivities, is referred to as the early stage branch, and the right-hand branch, corresponding to higher resistivities, is referred to as the late stage branch. (For a discussion of early and late stages, see Kaufmann and Keller (1983)). Note that two values of resistivity correspond to the same value of mutual impedance. This two-valued response was previously shown for the step function approximation by Raab and Frischknecht (1983) and by Spies and Eggers (1986). As can be seen in Figures 3a-c, the two-valued response also occurs for the ramp function approximation.

In order for the early stage branch of these curves to be appropriate in data reduction, the resistivities involved have to be very low; in most instances the late stage branch is the representative one.

Note that as time increases, late stage branches of the curves for the step function and ramp function approach each other. Also, both functions converge to the asymptotic early stage result given by (6) for decreasing resistivity.

An algorithm for processing TEM field data and solving for ramp function apparent resistivity was developed (computer program RAMPRES3). This algorithm uses a modified secant method iterative solution to obtain an apparent resistivity from an observed mutual impedance. The method uses the asymptotic late stage resistivity derived from solving (7) for ρ, which yields the first function point, and a second is calculated less than the first yielding a second function point. A third function point is calculated assuming a linear relationship between log resistivity and log mutual impedance. The process is repeated using the second and third values to obtain a fourth, and so on until a solution is obtained within a specified tolerance. To remain on a particular branch of the curve, the iterative step size is regulated. (The asymptotic early stage resistivity is used for the first function point if a solution on the early stage branch is desired).

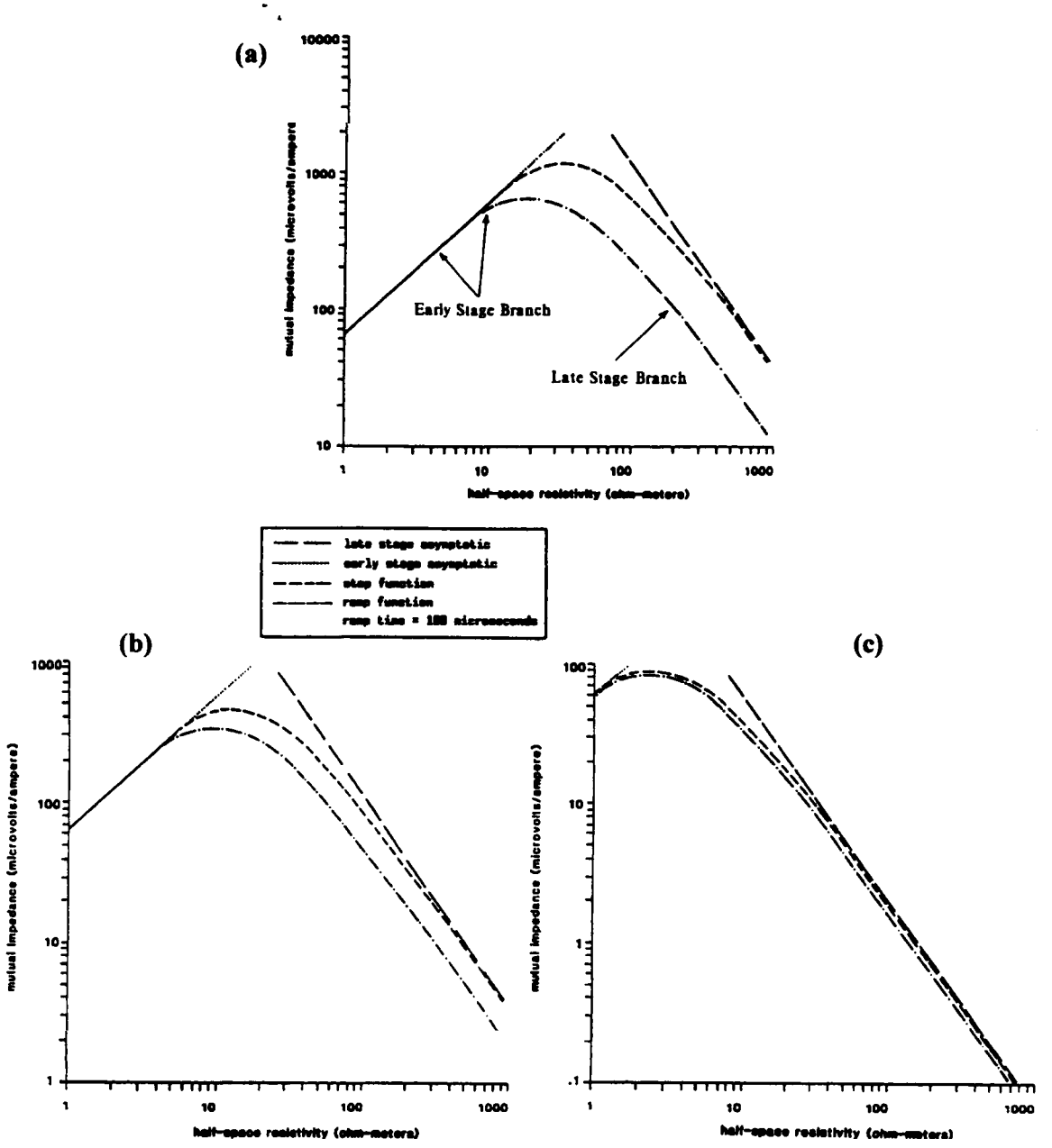

Figure 3. Mutual impedance for a homogeneous half-space using asymptotic relations, step function response, and ramp function response for (a) 0.109 ms, (b) 0.28 ms, and (c) 1.40 ms.

TEM APPARENT RESISTIVITY CALCULATION

TEM data are almost always reduced from *dB/dt* values (generated by the BASIC program T47INPUT or

READZONG above) to apparent resistivity. Two common reasons for this are: 1) it facilitates inspection of data quality and qualitative analysis, and 2) it enables one to make an initial guess for modeling.

An analysis of apparent resistivity algorithms for TEM central loop soundings was previously made under the heading of APPARENT RESISTIVITY ANALYSIS. Modification to the computer program RAMPRES (Sandberg, 1988) for the time channels of the EM-47 and EM-57 transmitters as well as the EM-37 transmitter, and for the Zonge equipment is included here as RAMPRES3. This algorithm accounts for the finite transmitter-turnoff ramp of the Geonics and Zonge transmitters.

The algorithm solves the equation

$$Z(\sigma,t) = \frac{\sqrt{\pi}\mu a}{2\delta} \times \frac{A_R}{A_T} \sum_{n=0}^{\infty} \frac{(-1)^n}{4^n n!(2n+3)(2n+5)} \times \left[\frac{1}{\tau'^{n+3/2}} - \frac{1}{\tau^{n+3/2}} \right] \tag{8}$$

for the apparent resistivity, ρ_a ($= 1/\sigma$) where

$$\tau' = \frac{t}{\sigma\mu a^2}$$

$$\tau = \frac{t+\delta}{\sigma\mu a^2}$$

In these expressions, Z is the mutual impedance (voltage in the receiver coil divided by the current in the transmitter loop), σ is the half-space conductivity, t is the measurement time, δ is the ramp time, μ is the magnetic permeability, a is the equivalent circular transmitter-loop radius, A_R is the area of the receiver coil, and A_T is the area of the transmitter loop.

The apparent resistivity derived from inverting (8) is referred to as the ramp-derived apparent resistivity. Problems associated with the two-valued response and the unreliability of this apparent resistivity definition were discussed previously. Many workers use the step-function asymptotic "early" and "late" stage apparent resistivities defined as follows. The asymptotic "early" stage apparent resistivity is

$$\rho_a^{early} = \frac{a^3 Z}{3A_R} \tag{9}$$

and the asymptotic "late" stage apparent resistivity is

$$\rho_a^{late} = \frac{a^{4/3} A_R^{2/3} \mu^{5/3}}{20^{2/3} \pi^{1/3} t^{5/3} Z^{2/3}} \tag{10}$$

Owing to problems associated with the ramp-derived apparent resistivity, the objective function used in the inversion program EINVRT6 is the asymptotic "late" stage apparent resistivity as defined in (10).

FORTRAN program RAMPRES3

The program RAMPRES3 operates much the same as its predecessor, RAMPRES (Sandberg, 1988). One added feature is the ability to add (or subtract) a fixed amount of time to each of the time gates. This is needed if the receiver was set incorrectly for the ramp-turnoff time of the transmitter (which can easily be done using the analog PROTEM). The update from RAMPRES2 is the ability to read Zonge data.

Input. The program RAMPRES3 requires one or more input files in the NJGS Standard TEM Data Format (generated by T47INPUT or equivalent), or the Zonge modification.

output. All input files are combined into one output-plot file. Note that entering a filename identical to that of a preexisting file causes an error exit of the program to protect previously created output files. A provision is made for including results from the asymptotic "early" stage or "late" stage approximations (9) and (10) respectively, in the output for comparison. Also, the program is designed to remain on either the "late" stage branch or the "early" stage branch of the rampderived function in looking for solutions.

Screen output consists of the following columns: channel number, sample time, "late" stage step-function asymptotic apparent resistivity, rampderived apparent resistivity, number of iterations of the secant method (which is used to solve (8) for the apparent resistivity), the branch of the mutual impedance curve to which the apparent resistivity corresponds, and the slope of the mutual impedance curve at the solution point in log-log space. During computation of the series in (8), if 70 terms are calculated without convergence, the statement "divergent sum" appears on the screen and no rampderived apparent resistivity is written to the plot file. If "no soln" and "not applicable" appear in the columns for resistivity and branch, either no solution for apparent resistivity exists for that data point., or a numerical instability of the method prevented solution.

In addition to the screen output, an output file in the NJGS Standard Plot Format (Sandberg, 1988) is generated. This format consists of three columns of numbers in free format: column 1 is the x-coordinate (or time in seconds for RAMPRES3), column 2 is the y-coordinate (or apparent resistivity in ohm-meters for RAMPRES3), and column 3 is the plotting-symbol number. The plotting-symbol number corresponds to a symbol used by the plotting program and usually ranges from 1 to 6 (see for example PLOT in Sandberg, 1988). Only one output-plot file is generated for each program run, no matter how many input files are processed.

FORWARD MODEL ALGORITHMS

This section provides details of the forward calculation for each of the methods: transient electromagnetics, resistivity, and induced polarization. Each of these forward solutions is numerical rather than analytical.

THEORY

TEM

The TEM central loop induction configuration is shown diagrammatically in Figure 1. The expression for the TEM mutual impedance in this configuration for a layered earth is given by Raiche (1984) as

$$Z(\rho,t) = \frac{\pi\mu a}{2\delta} \times \frac{A_R}{A_T} \int_0^\infty G(\xi^2\tau, P) J_1(\xi) \xi d\xi \tag{11}$$

the symbols are as defined previously with the addition of the following: ξ is the argument of the inverse Hankel transform, and J_1 is a Bessel function of order 1. The function G is

$$G(\xi^2\tau, P) = F(\xi^2\tau') - F(\xi^2\tau) \tag{12}$$

with τ and τ' as defined previously. For the layered earth case,

$$F(\xi^2\tau) = -L_q^{-1}\left[\frac{A_0(q)}{q}\right] \tag{13}$$

where L_q^{-1} is the inverse Laplace transform operator with respect to q, the transform pair is $(q, \xi^2\tau)$, A_0 is the layered earth impedance function, and the expression for q is

$$q = \frac{-i\omega\sigma\mu a^2}{\xi^2} \tag{14}$$

where ω is the angular frequency, and i is $\sqrt{-1}$. The layered earth impedance function, A_0, is derived following Raiche (1984) as follows. Define the exponential factor

$$E_j = e^{-2s_j h_j} \tag{15}$$

where h_j is the thickness of layer j and

$$S_j = \left[\left(\xi/a\right)^2 - i\omega\sigma_j\mu\right]^{1/2} \tag{16}$$

where σ_j is the conductivity of layer j. Next define a reflection coefficient, R_j, at the boundary of layers j and j+1 as

$$R_j = \frac{S_j - S_{j+1}}{S_j + S_{j+1}} \tag{17}$$

To obtain A_0, start at the bottom layer and work to the top. For N layers above a haif-space define

$$F_{N+1} = 0$$

$$F_N = R_N E_N$$

$$F_j = \frac{E_j(R_j + F_{j+1})}{1 + R_j F_{j+1}}$$

for all j except $j = 0$ or $j = N$. Then

$$A_0 = \frac{R_0 + F_1}{1 + R_0 F_1} \tag{18}$$

The inverse Laplace transform is calculated numerically using the Gaver - Stehfest method as described by Knight and Raiche (1982). The two formulas used in this algorithm are

$$f(t) \approx \left[\frac{\ln(2)}{t}\right]\sum_{j=1}^{J} d(i,J) \times F[j \cdot \ln(2)/t] \tag{19}$$

and

$$d(j,J) = (-1)^{j+M} \sum_{k=m}^{\min(j,M)} \frac{k^M (2k)!}{(M-k)!k!(k-1)!(j-k)!(2k-j)!} \tag{20}$$

where F is the Laplace transform of the function $f(t)$ defined for non-negative t, J is an even integer whose optimal value depends upon the computer word length, $M = J/2$, and m is the integer part of $(j+1)/2$. The optimal value of J for the IBM-compatible computer used in this development based upon testing known inverse Laplace transforms is 16. However, testing this software on a Sun minicomputer required changing this to 8.

The inverse Hankel transform in (11) is evaluated using the adaptive filter in function subroutine ZHANKS of Anderson (1979) in which the tolerance is initially set at 0.01 for a high rate of calculation. If the convolution diverges, the tolerance automatically decreases in succession by factors of 10 until convergence is achieved.

It has been shown by Asten (1987) that by not taking into account the entire transmitter waveform, the amplitude of the computed transient may be in error by 4 to more than 100 percent, depending upon the sample time and type of earth model. The greatest errors occur at sample times near the end of the transmitter off-time and for models with a conductive basement. The correction described by Asten has been incorporated in this computer program.

Resistivity

The Schlumberger resistivity array geometry is shown diagramatically in Figure 4. In a strict sense, the Schlumberger array is specific in that the AB, or current electrode separation distance is much greater than the MN, or potential electrode separation distance. In this dissertation, a less restrictive definition is adopted in which the array is a colinear array in which the outer two electrodes are the current sources and the inner two electrodes are the potential measuring points. This definition allows the Wenner array to be a special case. The forward solution used here assumes no restriction on the AB distance versus the MN distance.

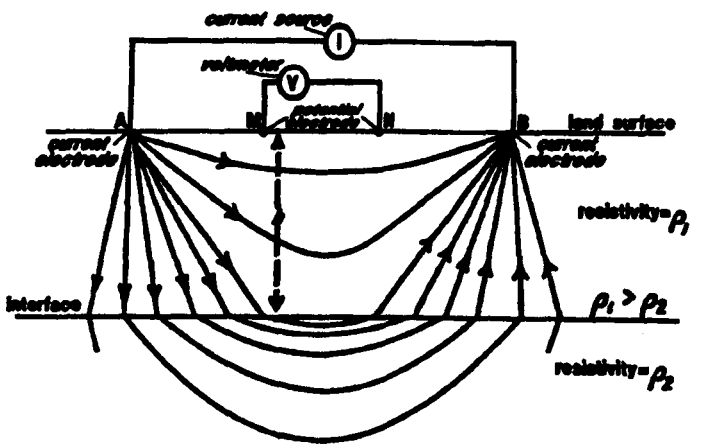

Figure 4. Schlumberger resistivity-array geometry showing lines of current flow in a two-layered earth with higher conductivity in the deeper layer.

Therefore, the apparent resistivity for this Schlumberger may is defined as

$$\rho_a = \frac{\pi \cdot MN \cdot V}{I}\left[\left(\frac{AB/2}{MN}\right)^2 - \frac{1}{4}\right] \tag{21}$$

where V is the voltage across the potential electrodes MN, and I is the current across the current electrodes AB. Note that if the Wenner array is being considered, the Wenner a-spacing = $MN = AB/3$, and (21) reduces to the familiar result

$$\rho_a^{(Wenner)} = \frac{\pi V}{I} \times a \tag{22}$$

From Sandberg (1979, p. 23) the potential over an N-layered earth at a distance r from a point current source is

$$V(r) = \frac{I\rho_1}{2\pi}\int_0^\infty R(\lambda) \cdot J_0(\lambda r) d\lambda \tag{23}$$

where

$$R(\lambda) = k_{12\cdots N} = \frac{1 - U_{12\cdots N} e^{-2\lambda d_1}}{1 + U_{12\cdots N} e^{-2\lambda d_1}} \tag{24}$$

$$U_{12\cdots N} = \frac{\rho_1 - \rho_2 k_{23\cdots N}}{\rho_1 + \rho_2 k_{23\cdots N}} \tag{25}$$

$$k_{(M-1)M\cdots N} = \frac{1 - U_{(M-1)M\cdots N} e^{-2\lambda d_{M-1}}}{1 + U_{(M-1)M\cdots N} e^{-2\lambda d_{M-1}}} \tag{26}$$

$$U_{(M-1)M\cdots N} = \frac{\rho_{M-1} - \rho_M k_{M(M+1)\cdots N}}{\rho_{M-1} + \rho_M k_{M(M+1)\cdots N}} \tag{27}$$

$$k_{(N-1)N} = \frac{1 - U_{(N-1)N} e^{-2\lambda d_{N-1}}}{1 + U_{(N-1)N} e^{-2\lambda d_{N-1}}} \tag{28}$$

and

$$U_{(N-1)N} = \frac{\rho_{N-1} - \rho_N}{\rho_{N-1} + \rho_N} \tag{29}$$

A similar development for 2 and 3-layer earth models is given in Wait (1982, p. 3 and 11, respectively). Following the development in Sandberg (1979, p. 15-16), substitute $\lambda = e^{-y}$ and $r = e^{x}$ in (23). The potential is then

$$V(r) = \frac{-I}{2\pi r} \int_{-\infty}^{\infty} R(y) e^{x-y} J_0(e^{x-y}) dy \tag{30}$$

which is in the form of a convolution integral

$$V(r) = \int_{-\infty}^{\infty} f(y) g(x-y) dy \tag{31}$$

where $R(y)$ can be considered as an input function $f(y)$, and $e^{x} J_0(e^{x})$ as the impulse response of a stationary filter. If $R(y)$ is evaluated at N discrete points, we can approximate $V(r)$ by a finite sum

$$V(r) \approx \frac{I}{2\pi r} \sum_{j=1}^{N} c_j R[\ln(r) - \eta_j] \tag{32}$$

where η_j are the abscissas of the stationary filter coefficients c_j. The algorithm used in the EINVRT6 program uses a 61-point filter to evaluate $V(r)$. The forward routine and filter were originally from an unpublished computer program written by Luiz Rijo which was later documented by Sandberg (1979). Rijo and others (1977) found that the 61-point filter provided adequate accuracy as long as the maximum

resistivity contrast did not exceed 200:1. This is an important restriction on interpretation using this software.

IP

Induced polarization (IP) data are collected in the Schlumberger array in the time domain. As successfully employed by Seara and Granda (1987), the apparent chargeability, m_a, as given by Roy and Poddar (1981) is

$$m_a = \frac{\rho_a(\rho_i + m_i\rho_i) - \rho_a(\rho_i)}{\rho_a(\rho_i)} \tag{33}$$

In this expression, m_a is the apparent chargeability due to altering the layer resistivities, ρ_i, by the layer chargeabilities, m_i, and then computing the difference with unaltered apparent resistivity, and finally normalizing, generating a percentage change. The IP equipment for which this software was designed is the Huntec M4 time-domain system, which is similar to the Phoenix V-5. Instrument readings from this system consist of the sum of 10 time windows of equal width following a specified delay. Experience gained from obtaining IP data while mapping hydrogeologic units for groundwater studies in New Jersey has shown that this reading (in milliseconds) has been found to range from about 1 to 25 when the gate widths and delay were both set to 100 ms. The chargeability m in (33) is not the same as the instrument reading fiom the Huntec receiver. To use Huntec instrument readings, a scale factor, chnorm, is introduced into (999) which becomes

$$m_a = \frac{\rho_a(\rho_i + chnorm \times m_i\rho_i) - \rho_a(\rho_i)}{chnorm \times \rho_a(\rho_i)} \tag{34}$$

In the program EINVRT6, subroutine SWITCH, *chnorm* is set to 0.01 which works well in ground-water applications. In addition, the inversion program operates in linear space for IP data compared to log space for the resistivity and TEM data, so a second scale factor is applied to the above apparent chargeability, $m_a/6$, so that the range of values is closer to the range of logarithmic apparent resistivities. The range of data values must be comparable to other types of data in simultaneous inversion so that one data set will not be emphasized over another.

INVERSE MODELING

Inverse modeling, or inversion, is the process by which adjustments to an earth model are made to improve the field versus model-computed data fit. The term normally refers to semi-automated methods where mathematical analysis (based on least squares or other criteria) rather than trial-and-error creates the parameter adjustments. Most electrical geophysical inverse models are nonlinear (meaning that the forward model is a nonlinear function of the parameters) so that the minimization is accomplished in steps, or iterations, each of which is a linearization of the problem over a small interval.

In this section, the inverse modeling process is examined by application of the EINVRT6 computer program. First, the inversion theory used in the modeling algorithm is presented. Next, the EINVRT6 computer program is presented.

THEORY

The Jupp-Vozoff algorithm

The inversion algorithm used in this software is that described by Jupp and Vozoff (1975). In particular, the application by Raiche and others (1985) which is restated and elaborated upon in Hohmann and Raiche (1988), employs simultaneous inverse modeling of Schlumberger resistivity and coincident loop TEM soundings. Although the software presented in this manual addresses resistivity, IP, and central loop TEM soundings, the same algorithm used by Raiche and others (1985) forms the framework for the inversion as used in the EINVRT6 computer program here. The following is a brief treatment of the method.

Let d be a vector of field-data values containing M observations. These are Schlumberger apparent resistivity values at particular current and potential electrode separations, IP chargeability measurements which are also obtained at these particular electrode separations, and/or TEM late time asymptotic apparent resistivities corresponding to particular sample times after transmitter-current shutoff.

Let x be a vector of layered-earth parameters containing N values corresponding to layer resistivities, chargeabilities, and thicknesses.

A forward problem generates model data at the same electrode separations and/or sample times after transmitter current shutoff as the field observations, as a function of the vector of parameters, x. Let $g(x)$ be that vector of model data, again containing M values. Therefore, g_i is the model-predicted data point corresponding to the field data value d_i.

The inverse problem is to determine values of x which are used to calculate the values of g so that they "match" the field observations d. This "match" corresponds to minimizing the Root Mean Squared (RMS) relative error between model-derived data and field data,

$$RMS = \left[\frac{1}{M} \sum_{i=1}^{M} \frac{(d_i - g_i)^2}{d_i^2} \right]^{1/2} \qquad (35)$$

Now it is possible to expand $g(x)$ about $\mathbf{x}$ in a Taylor expansion ignoring higher-order terms. Ignoring the higher-order terms amounts to assuming that the problem is linear. Then,

$$\left[g(x+\delta x)\right]_i = g_1(x) + \frac{\partial g_i}{\partial x_1}\delta x_1 + \frac{\partial g_i}{\partial x_2}\delta x_2 + \ldots + \frac{\partial g_i}{\partial x_N}\delta x_N \tag{36}$$

or

$$g(x+\delta x) = g(x) + \underline{J}\delta x \tag{37}$$

where

$$\left[\underline{J}\right]_{m,n} \equiv J_{mn} = \frac{\partial g_m}{\partial x_n} \tag{38}$$

In this development, **J** is the Jacobian matrix relating changes in the model data to changes in the parameters.

In solving the inverse problem an iterative scheme is used. It is assumed that the nonlinear problem is linear, and a correction to the current version of parameters is calculated. The parameters are modified and new model data are calculated and compared to the field data. This constitutes an iteration. Using the same notation and assuming that the problem is linear,

$$d = g(x) + \underline{J}\delta x \tag{39}$$

or

$$d - g(x) = \underline{J}\delta x \tag{40}$$

The parameter correction step is then

$$\delta x = \underline{J}^{+}\left[d - g(x)\right] \tag{41}$$

where J^{+} is a pseudoinverse of the Jacobian matrix **J**, and the updated parameter vector is given by

$$x^{new} = x^{old} + \delta x \tag{42}$$

Often in inversion algorithms iterations proceed until either 1) the error in **(35)** decreases below some predetermined value, 2) the new iteration does not decrease the error, or 3) the preset number of iterations is exceeded. In the EINVRT6 computer program, the program continues to iterate until the specified number of iterations in the input file has been satisfied, or the algorithm diverges (see section on input file under EINVRT6).

What now remains is to determine the pseudoinverse J^+ in **(41).** The matrix **J** is not a square matrix since it has dimensions M x ***N.*** The singular value decomposition (SVD) of ***J*** is calculated as

$$\underline{\underline{J}} = \underline{\underline{U}}\,\underline{\underline{S}}\underline{\underline{V}}^T \tag{43}$$

where U is an M x ***N*** matrix, ***S*** is an ***N*** x ***N*** diagonal **matrix,** and V is an N x ***N*** matrix. The matrices U and V are such that

$$\underline{\underline{U}}^T\underline{\underline{U}} = \underline{\underline{I}}_M \quad \text{and} \quad \underline{\underline{V}}^T\underline{\underline{V}} = \underline{\underline{I}}_N \tag{44}$$

where I_M and I_N are identity matrices of rank ***M*** and ***N,*** respectively. For convenience, the diagonal **S matrix** is defined to have elements

$$s_{jj} = s_j = \sqrt{\lambda_j / \lambda_1} \tag{45}$$

and

$$\lambda_1 \geq \lambda_2 \geq \ldots \geq \lambda_N \geq 0 \tag{46}$$

The λ_j values are eigenvalues of the matrix J^TJ. Therefore **(40)** becomes

$$d - g(x) = \sqrt{\lambda_1}\,\underline{\underline{U}}\,\underline{\underline{S}}\underline{\underline{V}}^T \delta x \tag{47}$$

At this point, define the eigenparameter vector

$$q = \underline{\underline{V}}^T x\,. \tag{48}$$

Then

$$\delta q = \underline{\underline{V}}^T \delta x \tag{49}$$

is the eigenparameter correction vector. Equation (47) is premultiplied on both sides by $\lambda_1^{-1/2} U^T (d - g)$,

$$r = \lambda_1^{-1/2} \underline{\underline{U}}^T [d - g(x)] . \tag{50}$$

Then,

$$r = \underline{\underline{S}} \delta q \tag{51}$$

or

$$\delta q_i = s_i^{-1} r_i \tag{52}$$

The eigenparameters and the V matrix are used in the resolution analysis described in the next section.

In general, the Jacobian matrix, J is ill-conditioned. A damping factor, t_i is incorporated into (52), so that

$$\delta q_i = \frac{t_i}{s_i} r_i , \tag{53}$$

with

$$t_i = \frac{s_i^{2k}}{s_i^{2k} + \mu^{2k}} . \tag{54}$$

The number, μ is called the relative singular value threshold, and k is the order of damping. In the computer program EINVRT6, a value $k = 2$ is used. The number, μ is varied for each iteration such that as the model fit improves, μ decreases. A smaller μ results in the incorporation of smaller eigenvalues into the process. This scheme of varying μ results in a more stable sequence of iterations. For TEM inversion in the program EINVRT6, the range of permissible values is $0.01 < \mu < 0.10$. The value of μ increases or decreases

(doubles or halves) depending upon the previous iteration's value (or the value specified in the input file), and upon whether the iteration decreases the squared error.

The concepts of important, unimportant, and irrelevant parameters must be discussed in this context. If a small change in the value of the parameter x_j results in a significant change in at least some of the model data g, then x_j is an important parameter. If a relatively large change in x_j results in only a minimal change in g, then x_j is termed an unimportant parameter. If a large change in x_j produces no effect in g, then x_j is an irrelevant parameter.

Therefore, if one of the x_j were irrelevant, then the jth column of the Jacobian, J in (38) would be zero, which in turn would produce a zero eigenvalue. If one of the x_j were unimportant, at least one of the eigenvalues would be very small. The modification of (52) to (53) serves to eliminate irrelevant parameters, and damps the oscillations produced by unimportant parameters in the iterative solution.

Parameter Resolution Statistics

It is possible to analyze the confidence of a particular model arrived at by inversion. Following Hohmann and Raiche (1988), one can determine the estimated standard error

$$\hat{\sigma} = \left[\frac{1}{M-N} \sum_{n=1}^{M} (D_n - G_n)^2 \right]^{1/2} \tag{55}$$

and the noise-to-signal ratio,

$$NSR = \frac{\hat{\sigma}}{\left[\frac{1}{N-1} \sum_{n=1}^{M} (G_n - \bar{G}_n)^2 \right]^{1/2}} \tag{56}$$

In these expressions D_n and G_n are scaled field data and model data values corresponding to unscaled values d_n and g_n. Scaling in the program EINVRT6 consists of the following: DC resistivity and TEM apparent resistivity data values are used in log space, whereas IP data is kept in linear space using a scaling factor of 1/6 for the chargeability values. A standard error of a few percent usually implies a good fit, whereas one greater than 20 percent implies problems with the inversion. Standard error in (55) is referred to as the *rcsq* parameter in the computer program EINVRT6 following the notation of Rijo and others (1977).

NSR is a measure of how well variations in the observed data are taken up by variations in the model data. A good inversion has an NSR of less than 2 percent. One greater than 10 percent would indicate an inappropriate model.

Confidence intervals for the layered earth parameters are calculated in the following manner. The Cramer-Rao multipliers δ_n are defined (Hohmann and Raiche, 1988, after Bard, 1974)

$$\beta_n = \left[\sum_{k=1}^{M} t_k (V_{nk} / S_k)^2 \right]^{1/2} \quad (57)$$

Inasmuch as the logarithms to the base 10 of the parameters are used in the program EINVRT6, the parameter confidence intervals are given by

$$p_n^{\pm} = p_n \times 10^{(\pm 1.96 \beta_n \sigma)} \quad (58)$$

where $p_n^{\pm}$ are the upper and lower bounds of a 95-percent confidence interval for the parameter p_n.

The V matrix is very useful in examining parameter resolution. From (48), $V_{i,j}$ is a measure of the relative contribution of physical parameter x_i to q_j. Each column of V corresponding to an eigenparameter q_j is a linear combination of physical parameters x_i. Any combination of x_i corresponding to a q_j with a damping factor (54) $t_j = 1$ will be well resolved, and combinations with $t_j << 1$ will be poorly resolved. Examples illustrating resolution for the coincident loop TEM - Schlumberger resistivity sounding case are discussed by Raiche and others (1985).

SOFTWARE

FORTRAN program ZONGE

This program substitutes for the data input part of EINVRT6 when data from the Zonge systems are to be modeled. The TEM output file from READZONG (see earlier section) is used, which is somewhat altered from the NJGS Standard TEM File Format. The output from this program is an input file which can be edited using an ascii text editor, and can then be run using the EINVRT6 inversion software.

FORTRAN program EINVRT6

This program was designed to individually or simultaneously invert resistivity, resistivity/IP, and TEM data for a horizontally stratified, or one-dimensional earth model.

Modes of operation.

The program is designed to operate, depending upon choice of option, in any of the following six modes:

1. TEM central loop induction configuration only
2. Schlumberger array resistivity only
3. Simultaneous Schlumberger resistivity and TEM
4. Simultaneous dipole-dipole resistivity and TEM
5. Simultaneous Schlumberger resistivity and IP
6. Simultaneous Schlumberger resistivity, IP, and TEM

Each of these modes has a characteristic graphics screen associated with the type of data to be depicted.

In addition, owing to the way that the resistivity forward solution is calculated, Wenner array resistivity (alone and with IP) data can be interpreted if the input data file is set up in the following way. The Wenner array data are put into the **NJGS** Standard Resistivity/IP Data File Format as described previously under field data reduction and storage. **But,** for the Wenner array, instead of an $AB/2$ distance use **1.5 x a ,** where a is the characteristic spacing for the distance between electrodes in the Wenner array. **And,** for the MN distance, use the a-spacing.

Input file.

Entry to the EINVRT6 program for the first time with a particular data set will mean that an input file is unavailable. This input file must be created prior to performing the inversion. Specifying that an input file is lacking causes prompts to be given through which an input file is created. This input file makes subsequent inversions easier in that program prompting is minimized, and changing program-control parameters and data can be accomplished by using a text editor, such as MS-DOS EDIT, the IBM Professional Editor, Wordstar (in the non-document mode), or other standard ASCII text editor.

The input files corresponding to differing modes of operation are fairly similar. A description of the input data lines is given next, along with the data format.

Line 1 output filename, and output plot filename
format(2a15)

Line 2 n,ic,icode,mr,mc,mt,ifwd,metric,igrf,iout
format(10i5)

n = total number of layered earth parameters (# resistivities + # chargeabilities + # thicknesses). The program will handle 15 layers, but the graphics screen will **only** accomodate **12.** If more than 12 layers are needed, do not use screen graphics.

ic = code for using thicknesses or depths
= **1** for thicknesses
= 2 for depths

icode = code for determining which problem is being solved (which mode of operation)
1 = **TEM** only
2 = Schlumberger resistivity only
3 = both **TEM** and Schlumberger resistivity
4 = TEM and dipoledipole resistivity
5 = Schlumberger resistivity and IP
6 = TEM, Schlumberger resistivity, and IP

mr = number of resistivity data points

mc = number of chargeability data points

mt = number of TEM data points

ifwd = maximum number of iterations to be performed
= 0 for forward calculation only
< 0 no iterations and also skip the forward calculation (used when a theoretical data set is being generated)

metric = 1 means thicknesses or depths will be in meters in the input file and the screen display
= 0 means thicknesses or depths will be in feet in the input file and the screen display.

igrf = 1 uses screen graphics (requires graphics driver)
= 0 echos selected portion of output file on screen (no graphics).
(default=1)

iout = 1-7 creates output data file (in NJGS Standard TEM Data File Format) From final model with corresponding time gates and name "einvrt5x.dat"
= 0 does not create output data file
(default=0)
>7 - [illegible] x 10

Line 3 deriv,ammu,khow
format(f10.4,f10.3,i10)

deriv = size of derivative increment in first forward difference approximation for calculating Jacobian matrix
(default=0.004)

ammu = starting value of μ in (54)
(default=0.01)

khow = 1 use RCSQ to monitor iterations
= 2 use 11 to monitor iterations
= 3 iterate anyway no matter what and hold ammu constant
= 4 if new RCSQ > old RCSQ then quit
(default=1)

Line 4 one,two,three,four,five,six
format(6f10.0)

Plot symbol numbers for the output plot file

one = Chargeability field data points
(default–2)

two = Chargeability calculated values
(default–3)

three = Schlumberger resistivity field-data points
(default=1)

four = TEM field-data points (default=4)

five = Schlumberger resistivity calculated values
(default–5)

six = TEM calculated values
(default=6)

Line 5 p0(i) layer resistivities
format(8f10.2)

Line 6 p0(i) layer chargeabilities (this line is omitted when IP is not being used [options 1-41)
format(8f10.2)

Line 7 p0(i) layer thicknesses
format(8f10.2)

Line 8 ipf(i), i = 1,n code for fixing of parameters
format(40i2)

ipf(i) = 1 hold parameter at its current value throughout inversion

ipf(i) = 0 allow parameter to vary

Next, several data lines corresponding to reduced data values follow. For resistivity/IP data lines:

ab2(i),amn(i),ai(i),v(i),rhoa(i),ch(i)
format(2f10.2,2f10.4,f10.1,f10.2)

ab2(i) = Schlumberger array AB/2 distance (m), or dipole-dipole n-value

amn(i) = Schlumberger array MN distance (m), or dipole-dipole a-spacing **(m)**

ai(i) = transmitter current reading (amperes)

v(i) = receiver voltage (volts)

rhoa(i) = calculated apparent resistivity [using (21) for Schlumberger array] (ohm-m)

ch(i) = measured apparent chargeability (ms), or 1 if no IP

For **TEM data** lines:

tt(i), temv(i), aba(i), ramp(i), al(i), area(I)
format(f15.4,e15.6,f5.0,e15.3,f5.0)

tt(i) = **TEM** sample time **(ms)**

temv(i) = TEM voltage in receiver coil divided by current at transmitter divided by coil effective area (μV/amp m^2)

aba(i) = key for particular transmitter **base** frequency and receiver coil effective area **(see** program **T47INPUT.BAS),** or for the Zonge systems this is the transmitter frequency (Hz)

ramp(i) = **TEM** current shutoff ramp duration (μs)

al(i) = transmitter loop side length (m)

area(i) = the receiver coil moment (m^2)

Output file of results.

The output file is designed so that if there is no graphics capability and this output is sent to the CRT screen, it is still possible to monitor the progress of the inversion.

The program title, date, beginning time, and input filename are output first. The initial guess results are then presented as a list of field data, theoretical data, and the percentage difference between the two for each data point. TEM data are presented as apparent resistivity using the asymptotic late time formula from (7). Following this, the standard error from (55) is calculated and displayed as *rcsq*, and the *l*1 norm is given. The *l*1 norm is the normalized sum of absolute value residuals, given by

$$l1 = \frac{1}{M}\sum_{n=1}^{M}|D_n - G_n| \tag{59}$$

using notation from the theory section under the INVERSE MODELING heading. In addition, the time to calculate the complete forward problem is given (in hours).

Next, the rows of the Jacobian matrix in (38) are presented. Each row consists of the following: the first 3 characters are RES, CHG, or TEM depending upon which data type the row represents, the next number is the iteration number, the next fraction is the current row number over the total number of rows for that particular data type (RES, CHG, or TEM), and the next number is the amount of time used to calculate that row (for RES and CHG this is in seconds, for TEM this is in hours). For a RES or CHG row, the next numbers are the Jacobian matrix values.

Following the Jacobian, the iteration number, current value of μ (ammu) in (54), and a list of eigenvalues for the Jacobian matrix are given. Parameter increments (in log_{10} space) are given, and the old-versus-new parameters are presented. Then, results of a forward calculation using the new parameters are shown as field-versus-theoretical data with the percentage difference.

If the new rcsq is lower than the previous one, a new Jacobian matrix is calculated. Otherwise, ammu is doubled and new parameters are again determined, followed by a forward calculation. This is repeated until either a new Jacobian matrix is calculated, the program satisfies the specified number of iterations and moves on to statistics, or ammu gets too large, resulting in a message that divergence has occurred.

A section on statistics is output next. The NSR from (56) is output followed by parameter confidence intervals calculated from (58). The V-matrix defined in (43) is output next, followed by the corresponding damping factors from (54).

Next, the final field-versus-model data are presented with the percentage difference, and relevant dependent parameters. Final layer parameters are listed next. The thickness (or depth-to-bottom) parameters have two columns; the first column is in meters, and the second, in feet.

Finally, the *rcsq* and *l1* values from the final parameters are listed, followed by the number of iterations completed, and the time of completion.

Output plot file.

A plot file of field-versus-model data is generated by EINVRT6 to display data fit. Field and model-derived TEM data are asymptotic late time apparent resistivity calculated using (7). If inversion of TEM data alone were performed, sample times would be in ms. If both resistivity and TEM data were being inverted, TEM sample times in the plot file would be scaled by a factor of 10 and the units would be in ms. If IP data were being inverted, the output plot file would contain field and theoretical chargeability data in the following form

$$IPvalue = 10^{(m_a/5)} \tag{60}$$

where m_a is the apparent chargeability (in ms).

This is done so that the entire plot file can be shown on a log-log plot in which the IP data are linear, with a scale of 5 ms per decade. This scale has been found to be useful for IP data collected for ground-water studies in New Jersey.

Graphics screens.

Different graphics screens are possible depending upon the choice of operation mode, parameterization (depths or thicknesses), and units (feet or meters).

On a color monitor, the calculated model response lines are in color to distinguish them from each other. The resistivity calculated line is drawn in white, the TEM calculated line is in green, and the IP calculated line is in red.

Data plotting area. Field and calculated data are plotted in the data plotting area. The range of field data is used to adjust the plot axes so that the data sets are centered in the plotting area. There are no checks on the data span, so that data can conceivably plot anywhere on the graphics screen if the span is great enough. DC resistivity and TEM apparent resistivity, electrode AB/2 distance, and TEM sample time are all plotted logarithmically in ohm-m, m, and ms respectively. IP apparent chargeability data are plotted on a linear scale in ms. One or two of these axes are omitted when run modes are selected which do not use these data types.

As model data are calculated, the results are plotted as straight-line segments in the color scheme explained above.

Bottom of screen. One line from the bottom on the left side is the name of the input data file. Along the bottom line to the left is the status line. The status line displays what operation is currently being performed in the program. The term "calc. forward" means that the forward solution given the current model is being calculated. The fraction directly after that displays the number of data values calculated over the total number.

The term "sys matrix" in the status line means that the Jacobian matrix is being computed. The fraction directly following is the number of rows of the matrix which are completed over the total number.

On the bottom line, in the center and to the right, is one of two messages. One message displayed is "forward elapsed time" and a clock is shown displaying the number of seconds, minutes, and hours that have elapsed while the forward routine calculates the initial guess response. The other message is "estim. completion" and a countdown clock is shown displaying an estimate of how much time remains to complete the current task shown in the status line.

At the bottom right, is the current value of mu (which is *ammu*, or μ) in (54). This value is updated depending on whether the inversion is converging or not.

Parameter area. Below the data plot key box, the iteration number is shown as a fraction over the total number of iterations to be performed. This is updated after new parameters have been obtained fiom a new system matrix.

Below the iteration number, the rcsq and *l*1 values fiom the forward calculation for the current parameters are shown. These are updated after completion of a complete forward calculation.

Below the *rcsq* and *l*1 values, the current parameters are listed. Layer resistivities in ohm-m are under the heading rho, and layer chargeabilities in msec are under the heading chg. Layer thicknesses are either in m or ft under the headings thk(m) or thk(ft). If depth-to-bottom parameters are used, these are either dpth(m) or dpth(ft). An asterisk (*) appears to the left of a parameter being inverted. If no asterisk appears, then that parameter is fixed in the inversion.

REFERENCES

Anderson, W. L., 1979, Numerical integration of related Hankel transforms of orders 0 and 1 by adaptive digital filtering: Geophysics, v. 44, p. 1287-1305.

Asten, M. W., 1987, Full transmitter waveform transient electromagnetic modeling and inversion for soundings over coal measures: Geophysics, v. 52, p. 279-288.

Bard, Y., 1974, Nonlinear parameter estimation: New York, Academic Press, 216 p.

Geonics Limited, 1988, GSPx7 transient EM data handling & modelling for Geonics' EM37 & PROTEM systems and IBM PC/XT MS-DOS 2.0 – December, 1988: Geonics Limited, Mississauga, Ontario, Canada, 64 p.

Gustafson, E., and McEuen, R., 1987, Minimizing interpretation ambiguities through joint inversion of surface electrical data: Ground Water Monitoring Review, v. 7, no. 4, p. 101-113.

Hohmann, G. W., and Raiche, A. P., 1988, Inversion of controlled-source electromagnetic data: In Electromagnetic Methods in Applied Geophysics, Volume I: Theory: Investigations in Geophysics, No. 3, M. N. Nabighian (ed.), Society of Exploration Geophysicists, p. 469-503.

Jupp, D. L. B., and Vozofff, K., 1975, Stable iterative methods for geophysical inversion: Geophys. J. Roy. Astr. Soc., v. 42, p. 957-976.

Kaufmann, A. A., and Keller, G. V., 1983, Frequency and transient soundings: Elsevier, Amsterdam, 685 p.

Knight, J. H., and Raiche, A. P., 1982, Transient electromagnetic calculations using the Gaver-Stehfest inverse Laplace transform method: Geophysics, v. 47, p. 47-50.

Meju, M. A., 1998, Short Note: A simple method of transient electromagnetic data analysis: Geophysics, vol. 63, no. 2, p. 405-410.

Raab, P. V., and Frischknecht, F. C., 1983, Desktop computer processing of coincident and central loop time domain electromagnetic data: U.S. Geol. Surv. Open-File Report 83-240, 43 p.

Raiche, A. P., 1984, The effect of ramp function turnoff on the TEM response of a layered ground: Exploration Geophysics, v. 15, p. 37-41.

Raiche, A. P., 1987, Transient electromagnetic field computations for polygonal loops on layered earths: Geophysics, v. 52, p. 785-793.

Raiche, A. P., Jupp, D. L. B., Rutter, H., and Vozoff, K., 1985, The joint use of coincident loop transient electromagnetic and Schlumberger sounding to resolve layered structures: Geophysics, v. 50, p. 1618-1627.

Rijo, L., Pelton, W. H., Feitosa, E. C., and Ward, S. H., 1977, Interpretation of apparent resistivity data from Apodi Valley, Rio Grande Do Norte, Brazil: Geophysics, v. 42, p. 811-822.

Roy, A., and Poddar, M., 1981, A simple derivation of Seigel's time domain induced polarization formula: Geophysical Prospecting, v. 29, p. 432-437.

Sandberg, S. K., 1979, Documentation and analysis of the Schlumberger interactive 1-D inversion program SLUMB: Univ. of Utah Dept. Geol. and Geophys. Report DOE/ET/27002-2, 84 p.

Sandberg, S. K., 1988, Microcomputer software for the processing and forward modeling of transient electromagnetic data taken in the central loop sounding configuration: New Jersey Geological Survey Open-File Report 88-1, 88p., 1 diskette.

Sandberg, S. K., 1990, Microcomputer software for individual or simultaneous inverse modeling of transient electromagnetic, resistivity, and induced polarization soundings: New Jersey Geological Survey Open-File Report OFR 90-1, 160 p., 2 diskettes.

Sandberg, S. K., 1993, Examples of resolution improvement in geoelectrical soundings applied to groundwater investigations: Geophysical Prospecting, v. 41, p. 207-227.

Seara, J. L., and Granda, A., 1987, Interpretation of I.P. time domain/resistivity soundings for delineating sea-water intrusions in some coastal areas of the northeast of Spain: Geoexploration, v. 24, p. 153-167.

Spies, B. R., and Eggers, D. E., 1986, The use and misuse of apparent resistivity in electromagnetic methods: Geophysics, v. 51, p. 1462-1471.

Vozoff, K., and Jupp, D. L. B., 1975, Joint inversion of geophysical data: Geophys. J. Roy. Astr. Soc., v. 42, p. 977-991.

Wait, J. R., 1982, Geo-electromagnetism: New York, Academic Press, 268 p.

Walker, G. G., and Kawasaki, K., 1988, Observation of double sign reversals in trannsient electromagnetic central induction soundings: Geoexploration, v. 25, p. 245-254.

Appendix 2

FACSIMILE COVER SHEET

TO: DAVID FARRELL

CNWRA

FAX #: 210 522 5155

FROM: STEWART SANDBERG

GEOPHYSICAL SOLUTIONS

FAX #: 207 780 5167

DATE: JUNE 9, 1999

Number of Pages (including cover sheet) ~~44~~ 22

MESSAGE: Fieldbook PAGES ~~2-23 24-43~~ ~~27~~ 2-43

RECEIVED
JUN 9

2 544712E 4059219N Jan 15, 1999
Next to cinder cone Overcast (19?? Flows)

AB/2	MN	I	V	CHARGE	ρa
2.08m	1.0m	16mA	1494mV	1.246	1196.
2.5	1.0m	~~14.7~~	927	1.469	1189
3.16	1.0	.025A	823	2.089	1007
4	1.0	.020	311.8	2.092	771
5	1.0	.040	303.99	2.674	59.11
6.31	1.0	.040	135.5	2.19	421.1
8	1.0	.032	48.6	2.90	304
10	1.0	.036	27.4	2.95	283
12.6	1.0	.03?	16.94	2.65	222
~~15.8~~	1.0	.042	10.9	2.69	203.5
~~20.0~~	~~1.0~~	~~.026~~		2.15	
20.0	1.0	.027	4.64	~~2165~~	2165
20.0	3.0	.029	15.59	2.385	233.9
25	3.0	.028	10.03	2.163	~~284~~
31.6	3.0	.030	7.27	2.14	253
40	3.0	.058	8.93	2.4	258
40.0	~~7.4~~	.058	20.23	1.97	235
50.0	7.4	.062	14.73	2.142	251
63.1	7.4	.031	5.18	1.89	281
80.0	7.4	.062	5.3	2.06	231
100.0	7.4	.067	3.149	3.75	~~195~~
~~186.0~~	7.4	.065	1.303	NJ	135
126.0	17.1 ~~8.55~~	.066	3.272	1.9	145
~~126.0~~		.066	3.29		1116

1/15/99

8/24/2000

AB/2	MN	I	V	Charge	ρa
158	~~8.55~~	.070	1.37	3.38	89
200	~~8.55~~	.055	.403	10.51	54
250	~~8.55~~	.057	.189	8.23	38
268	8.55	058	.166	14.0	38

cross-spread (E-W)

AB/2	MN	I	V	CH	ρa
1.58	0.80	.010	2046	1.256	878
2.5	0.80	.010	579	1.682	639
4.0	0.80	.010	150	2.378	933
6.31	0.8	.010	28.5	2.989	444
10.0	0.8/4	.035	21.8	2.753	344
15.8	0.8/4	.055	~~25.6~~	2.51	205
15.8	80/4.0	.055	119.3	260	199
25.0	8/4.0	.054	50.9	2.43	227
40.0	8.0/4.0	.030	11.65	2.55	241
63.1	8.0	.030	4.68	1.54	243
100	8.0/4	.038	1.[illegible] 1.54	1.9	158

D.A.T.
8/24/2000

1/15/99

$$\rho_a = \left[\left(\frac{AB/2}{MN}\right)^2 - \frac{1}{4}\right] \pi MN \frac{V}{I}$$

6 SAT. JAN 16, 1999

TEM at IP site near Cinder cone

Coordinates:

(1) 544700E
4059215N

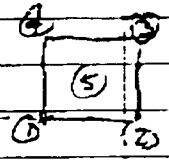

544526E (2)
4058971N

(D.A.H. 8/24/2000)

5448[53]E (3)
4058740N

545027E (4)
4058984N

327E
231

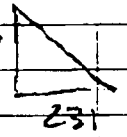

106929 +
53361
160290

1/16/99

7

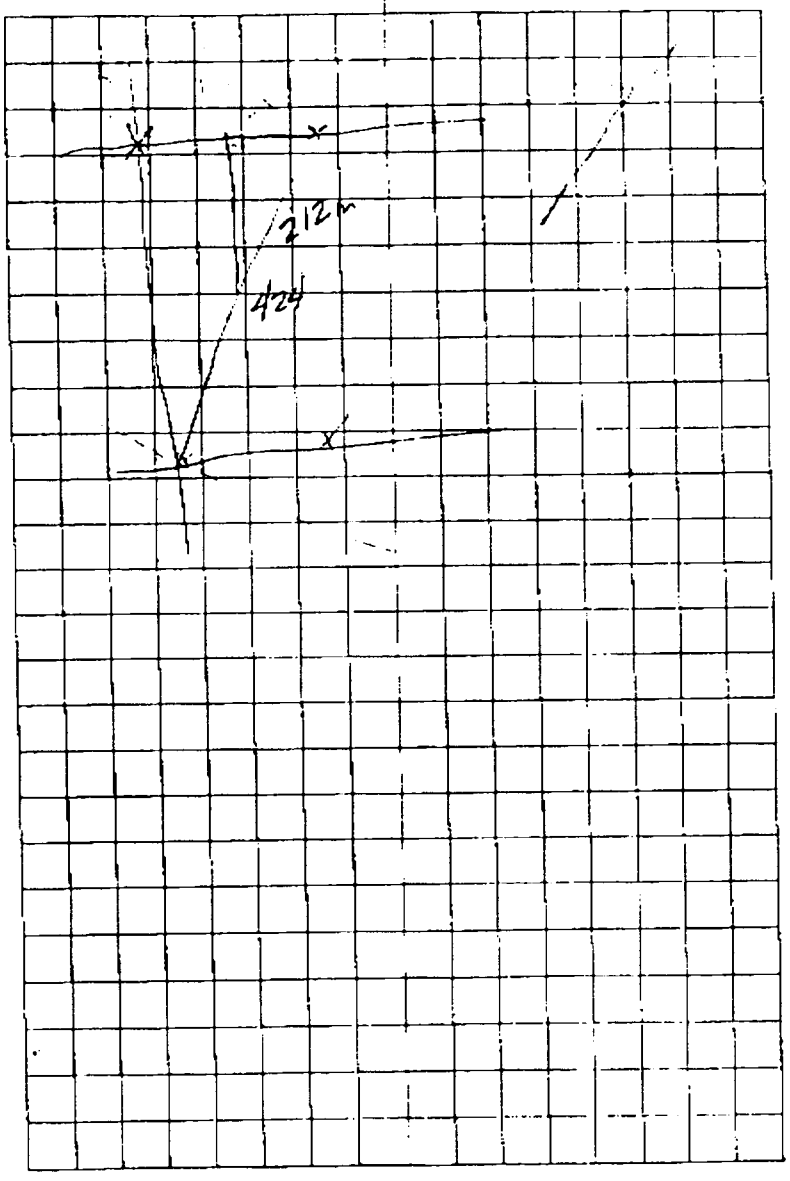

Loop dimension 300m

Current = 5A (freq LO)

T/O time = 65 μs (freq HI)

9E LO

HI

I = 11A

T/O time 140 μs

Rec 2258 Line IN LO

STATION 13E

SOUNDING 2 2:51pm

Line IN STA 14E

LOW POWER Current = 5A LOW FREQ

T/O time = 70 μs 2260 NO GOOD

HIGH FREQ

2261

LOW FREQ

2262

17E HIGH FREQ 2263

NO GOOD 18E MED FREQ 2264

~~HIGH POWER~~

T/O = 130

CURRENT = 11 19E LOW FREQ 2266

NO GOOD

1/16/99

TEM 3 site, 1/17/99

Next to drilling

300m Loop

0IN I = 5A LOW FREQ LOW POWER

20E T/O = 70 μs Noise in last 5 gates

GAIN 3

21E GAIN 4

1 -.602E3

2 -.429E3

22E GAIN 5 -.342 E3 (primary)

1 -.601E3

2 -.426E3

8/24/2008

23E GAIN 6 -.331E3

1 -.597E3

2 -.426E3

24E GAIN 7 -.342E3

1 -.598E3

2 -.426E3

1/17/99

25E HIGH FREQ GAIN 7
1 -.196E5 -.345E5
2 -.190E5

GAIN 5
26E
1 -.254E5 -.342E5
2 -.204E5

GAIN 4
27E
1 -.255E5 -.342E5
☆ 2 -.205E5

40m Tx Loop TEM3A
28E T/O = 50 FREQ = HI POWER = LOW
I = 23A GAIN = 1
29E REPEAT

30E USING REFERENCE CABLE

11:15am Using V-5 and motor generator
doesn't work
V-5 and TEM 47 - doesn't work

1/17/99 [illegible]

PROTEM RECEIVER
31E 30HZ TEM47 Transmitter
32E 7.5HZ
33E 285 HZ gain 2
34E gain 1
35E repeat gain 1

3L.dat
3H.dat } 300m loop
347H.dat
347V.dat } 40m loop
347U.dat

1/17/99 [illegible]

1/17.99 IP Sounding near drill rig

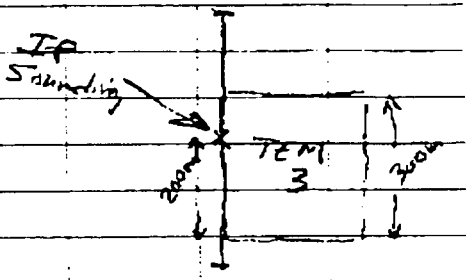

1256

AB/2	MN/2	I	V	ρa	Chargeability
2.0	.4	.030A	1370mv	687	2.816
2.5	.4	.030	789	629	3.271
2.5	.4	.030	767	611.7	3.224
3.16	.4	.030	430.7	554	3.386
4.0	.4	.030	212	440	3.638
5.0	.4	.040	136.6	333	3.854
6.31	.4	.040	66.7	259.7	3.799
8.0	.4	.090	75.9	211.5	3.396
10.0	.4	.225	108.	188.5	3.029
12.6	.4	.215	66	191.4	2.788
15.8	.4	.170	34.32	197.9	2.604
15.8	2.5	.170	208	187.8	247
20.0	2.5	.210	157	186	2.336
25.0	2.5	.145	71.3	191	2.136
31.6	2.5	.225	68.96	191	2.04

1/17/99

14

AB/2	MN/2	I	V	ρa	Ch
40	2.5	.16	29.3	183	1.919
50	2.5	.19	21.78	179	1.808
50	8.0	.19	70.39	177	1.74
63.1	8.0	.19	41.022	167	1.705
80	8.0	.19	22.86	149	1.75
100	8.0	.22	15.33	136	1.759
126	8.0	.21	8.2	121	2.249
158	8.0	.20	4.01	98	3.31
200	8.0	.16	1.58	77	3.63
250	8.0	.17	0.793	57.3	6.07
250	15.8	.17	.686	23.27	-24 BD
316	15.8	.320	1.995	46.8	6.415

1/17/99

15

Antarctica reference

Behrendt Geology 1994

V22 P.527

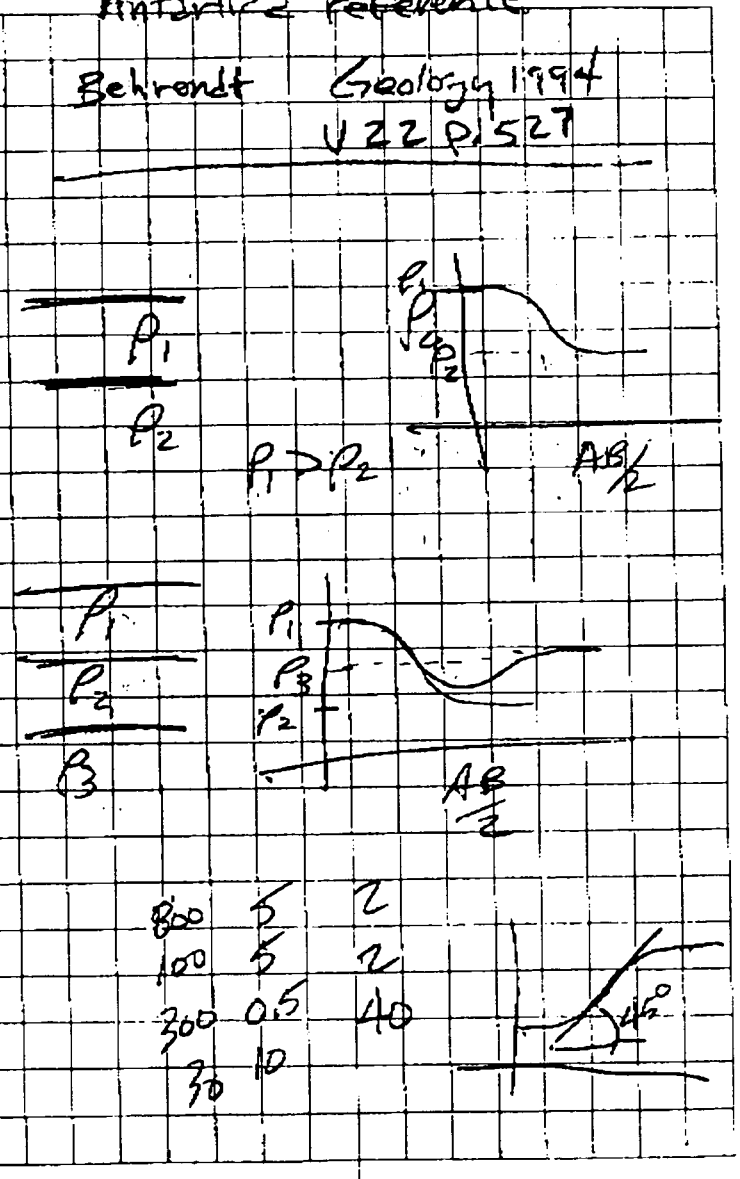

modeling

347u.dat

3H.dat

3L.dat

97 96 10 29

59 58 16 7

52 100 68 10

11 14

Monday JAN 18, 1999

TEM 4 40m Loop

Line IN STA 36E 285HZ

37E repeat

38E 75 HZ gain 1

39E repeat gain 2

40E repeat gain 3

41E 30Hz gain 4

42E repeat gain 5

near middle of nowhere, flat area, excavated hole

300m Loop

TEM 5

43E Low Freq gain 3

current 5A

T/O Time 73 70 μs

44E repeat

45E Hi freq Low Power gain 1

46E Hi repeat gain 3

47E MED freq gain 3

doesn't work

11:08 am

1/18/99

TEM 6

I = 5A

T/O = 70μs

48E LOW F GAIN = 1

49E LOW F GAIN = 3

50E HIGH F GAIN = 3

51E HIGH F GAIN = 1

HIGH POWER

I = 10.75 A

T/O = 130μs

52E LOW F GAIN = 1

BAD DATA

53E LOW F GAIN 7

BAD DATA

seems lost sync.

Low Power

54E LOW F GAIN 7

55E LOW F GAIN 1

1/18/99

18

TEM7 along phone cable road N 20 mW near junction 30 Ohm

IN	I = 5A	Low Power	300m Loop
	T/O =		
56E	Low freq	gain = 1	
57E	"	gain = 3	
58E	"	gain = 5	
59E	high freq	gain = 1	
60E	"	gain = 2	
61E	Low freq	gain 2	

BAD DATA — Lost Sync?

1/18/99

19

1/19/99

ON TEST SITE ref cable

40m loop TEM8 I = 3.0A

→ 62E	30Hz	GAIN2	Low F coil
63E	repeat		
64E	30Hz	GAIN2	High F coil
65E	"	GAIN4	"
→ 66E	"	GAIN6	
67E	75Hz	GAIN2	
→ 68E	"	GAIN5	
69E	285Hz	GAIN1	
70E	↓	GAIN3	
71E	↓	GAIN2	
→ 72E	repeat	GAIN 2	
73E		GAIN1	I = 2.89A

I = 2.0A

74E	285	GAIN1	

I = 4.0A

75E	285	GAIN1	11:53AM

1/19/99

TEM 9 Next to Wash

300m Loop
I = 5Amps
T/o = 70μs

76E	LOW F	GAIN 3
77E	repeat	
78E	LOW	GAIN 6
79E	LOW	GAIN 7
80E	HIGH F	GAIN 1
81E	repeat	
82E	HIGH F	GAIN 3

40m loop TEM 10 (DAH. 8/24/2000)
I = ~~3A~~ 4A
T/o = 2.5μs

83E	LOW F (30Hz)	Low F coil gain 3
84E	repeat	

I = 3A High F coil

85E	30Hz	gain 3
86E	75Hz	gain 2
87E	repeat	
88E	285Hz	gain
89E	"	gain 2

1/19/99

90E	285	gain 3
91E	285	gain 1

3:56pm

TEM 11 IN THE WASH (40mile wash)
4A 40m Loop

92E	30Hz	Gain 2
93E	30	Gain 4
→ 94E	30	Gain 7
95E	75Hz	Gain 2
→ 96E	75	Gain 4
97E	repeat	4
→ 98E	285Hz	GAIN 1
99E	repeat	
100E	285	GAIN 3
101E	285	GAIN 2

4:22pm

1/19/99

1/20/99

Test site
Near Busted Butte
TEM12

LowF Low Power 300m loop along road 2nd south
T/0 = 70μs
I = 5A

103E	LowF	GAIN4	
104E		GAIN7	
⊖ 105E	repeat		
106E	HighF	GAIN1	
⊖ 107E	repeat		
108E	HIGH	GAIN3	
109E	repeat		
		TEM13	
40m	loop	4.0 Amp	
110E	30 Hz	GAIN3	LOW F coil
⊖ 111E	30Hz	GAIN5	"
112E	30Hz	GAIN2	HIGH F COIL
113E	"	GAIN5	
114E	"	GAIN7	
⊖ 115E	75Hz	GAIN3	
116E	"	GAIN1	
117E	285Hz	GAIN1	
- 118E	repeat		
119E	285	GAIN2	
120E	285	GAIN	

1/20/99

TEM14
4.0A

121E	30Hz	GAIN 3
- 122E	"	7
- 123E	75Hz	3
- 124E	285Hz	1
125E	repeat	

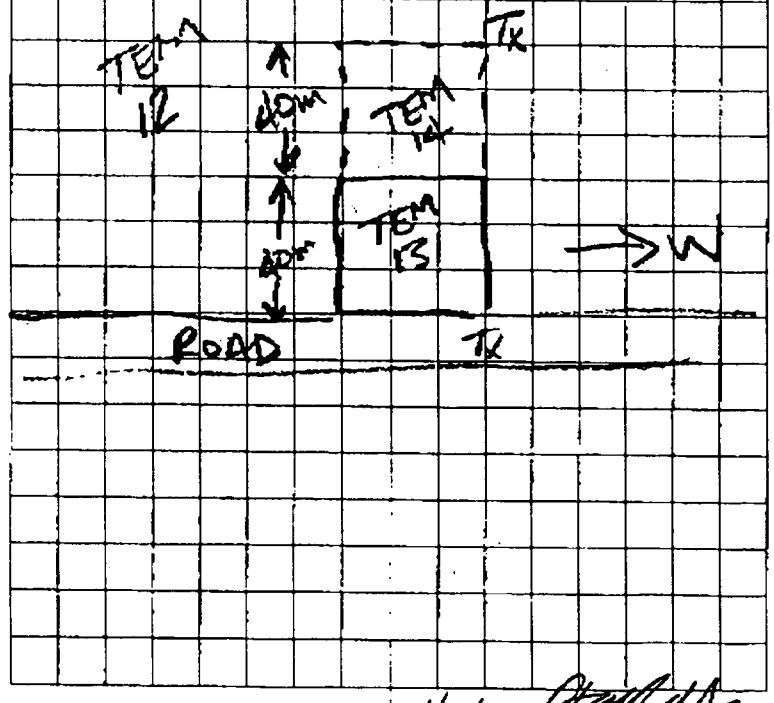

1/20/99

IP-3 @ TEM 12

1:27 1/20/99

AB/2	MN/2	I	V	ρ_a	Chg.
1.58	.4	.025	717.3	279.55	1731
2.0	.4	.025	320.7	193.9	2.467
2.5	.4	.025	188.8	180.0	2.933
3.16	.4	.036	154.5	165.61	3.209
4.00	.4	.060	149.89	155.4	3.304
5.00	.4	.065	95.34	143.11	3.218
6.31	.4	.065	57.98	138.6	2.907
8.0	.4	.10	58.1	146.4	2.926
10.0	.4	.10	39.3	156.8	2.874
12.6	.4	.10	25.26	157.4	2.561
[illegible]	3.16	.10	217.5	160.8	2.851
15.8	3.16	.09	129.8	169.53	2.463
20.0	3.16	.12	119.8	193.59	2.199
25.0	3.16	.12	86.44	220.3	1.849
31.6	3.16	.12	59.30	242.9	1.779
40.0	3.16	.13	38.895	257.73	1.947
50.0	3.16	.125	26.45	262.1	1.953
63.1	3.16	.08	11.56	285.3	2.017
63.1	6.31	.095	25.43	263.5	1.9435
80.0	6.31	.100	17.6	279.75	1.658
100.0	6.31	.200	21.319	264.6	1.655
126.0	6.31	.14	9.75	274.5	1.703
126.0	15.8	.14	24.47	271.7	2.188
158.0	15.8	.14	16.17	283.9	2275

1/20/99

26 IP-3 3:09

AB/2	MN/2	I	V	ρa	Ch.
200	15.8	.360	~~22.52~~	~~207.5~~	2.633
~~250~~	15.8	~~.20.25~~	9.612	~~303~~	3.02
200	15.8	.24	17.37	285.15	2.442
250	15.8	.25	12.87	3187	2.776
316	15.8	.35	13.735	388	~~9.450~~

TEM15

T/o = 70ms 300m Loop
I = 5A

126E 3Hz (low) GAIN
127E GAIN 7
-128E GAIN 5
129E repeat
30 Hz (HIGH) GAIN 1
131E HIGH F GAIN 1
-132E repeat
133E GAIN 2

130E BAD dipole switch Tx to 30

1/20/99

8 - ones
3 - threes
4 - fives

617	.39	.52
134	3.2	6.8
304	1.3	56
73	2	80
1000	5	80
30	5	230
900	5	

Thur. 1/21/99

Walk 1 ~ 1 km across from TEM15

TEM16 300m loop

T/O = 70

LINE IN

I = 5

134E	low f	gain1
135E	low f	gain7
136E	repeat	
137E	repeat	
139E	Hi freq 30Hz	gain1
139E	repeat	
140E	HI	gain2

TEM17 T/O = 54 μs

142E	HI	GAIN1	I = 22.5A
143E	HI	repeat	50m Loop
144E		repeat	40

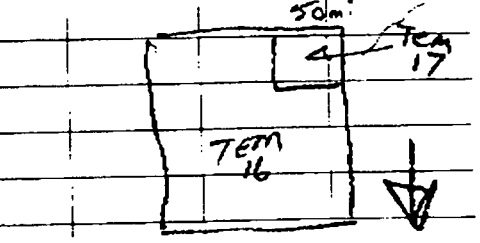

D.A.F. 8/24/2000

1/21/99

67
36
27
27
30

3
3
4

175 ft =
305
875
5256
53.3

TEM 18 1 km S/W of TEM 16

300m loop

146E	Lo freq	GAIN1	T/O = 70 ms
147E		GAIN7	I = 5.0A
148E	repeat	GAIN7	
149E	repeat	GAIN7	
150E	Hi Freq	gain 1	
151E	repeat		
152E	Hi	gain2	

TEM 19 T/O = 54

40m loop I = 22.5

153E	Hi	gain1
154E	repeat	
155E	Hi	gain2

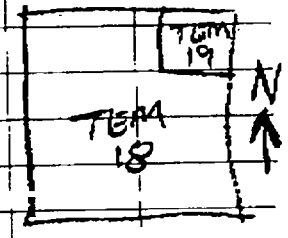

1/21/99

TEST SITE

FRI 1/22/99

TEM20
I = 5A
T_b = 70μs
157E high gain
158E " gain7
159E " gain5
160E " gain7
161E high gain ← BAD
162E " gain
165E repeat

300m loop
found single strand of wire crossing East portion of loop
Loop already laid out and will read it anyway
wire trends N13°E

40m loop
TEM21
I = 4A

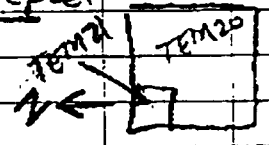

cut the wire to exactly 40m
16.8m ← cut off on 2 side.
switch = 40m

HI GAIN5 164E
I = 3A HI GAIN5 165E
VH GAIN2 166E
repeat 167E
– UH GAIN1 168E
I = 2A
– UH GAIN1 169E
– UH GAIN1 170E
I = 1A UH " 171E
– UH " 172E
I = 2A HI " 173E
HI GAIN7 174E
UH GAIN1 175E

switch ≥ 40m
switch = 40m
forgot to set I = 1A in header

1/22/99 1:56pm

TEM22 300m W of TEM21
40m
I = 2A
176E HI(30HZ) GAIN=7
177E repeat
178E VH GAIN3
179E VH repeat
180E UH GAIN1
181E UH GAIN3
182E UH GAIN1

TEM23 300m W of TEM22
I = 2
183E HI GAIN7
184E HI GAIN5
185E VH GAIN3
186E repeat
187E UH GAIN1
188E repeat

TEM24 300m W of TEM23
Lost pencil – no notes

1/22/99

TEM25 300m E of TEM20?

202E	HI	GAIN7
	HI	GAIN5
	VH	GAIN5
203E	VH	repeat
204E	UH	GAIN1
205E	repeat	
206E	UH	GAIN3
207E	repeat	

TEM26 next to wash 2A = I

208E	HI	GAIN7
209E	HI	repeat
210E	VH	GAIN5
211		
212E	UH	GAIN1
213E	repeat	
214E	UH	GAIN2

4:17pm

1/22/99

Amargosa Valley SAT. 1/23/99

TEM27 300m loop

I = 5.0A
T_0 = 70μs

215E	LO	GAIN7	
- 216E	repeat		
217E	HI	GAIN3	
- 218E	HI	GAIN3	repeat

TEM28 40m loop I = 2.0A
T_0 = 2.5μs

219E	HI	GAIN5	
- 220E	HI	GAIN7	
221E	repeat		
222E	VH	5	
- 223E	repeat		
- 224E	VH	GAIN2	
225E	repeat		

1/23/99

TEM 29

Center at 4055732 N
545100 E
780 elev.

I = 4 3/4 Amp
T/O = 65 as 30m loop
(Diff. 8/24/2000)

226E LO gain=7
227E repeat
228E GARBAGE gain=5
229E HI gain 5
230E repeat

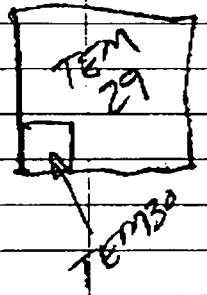

TEM 30 40m loop

231E HI gain7
232E repeat
233E VH gain5
234E repeat
235E UH gain2
236E repeat
237E repeat + sat 1st 2 chimes?
238E UH gain1

1/23/99

1-23-99 IP-4 (NW corner of TEM29)

AB/2	MN/2	I	V	ρa	Chi
2.0	.4	.03	1556	782	2.493
2.5	.4	.03	936.6	746.7	2.881
3.16	.4	.03	487.8	627.8	3.254
4.0	.4	.03	240.8	499	3.561
5.0	.4	.03	120.7	392.8	3.804
6.31	.4	.03	59.11	306.9	3.781
8.0	.4	.05	45.56	228.7	3.782
10.	.4	.05	23.74	186.3	2.826
12.6	.4	.05	13.83	172.48	2.791
12.6	3.16	.05	123.75	1548.78	2.776 → File has MN/2 of .4 really 3.16
15.8	3.16	.07	101.25	172	1.988 → 1.946
20.0	3.16	.07	62.07	169.7	1.912
25.0	3.16	.06	34.27	174.61	1.541
31.6	3.16	.06	21.15	171.09	1.596
40.0	3.16	.05	11.39	177.79	1.258
50.0	3.16	.075	9.85	160.5	1.392 → 1.516
63.1	3.16	.10	8.0	157.6	1.543 → 1.826 → 1.444
~~63.1~~	~~6.31~~	~~.105~~	~~15.1~~	~~140.96~~	Bad IP
63.1	6.31	.105	15.0	140.8	1.40 DAT-8/24/2000

1/23/99

42

SUN. JAN 24, 1999

TEM31 Amargosa Valley, SE of TEM 29

300m loop (15th one)

I = 4.75A

$T_{1/2}$ = 68 μs

239E	LO 3Hz	GAIN7
240E	repeat	
241E	LO	GAIN5
242E	HI	GAIN3
243E	repeat	

TEM32 40m loop

244E	HI	gain5
245E	HI	gain7
246E	repeat	
247E	VH	gain5
248E	repeat	
249E	UH	gain1
250E	repeat	

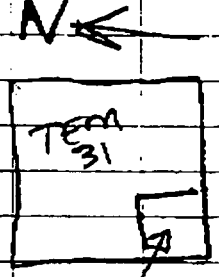

1/24/99

43

TEM33

300m loop

I = 4.8A

$T_{1/2}$ = 68 μs

251E	GAIN7	
252E	repeat	
253E	repeat	
254E	HI	GAIN3
255E	repeat	

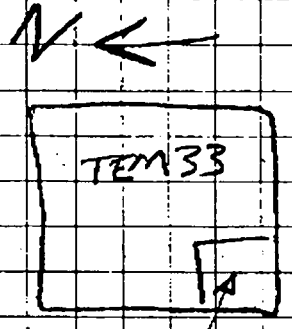

TEM34

40m loop

256E	GAIN7	HI
257E	repeat	
258E	repeat	
259E	GAIN3	VH
260E	repeat	
261E	GAIN1	UH
262E	repeat	

1/24/99

Appendix 3

INTERIM REPORT

GEOPHYSICAL SURVEY AT FORTYMILE WASH, YUCCA MOUNTAIN, NEVADA

February 10, 1999

Prepared by:

Geophysical Solutions

Geophysical Contracting & Consulting
22 Crescent View Avenue
Cape Elizabeth, Maine 04107
(267) 780-5154 e-mail: geophysh@aol.com
http://members.aol.com/geophysh/index.html

Stewart K. Sandberg, Ph.D., P.G.
Project Lead

Prepared for:

Center for Nuclear Waste
Regulatory Analyses
6220 Culebra Rd., Bldg. 189
San Antonio, TX 78238

Subcontract No. 9899052VE

I. INTRODUCTION

CNWRA completed a preliminary data collection phase in which TEM data from 13 sites were obtained using the Zonge equipment with 60 and 200 meter transmitter loops at each site. A preliminary hydrogeological model was produced with boundaries inferred from the geoelectrical model resulting from the TEM interpretations. Hydrogeological features of continued interest include:

1. Depth to the top of the water table aquifer,
2. Thickness of the unconsolidated portion of this aquifer (depth to bedrock),
3. The location where the water table transfers from the bedrock aquifer to the unconsolidated aquifer, and
4. The geometry of a bedrock horst and graben structure interpreted from the preliminary TEM data and subsequently identified in gravity data. This structure appears to be capable of significantly altering the groundwater flow velocity (magnitude and direction) directly down gradient from the proposed high-level radioactive waste repository at Yucca Mountain.

This work includes the collection and interpretation of additional TEM sites, resistivity soundings, and IP soundings to further delineate the four hydrogeological features identified above, expanding upon data obtained in the prelimary data collection phase. This report is an interim report describing what fieldwork was accomplished, and some preliminary data analysis.

II. DATA COLLECTION

Data collection occurred during January 15-24, 1999. During that period, 35 central-loop TEM soundings were collected, along with 4 Schlumberger-array resistivity/IP soundings. Of the 35 TEM soundings, 16 were collected using 300 m square transmitter loops, and 19 were collected using 40 m transmitter loops. Sounding numbers and locations are shown in Figure 1. Also shown for location purposes in the figure are the 4 wells: 5-12, JF-3, the Cind-R-Lite well, and Amargosa Town C. Geophysical sounding and transmitter loop locations shown were determined based on GPS data obtained during the data collection period.

TEM data were collected using the Geonics PROTEM digital receiver. The transmitter used for the 300 m loops was the Geonics EM-57 transmitter, using a portable Honda 1000 W gasoline motor generator. Both the PROTEM and EM-57 instruments were rented from TerraPlus in Denver, Colorado. For 40 m loops, the Geonics TEM-47 transmitter was used. Resistivity and induced polarization (IP) data were collected using the Phoenix V-5 receiver, and the Phoenix T-3 transmitter. The TEM-47, V-5, and T-3 instruments were on temporary loan from the University of Southern Maine.

III. PRELIMINARY DATA ANALYSIS

Data handling and analysis, both in the field and subsequently, was done using software available from GEOPHYSICAL SOLUTIONS. Specific computer programs include **READ,** SLUMBER, RAMPRES3, and EINVRT6, version 6.0, dated August 7, 1998. The PROTEM digital receiver sample time gates needed to be incorporated, which are substantially different from the PROTEM analog receiver sample time gates provided in the basic software. These newer time gates were obtained from a data file provided by

TerraPlus along with the PROTEM receiver rental. All preliminary data analysis which took place in the field used the incorrect time gates. All subsequent analysis will incorporate the correct time gates.

Apparent resistivity versus sample time for sounding TEM-1 (located in Figure 1) is shown in Figure 2. The correct time gates have been used, and the high quality of data is illustrated by the smooth curves, and convergence of curves at early 3 Hz (tem 1L) time gates with those at intermediate times from the 30 Hz dataset (tem 1H). Late time data with $t > 0.01$ s are in the background noise.

Figure 3 shows field data from TEM-1 and IP-1, along with data generated from a least-squares best fit model incorporating all four datasets (TEM-1L, TEM-1H, IP, and resistivity), illustrating the data fit. The 5-layer model produced is shown in Figure **4,** along with the water level elevation for the nearby Cind-R-Lite well (Figure 1). **A** discrepancy of 40 m exists between the 17 ohm-m bottom layer, and the water table elevation in the Cind-R-Lite well. Using the previously determined notion that a conductive layer at depth would likely correspond to the saturated zone below the water table, one possible interpretation is that Layer 5, at 770.2 m elevation, is a perched water table. Various attempts to model a layer at about 730 m elevation failed, indicating that there is no information in the data acquired concerning a geoelectrical boundary at that elevation.

Preliminary modeling of other soundings during the data collection period has indicated that conductive layers are detected at depths correlating generally with the water table. These preliminary results will not be presented here, since the TEM sample times were incorrect. They will be remodeled using the corrected sample times and presented in the near future.

IV. FURTHER WORK

The analysis of all soundings collected will continue, with results to be presented in a subsequent report.

V. STATEMENT

The Subcontractor, Geophysical Solutions, hereby certifies that, to the best of its knowledge and belief, the technical data delivered herewith under Subcontract No. 9899052VE is complete, accurate, and complies with all requirements of the Subcontract.

_____ _____

Date Name and Title of Certifying Official

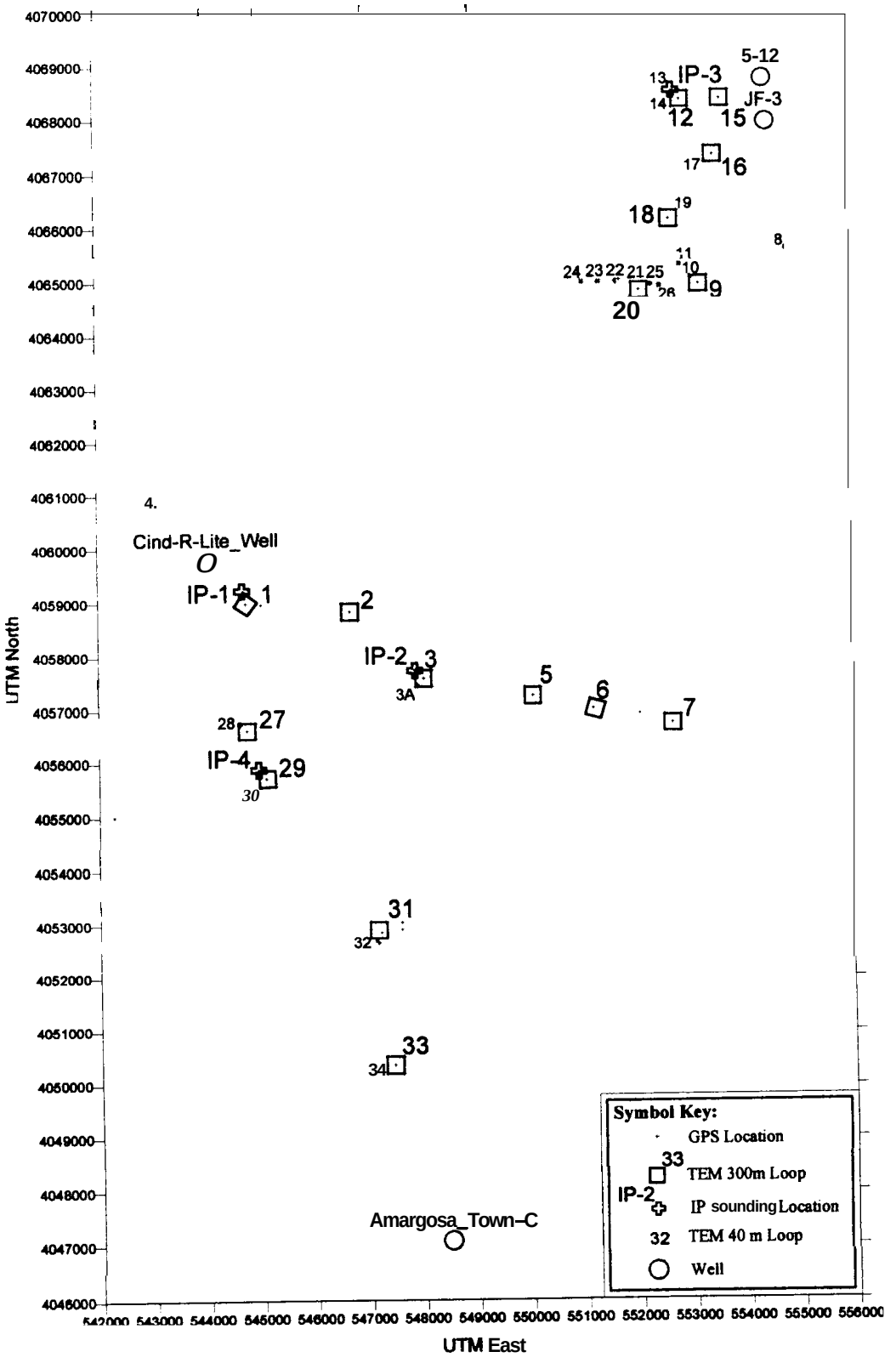

Figure 1. Geophysical data locations. 35 TEM central-loop soundings and 4 Schlumberger-array resistivity/IP soundings are shown.

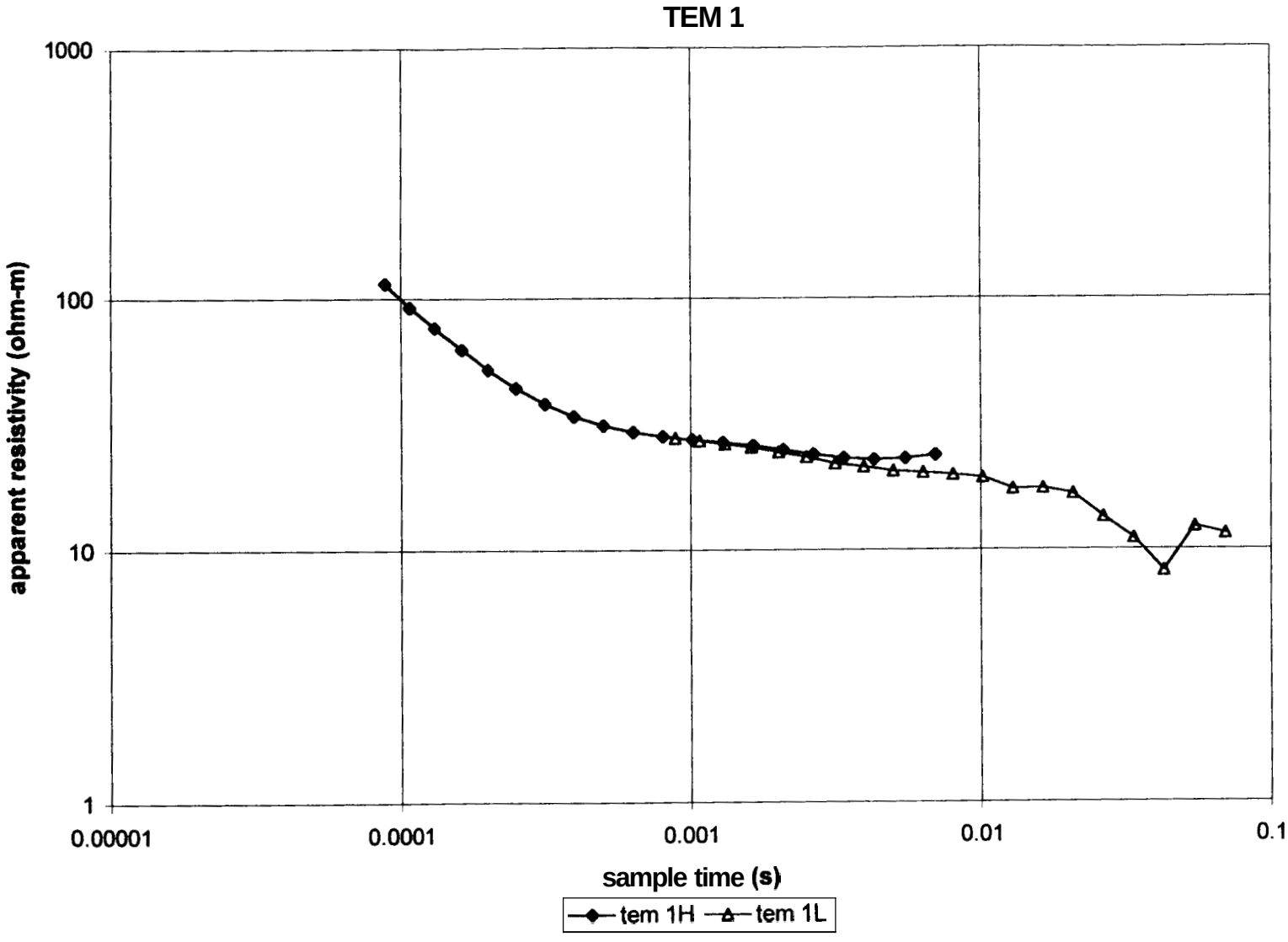

Figure 2. Ramp-corrected TEM apparent resistivity curves for TEM-1.

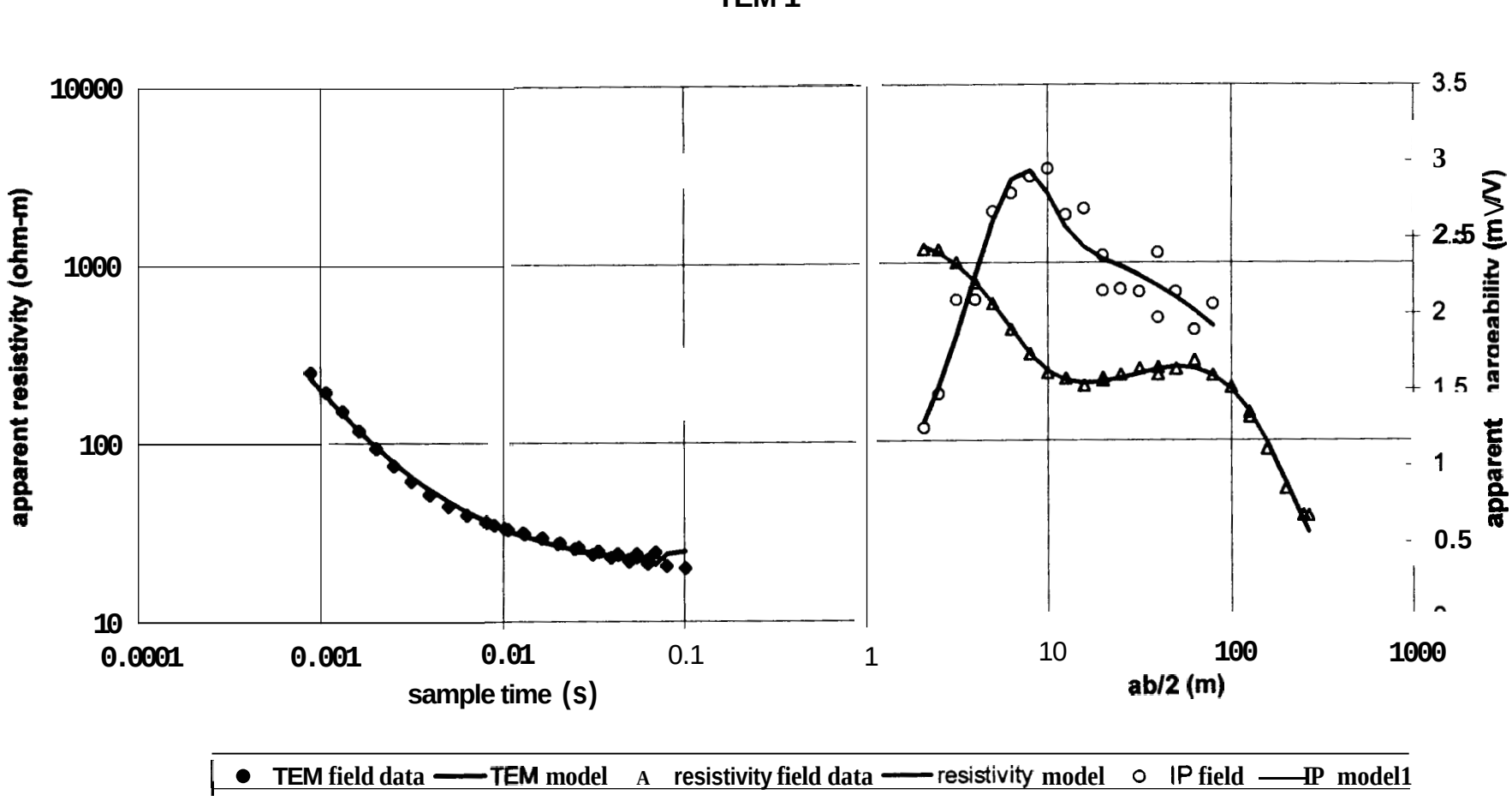

Figure 3. Modeling results showing data fit for simultaneous inverse modeling of TEM, resistivity, and IP datasets at TEM-1/IP-1. TEM apparent resistivities are late-time asymptotic values.

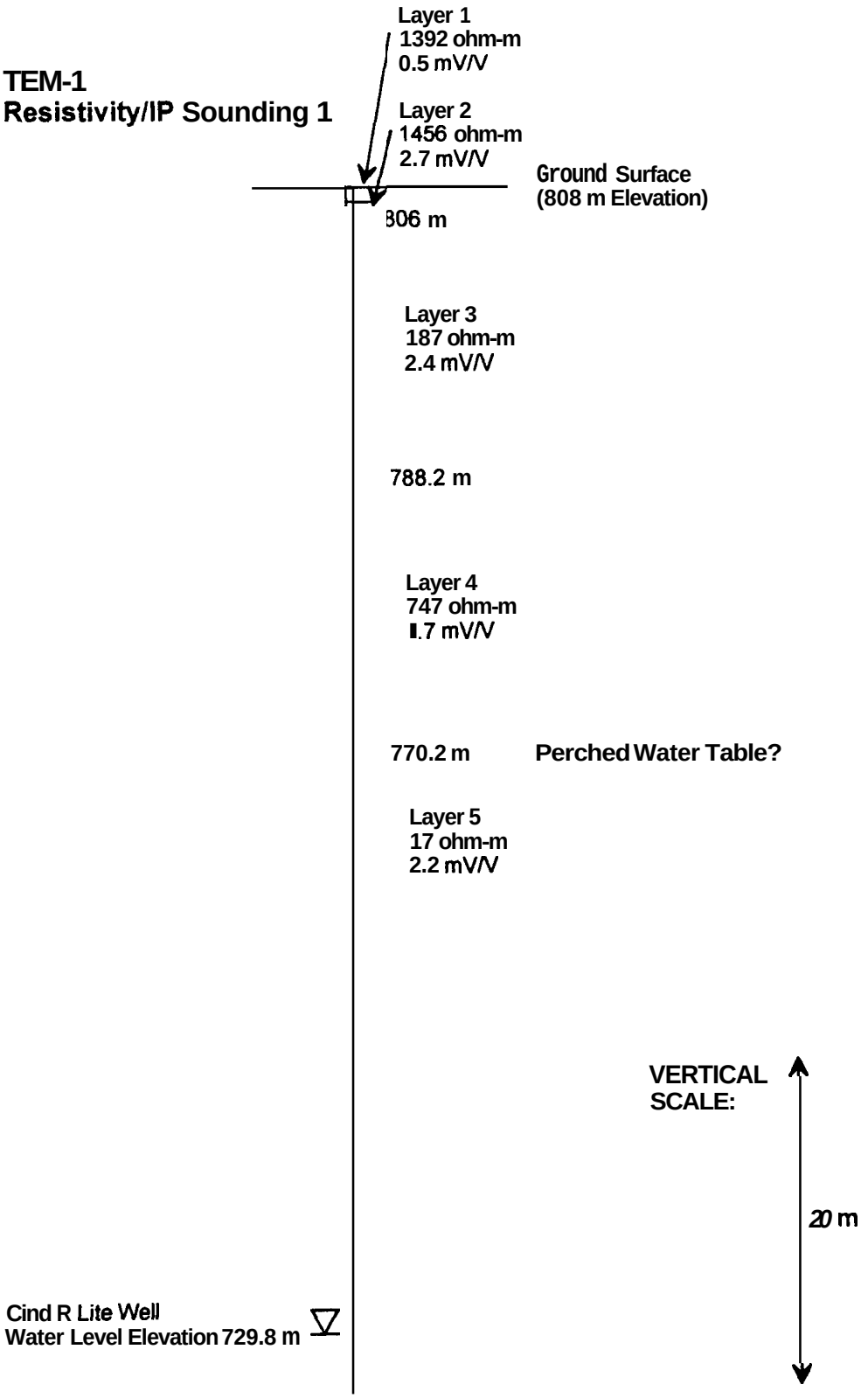

Figure 4. Interpretation of Resistivity/IP and TEM data at the TEM-I site near **Lathrop Wells.**

Appendix 4

INTERIM REPORT

INTERPRETATION OF AN EAST-WEST PROFILE ALONG STATE ROUTE 95

GEOPHYSICAL SURVEY AT FORTYMILE WASH, YUCCA MOUNTAIN, NEVADA

March 25, 1999

Prepared by:

Geophysical Solutions

Geophysical Contracting & Consulting
22 Crescent View ;\venue
Cape Elizabeth, Maine 04107
(207) 780-5154 e-mail: geophysh@aol.com
http://members.aol.com/geophysh/index.html

Stewart K. Sandberg, Ph.D., P.G.
Project Lead

Prepared for:

Center for Nuclear Waste
Regulatory Analyses
6220 Culebra Rd., Bldg. 189
San Antonio, TX 78238

Subcontract No. 9899052VE

I. INTRODUCTION AND BACKGROUND

During the summer of **1998,** CNWRA completed a preliminary geophysical data collection phase in which TEM data fiom 13 sites were obtained using a Zonge TEM and NANOTEM system with 60 and **200** meter transmitter loops at each site. A preliminary hydrogeological model was generated fiom modeling these data to produce boundaries inferred from the derived geoelectrical model. Hydrogeological features of continued interest include:

1. Depth to the top of the water table aquifer,
2. Thickness of the unconsolidated portion of this aquifer (depth to bedrock),
3. The location where the water table transfers from the bedrock aquifer to the unconsolidated aquifer, and
4. The geometry of a bedrock horst and graben structure interpreted fiom the preliminary TEM data and subsequently identified in gravity data. This structure appears to be capable of significantly altering the groundwater flow velocity (magnitude and direction) directly down gradient from the proposed high-level radioactive waste repository at Yucca Mountain.

A second geophysical data collection phase occurred fiom January **15-24, 1999.** This work generated an additional **35** TEM soundings, and **4** resistivity and IP soundings to further delineate **the** four hydrogeological features identified above, expanding upon data obtained in the prelimary data collection phase.

An interim report dated February **10,1999** discussed the locations of these additional data, and described the field logistics. This report is a second interim report presenting an interpretation of TEM sites 1 through 7, and resistivity/IP soundings 1 and 2.

Geophysical data sites collected in the second phase are shown in Figure 1. Also shown in the figure are the locations of 6 wells located near the geophysical soundings. Data **from** the following wells will be referenced in this report: Cind-R-Lite Well, NC-EWDP-2D, and NC-EWDP-Washburn.

II. DATA PROCESSING AND MODELING

Data handling and analysis software used is available from GEOPHYSICAL SOLUTIONS. Specific computer programs used in the data analysis presented in this report include RAMPRES3, and EINVRT6, version 6.0, dated August 7, **1998.**

TEM apparent resistivities were calculated using two methods. The first method is the late stage (also called "late time") asymptotic relation

$$\rho_a^{late} = \frac{a^{4/3} A_R^{2/3} \mu^{5/3}}{20^{2/3} \pi^{1/3} t^{5/3} Z^{2/3}},$$

where a is the radius of an equivalent circular transmitter loop (we used square loops 300 m and 40 m on a side, yielding a = 169 m and 22.6 m, respectively), A_R is the area of the receiver coil (in our survey, we used two receiver coils with areas 100 m^2 and 31.4 m^2), $\mu = 4\pi \times 10^{-7}$, t is the sample time, and Z is the received voltage divided by the

transmitted current. This solution assumes a step function transmitter turnoff and is only accurate at late sample times. Since this solution is a simple expression, it is used as the objective function in the inverse modeling, and hence the modeling outputs are presented using this solution.

The second method of calculating TEM apparent resistivity is the so-called "all-time" or "ramp-corrected" apparent resistivity, which is implemented in the **RAMPRES3** software. This method accounts for the finite transmitter **turnoff** ramp, and is therefore more accurate for determining near-surface (early time) resistivity structure. Because of this, field data are presented using this solution for preliminary inspection. Data from TEM 1 is plotted using this solution in Figure 2.

Approximate resistivity versus depth can be calculated using the "ramp-corrected resistivity values in the following expression (Meju, 1998, p. 405, equation 2)'

$$\delta_{eff} = (3.9\rho_a t / 2\pi\mu_0)^{1/2}.$$

This expression is applied to TEM 1 data in Figure 3. **As** a form of rapid and preliminary interpretation, the data from soundings TEM **1**, 2, 3, **3A**, **4**, 5, 6, and 7 were reduced to approximate resistivity versus depth and contoured in Figure **4.**

A more accurate interpretation results from computer modeling. **A** non-linear least-squares inversion program was used (EINVRT6) to model data fiom this survey. This program assumes a layered-earth model, and derived model parameters include layer resistivities and thicknesses for TEM and resistivity soundings, and also layer chargeabilities for **IP** soundings. **A** comparison of field versus computed data for TEM 1 showing data fit is shown in Figure 5. The derived model is shown in Table 2, which also indicates the high and low bounds of a 95% confidence interval for each parameter.

Simultaneous modeling was employed to improve resolution, by fitting TEM, resistivity, and IP data together to the same layered-earth model. Data fit for the three data sets, TEM 1, and resistivity/IP data fiom IP 1, is shown in Figure 6, with the derived model shown in Table 1.

III. INTERPRETATION OF CROSS-SECTION A – A'

Field data and modeling data fits for soundings along cross-section **A-A'** (indexed in Figure 1) are presented in Figures **5** through 20. **An** interpreted cross-section showing all the modeling results is shown in Figure 21. It should be noted that elevations are not available for any of the soundings along **A – A'** except for TEM 7.

TEM 1, IP 1

As can be seen in Figure 21, the model produced from simultaneously modeling soundings TEM 1 and IP 1 appears unable to resolve the water table. This was noted in

[1] Meju, M. **A.,** 1998, Short Note: **A** simple method of transient electromagnetic data analysis: Geophysics, vol. 63, no. 2, p. **405-410.**

the previous report (GEOPHYSICAL SOLUTIONS, February 10, 1999). However, note that the approximate depth calculation shown in Figure 3 has a resistive to conductive interface at 70 m depth, which better fits with the extrapolated water table depth in Figure 21. Modeling, which should produce a more accurate result, indicates this interface at 42 m depth (TABLE 1, sum of thicknesses for layers 1 through 4) for TEM/resistivity/IP simultaneous modeling, and also at 42 m depth (TABLE 2, parameter t1) when modeling only the TEM data. Confidence intervals indicate that this depth is fairly well resolved. Also, the data fit shown in Figures 5 and 6 is excellent.

The elevation of TEM 1 is not precisely known, but estimates of the error of the elevation used in Figure 21 are much smaller than the difference between the extrapolated water table and the top of the upper conductive layer.

The interpretation of TEM 1 / IP 1 is that the sounding site is likely located on or near a lateral resistivity boundary, perhaps resulting from lithological variation within the bedrock, or from structural inhomogeneity of the bedrock surface, such as faulting. Unfortunately, the design of the geophysical survey did not allow resolution of this lateral variation.

TEM 2

The model derived for TEM 2 is shown in Table 3, and is also shown in Figure 21. Data fit shown in Figure 8 is excellent, and the confidence interval for the depth to the conductive layer is small, indicating good resolution. Layer 2 of the model, with a resistivity of 11.1 ohm-m, is interpreted to be the top of the saturated zone.

TEM 3, TEM 3A, IP 2

The model resulting from simultaneous modeling TEM 3 and TEM3A data is shown in Table 4 and Figure 21. The model from simultaneous resistivity and IP modeling IP 2 data is shown in Table 5 and Figure 21.

It was not possible to fit all these data sets with the same model. However, note that the interface between layers 2 and 3 in the TEM model, and that between layers 3 and 4 in the resistivity/IP model is modeled at a similar depth. This depth is interpreted to be the top of the saturated zone, and is modeled at 78 and 73 m depth from TEM (300 and 40 m loops) and resistivity/IP modeling, respectively. Resolution of these depth estimates are good, as indicated in Tables 4 and 5, and data fit is also good as shown in Figures 11 and 12. Despite numerous attempts, the data fit for early time data from the 40 m 285 Hz data set is not perfect, as can be seen in Figure 11. However, this is considered a good fit, given the disparate data sets and possible surficial inhomogeneities.

A comparison with the water level in nearby well NC-EWDP-2D, indicates that the interpreted water table from the geophysical data is too shallow by about 20 m. The geophysical data were collected about 400 m NNE of the well (Figure 1), and Forty Mile Wash runs between them. It could be that some lateral inhomogeneity or variation resulting from this feature is causing this discrepancy, or that the water level in the well is not accurate.

The fact that the resistivity/IP sounding was centered at the northwest corner of the 300 m TEM loop may be significant. If the water table surface has a high gradient toward the

south in this area, the decrease in elevation of this surface from IP 2 to TEM 3 south to the well, would be consistent with that decrease.

TEM 4

TEM sounding TEM 4 is located to the northwest of the Cind-R-Lite well, as shown in Figure 1. Modeling results are shown in Figure 21 and in Table 6. The interface between layers 2 and 3 is interpreted to be the water table. Resolution of this depth is considered excellent, as is shown in Table 6, and as indicated by the data fit in Figure 14. This interpreted water table can easily be extrapolated from the water level in the nearby well.

TEM 5

The model for TEM 5 is shown in Figure 21 and Table 7. The depth to the top of layer 2 of the model is interpreted to be the depth to the water table. Resolution of this depth is considered good, based on the data in Table 7 and the data fit shown in Figure 16.

As can be seen in Figure 21, the water level in nearby well NC-EWDP-Washburn is somewhat lower than that interpreted from TEM 5. Again, note that the elevation of TEM 5 is not known, and has been estimated in Figure 21.

TEM 6

Modeling results for TEM 6 are shown in Table 8 and in Figure 21. Data fit is excellent as shown in Figure 18, and resolution of the depth to the conductive layer interpreted to be the water table (layer 2 in the model), is good. Also there is excellent agreement between this depth and the water level in nearby well NC-EWDP-Washburn.

TEM 7

Modeling results, data fit, and interpretation for TEM 7 are shown in Table 9, Figure 20, and Figure 21, respectively. Resolution is considered excellent, and agreement with the water table trend extrapolated from well NC-EWDP-Washburn is good.

IV. PRELIMINARY ANALYSIS OF MODELED RESISTIVITY ALONG A – A'

The upper layer modeled resistivity along the eastern extent of A – A', shown in Figure 21, is quite consistent. Values range from 100 (TEM 2) to 105 (TEM 3) to 92 (TEM 5) to 88 (TEM 6) to 81 ohm-m (TEM 7). An interpretation is that surficial lithologic variability is minor in this area. This is based on the observation that this unsaturated material has very little variation in resistivity along 6 km of transect.

Resistivities of the modeled layer corresponding to the top of the saturated zone show a Consistent spatial trend. As can be seen in Figure 21, modeled resistivity of the upper saturated zone increases toward the topographic low coincident with Forty Mile Wash, which is near TEM 3. The trend from the east extent toward the west shows resistivity increasing from 7.5 (TEM 7) to 13.2 (TEM 6), to 25 (TEM 5), to 33 ohm-m (IP 2). Going from west to east, the resistivity is from 11.1 (TEM 2) to 18.6 (TEM 3) or 33 ohm-m (IP ;).

An intapretation of this trend in subsurface resistivity is that groundwater flow is more rapid near Forty Mile Wash. Higher resistivity would be indicative of younger water in which fewer ions have been allowed to dissolve. This is due to the slow dissolution reactions between pore water and the silicate minerals through which they flow.

V. FURTHER WORK

The analysis of all soundings collected will continue, with results to be presented in subsequent reports.

VI. STATEMENT

The Subcontractor, Geophysical Solutions, hereby certifies that, to the best of its knowledge and belief, the technical data delivered herewith under Subcontract No. 9899052VE is complete, accurate, and complies with all requirements of the Subcontract.

MARCH 25, 1999
Date

STEWART K. SANDBERG, General Partner
Name and Title of Certifying Official

TABLE 1 (TEM 1 and IP 1 simultaneous)

		95% confidence interval	
parameter	final value	high	low
ρ1(Ω-m)	1440.60	3605.93	575.53
ρ2	1235.77	470704.13	3.24
P3	174.81	201.03	152.00
ρ4	507.57	837.31	307.69
P5	13.50	20.21	9.01
ρ6	13184	38180.25	0.46
P7	13.46	17.01	10.65
c 1(mV/V)	0.49	++++++++++++++++	0.00
c2	2.67	1352.46	0.01
c3	2.44	2.53	2.36
c4	1.80	2.13	1.52
c5	2.20	fixed	
c6	2.20	fixed	
c7	2.20	fixed	
t 1(m)	0.96	1332357380.00	0.00
t2	1.26	219835.25	0.00
t3	12.97	26.83	6.27
t4	27.33	54.95	13.59
t5	68.02	708.12	6.53
t6	40.86	194.99	8.56

TABLE 2 (TEM 1 only)

		95% confidence interval	
parameter	final value	high	low
p l(Ω-m)	434.01	96324262300000000.00	0.00
ρ2	13.38	17.76	10.07
P3	656.59	++++++++++++++++	0.00
ρ4	13.41	14.75	12.20
t 1(m)	41.77	52.26	33.38
t2	67.34	268.91	16.86
t3	38.03	73.54	19.67

TABLE 3 (TEM 2)

parameter	final value	95% confidence interval high	low
ρ1(Ω-m)	100.36	129.33	77.88
ρ2	11.14	12.40	10.02
P3	666.08	++++++++++++++++	0.00
ρ4	9.29	247.27	0.35
t 1(m)	75.60	79.71	71.70
t2	105.08	186.98	59.05
t3	106.77	226.47	50.33

TABLE 4 (TEM 3 and TEM 3A)

parameter	final value	95% confidence interval high	low
ρ1(Ω-m)	36.45	41.67	31.88
ρ2	104.70	106.18	103.24
P3	18.63	916921.44	0.00
ρ4	86.12	2771585250000000000000000.00	0.00
ρ5	8.26	9.41	7.25
t 1(m)	1.15	1.21	1.09
t2	77.12	94.33	63.05
t3	28.27	204120.78	0.00
t4	75.53	143.70	39.70

TABLE 5 (IP 2)

parameter	final value	95% confidence interval high	low
ρ1(Ω-m)	832.67	1008.84	687.26
ρ2	156.52	938.28	26.11
P3	188.20	194.02	182.56
ρ4	32.97	39.35	27.62
c 1(mV/V)	3.00	3.20	2.81
c2	4.91	16.85	1.43
c3	1.52	1.69	1.37
c4	7.86	8.44	7.32
t 1(m)	1.73	2.57	1.17
t2	3.09	485.21	0.02
t3	67.81	73.11	62.90

TABLE 6 (TEM 4)

		95% confidence interval	
parameter	final value	high	low
ρ1(Ω-m)	50.71	50.98	50.44
ρ2	1191.42	1215.16	1168.14
P3	21.29	21.92	20.68
ρ4	5.53	5.69	5.37
t 1(m)	3.38	3.44	3.33
t2	102.22	102.43	102.00
t3	94.85	101.33	88.78

TABLE 7 (TEM 5)

		95% confidence interval	
parameter	final value	high	low
ρ1(Ω-m)	92.18	105.09	80.86
ρ2	24.59	25.36	23.84
P3	29.27	161501824.00	0.00
ρ4	5.43	9.36	3.15
t 1(m)	82.74	93.25	73.41
t2	284.70	334.67	242.19
t3	26.42	47516040.00	0.00

TABLE 8 (TEM 6)

parameter	final value	high	low
ρ1(Ω-m)	87.94	89.82	86.11
ρ2	13.19	14.89	11.68
P3	18.00	30.50	10.62
t 1(m)	109.16	112.34	106.07
t2	149.95	877107.31	0.03

TABLE 9 (TEM 7)

		95% confidence interval	
parameter	final value	high	low
ρ1(Ω-m)	80.99	81.91	80.07
ρ2	7.54	7.83	7.27
P3	19.67	140.39	2.75
t 1(m)	114.02	114.73	113.31
t2	151.83	276.60	83.34

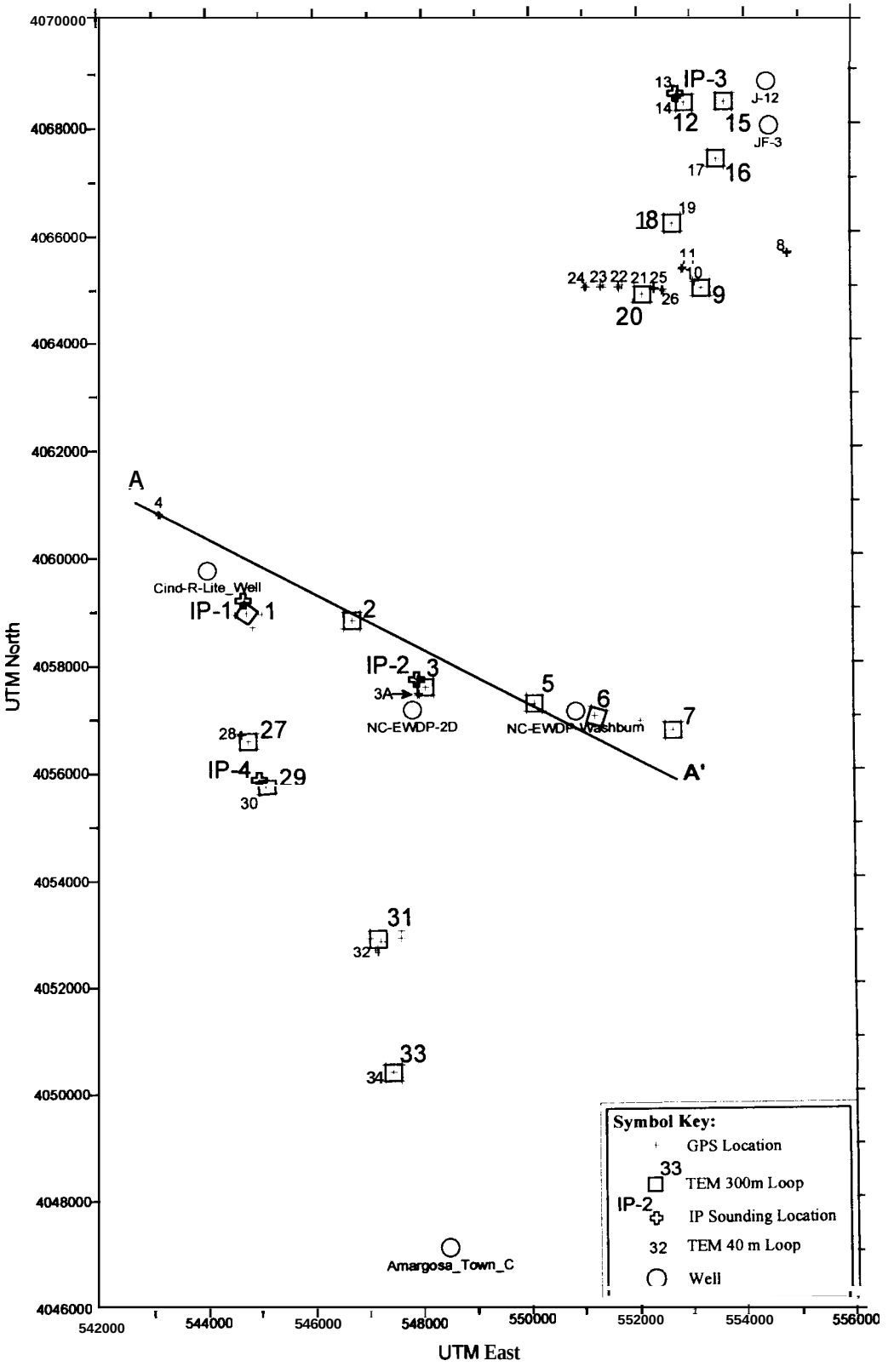

Figure 1. Geophysical data locations. Cross-section **A - A'** is shown, along with relevant well locations.

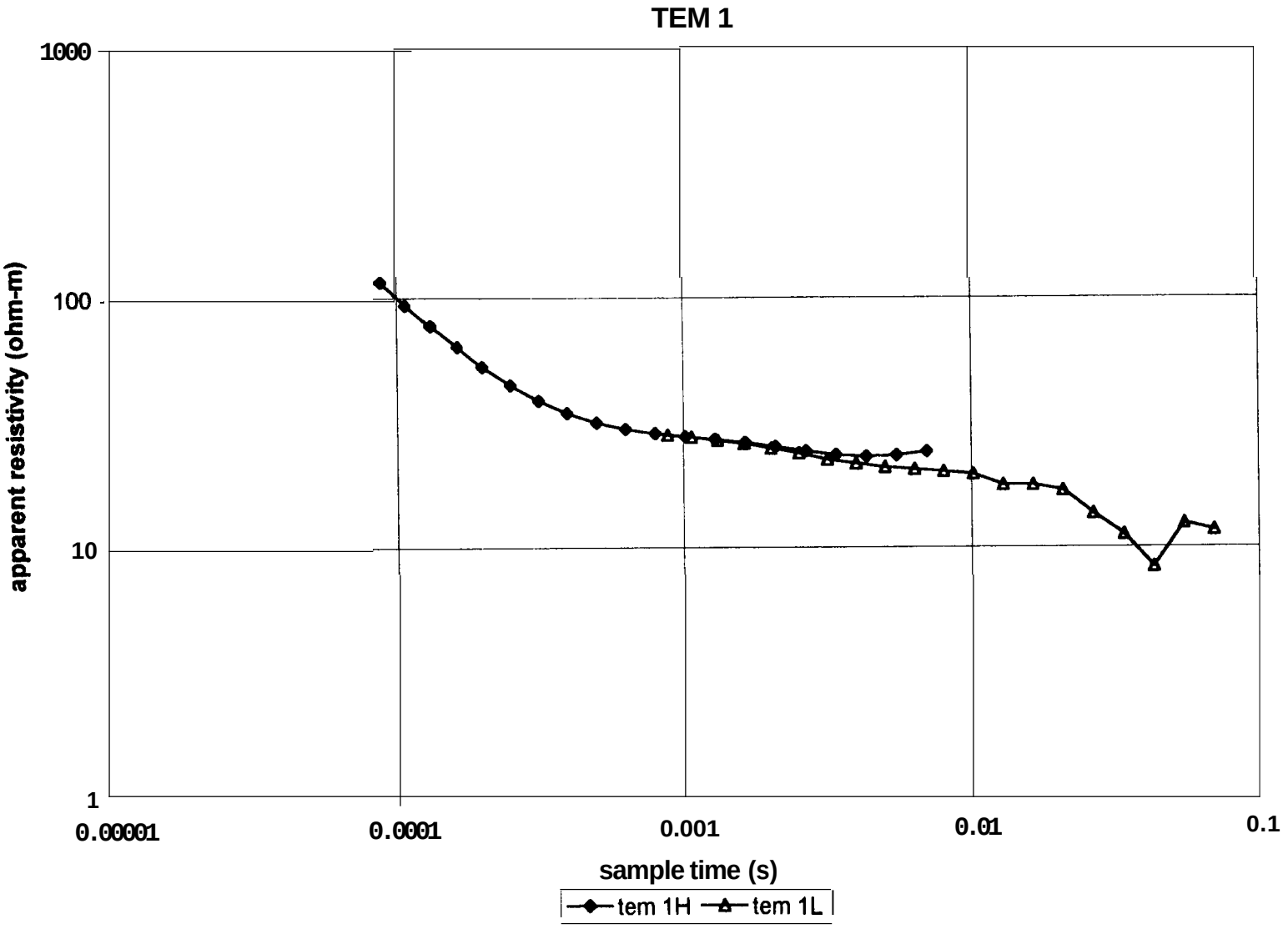

Figure 2. Ramp-corrected TEM apparent resistivity curves for TEM 1·

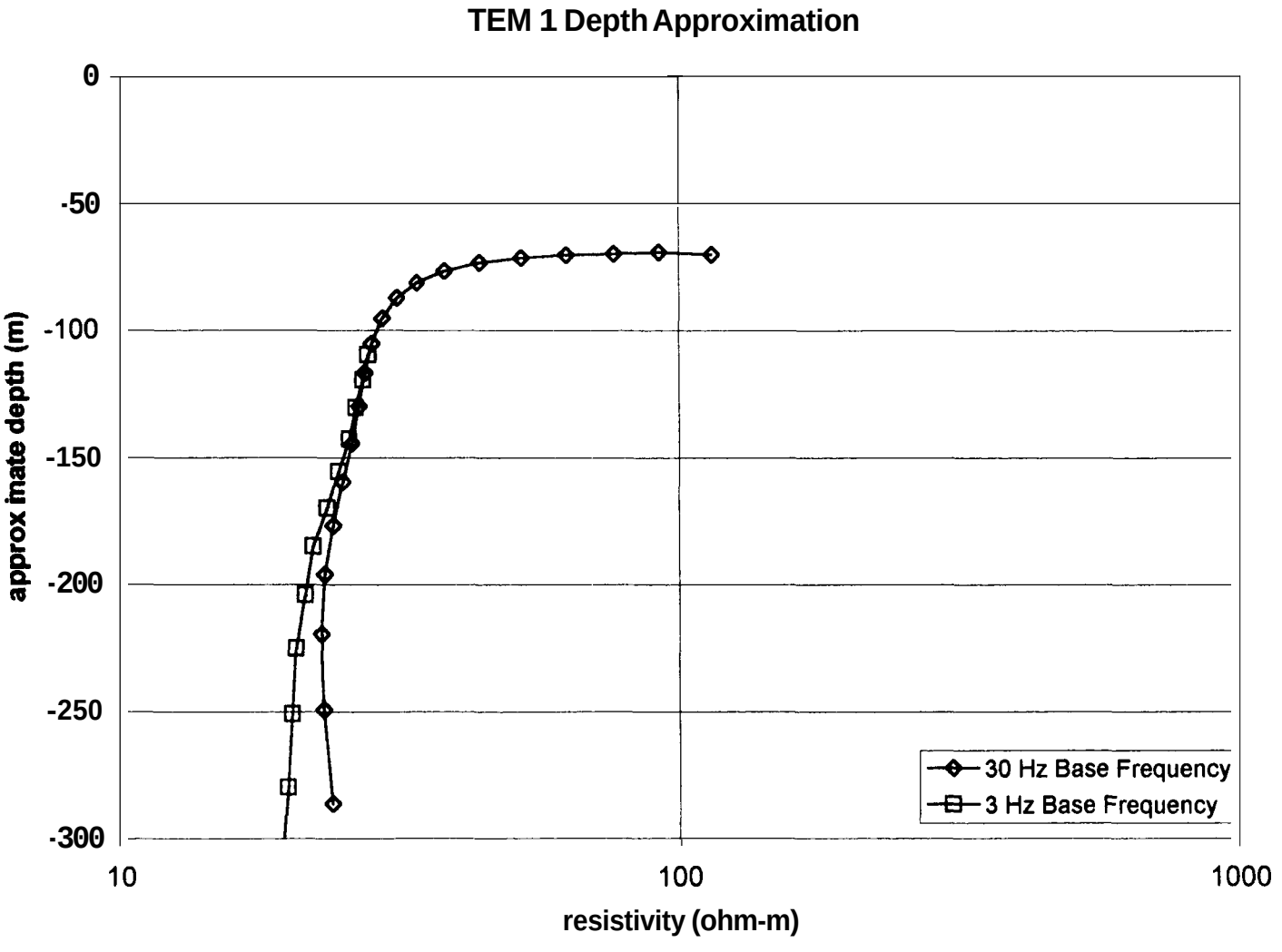

Figure 3. Result from applying approximate depth calculation to data from TEM 1.

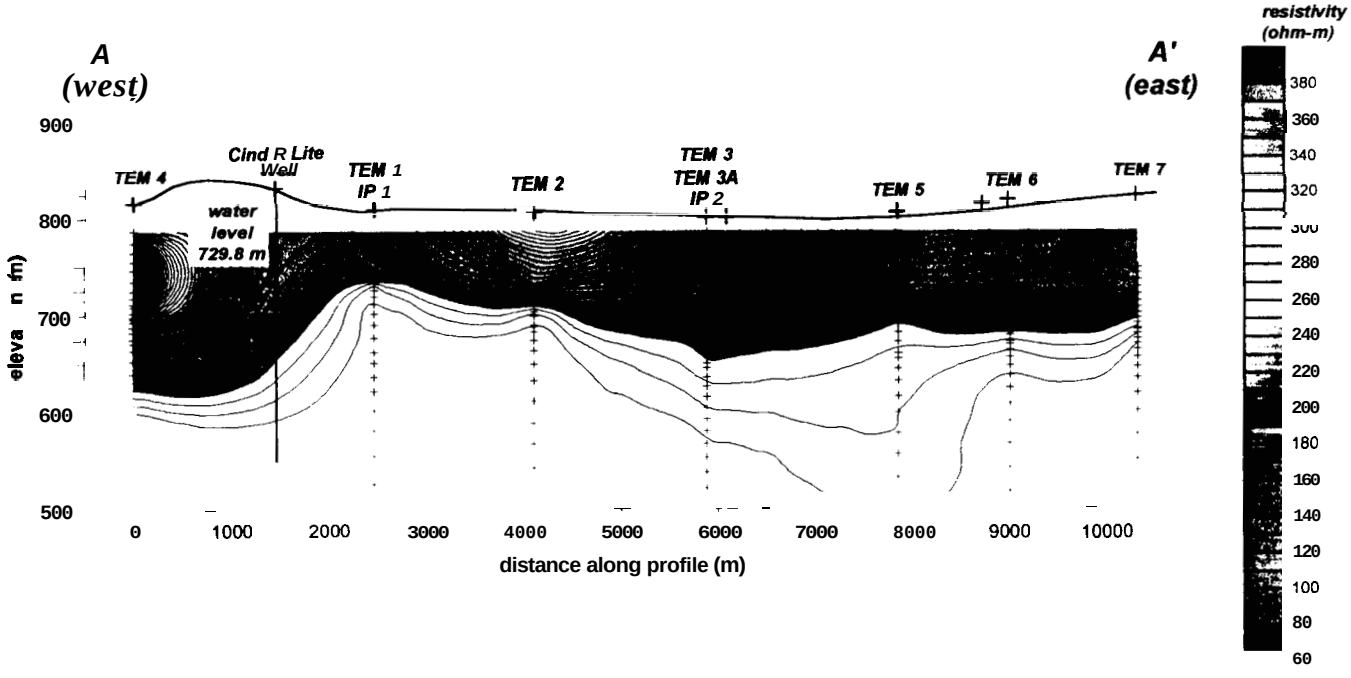

Figure 4. Approximate depth section for A-A' showing resistivity versus depth.

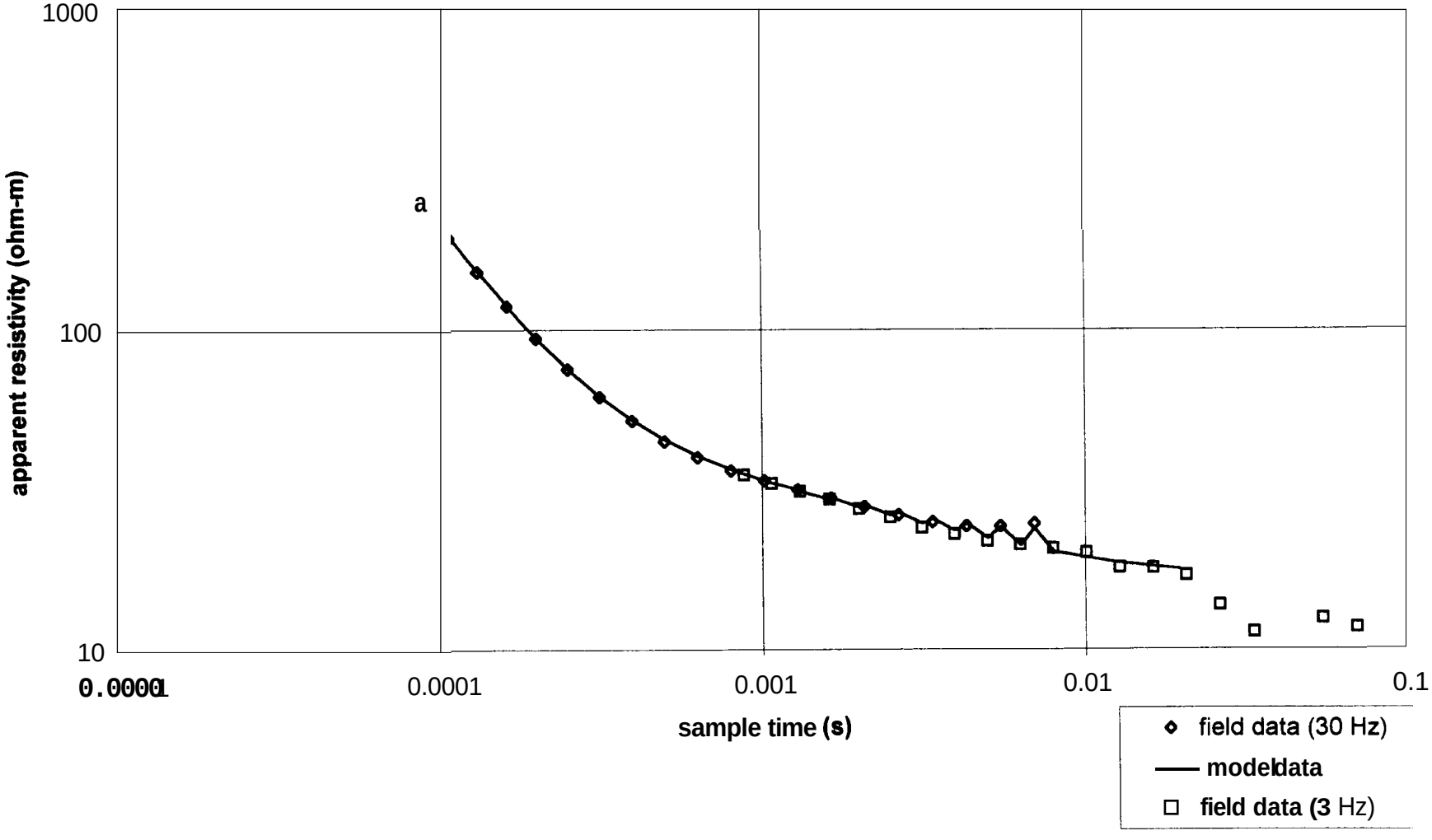

Figure 5. TEM 1 **field data versus model data showing data fit. Values shown are late-time asymptotic apparent resistivities. Model is derived from** TEM **data only.**

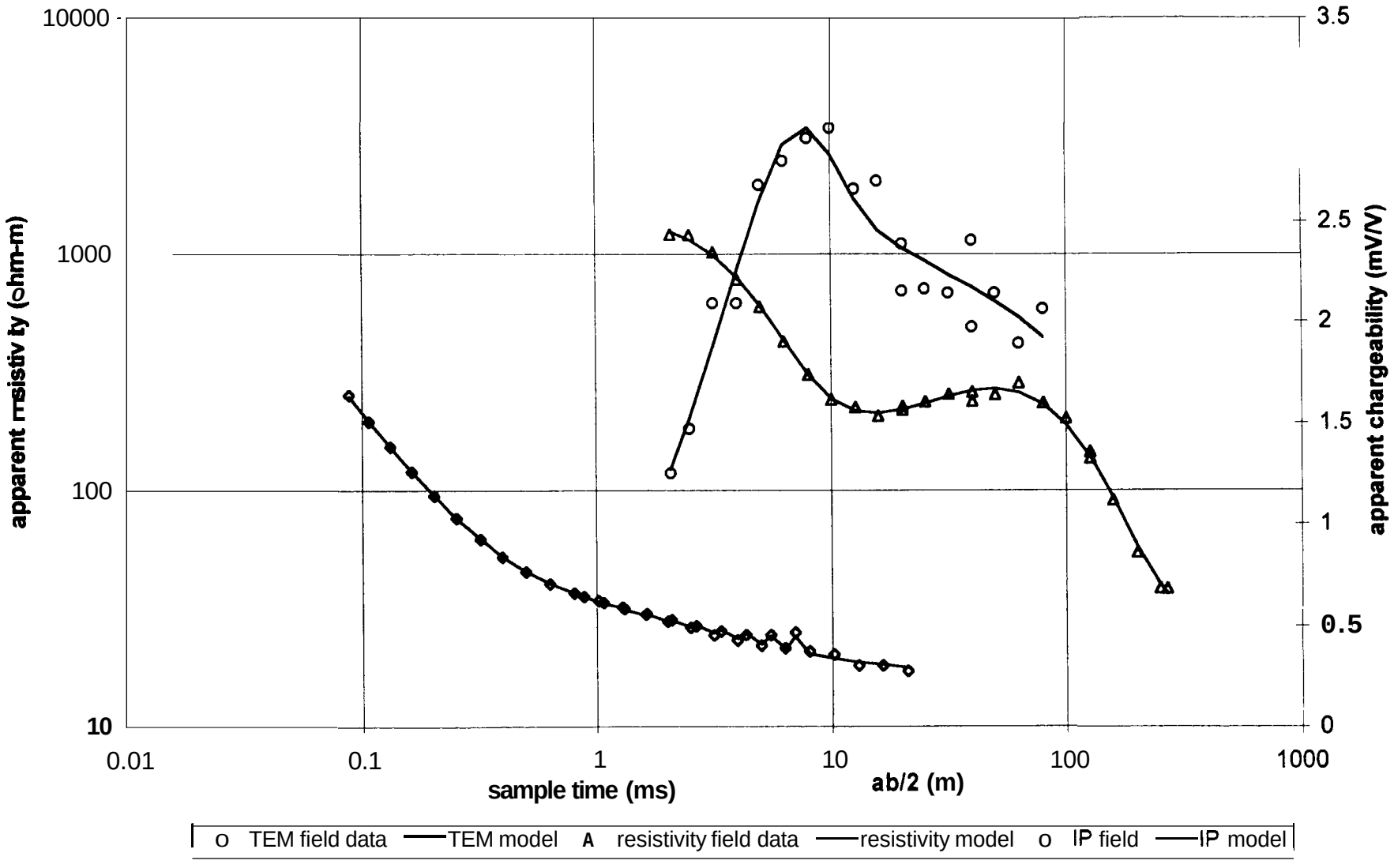

Figure 6. Modeling results showing data fit for simultaneous inverse modeling of TEM, resistivity, and IP datasets at TEM 1/IP 1. TEM apparent resistivities are late-time asymptotic values.

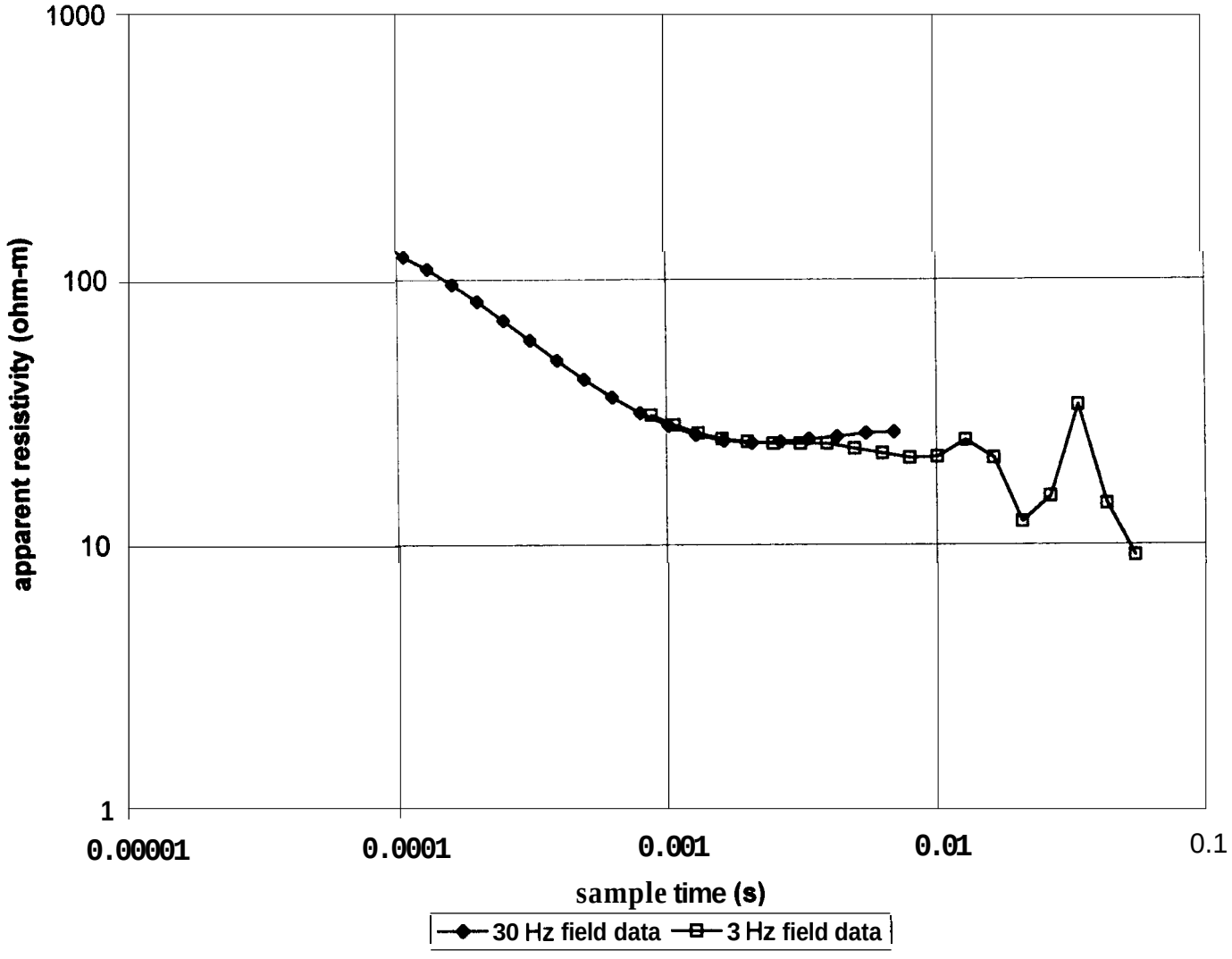

Figure 7. Ramp-corrected TEM apparent resistivity curves for TEM 2.

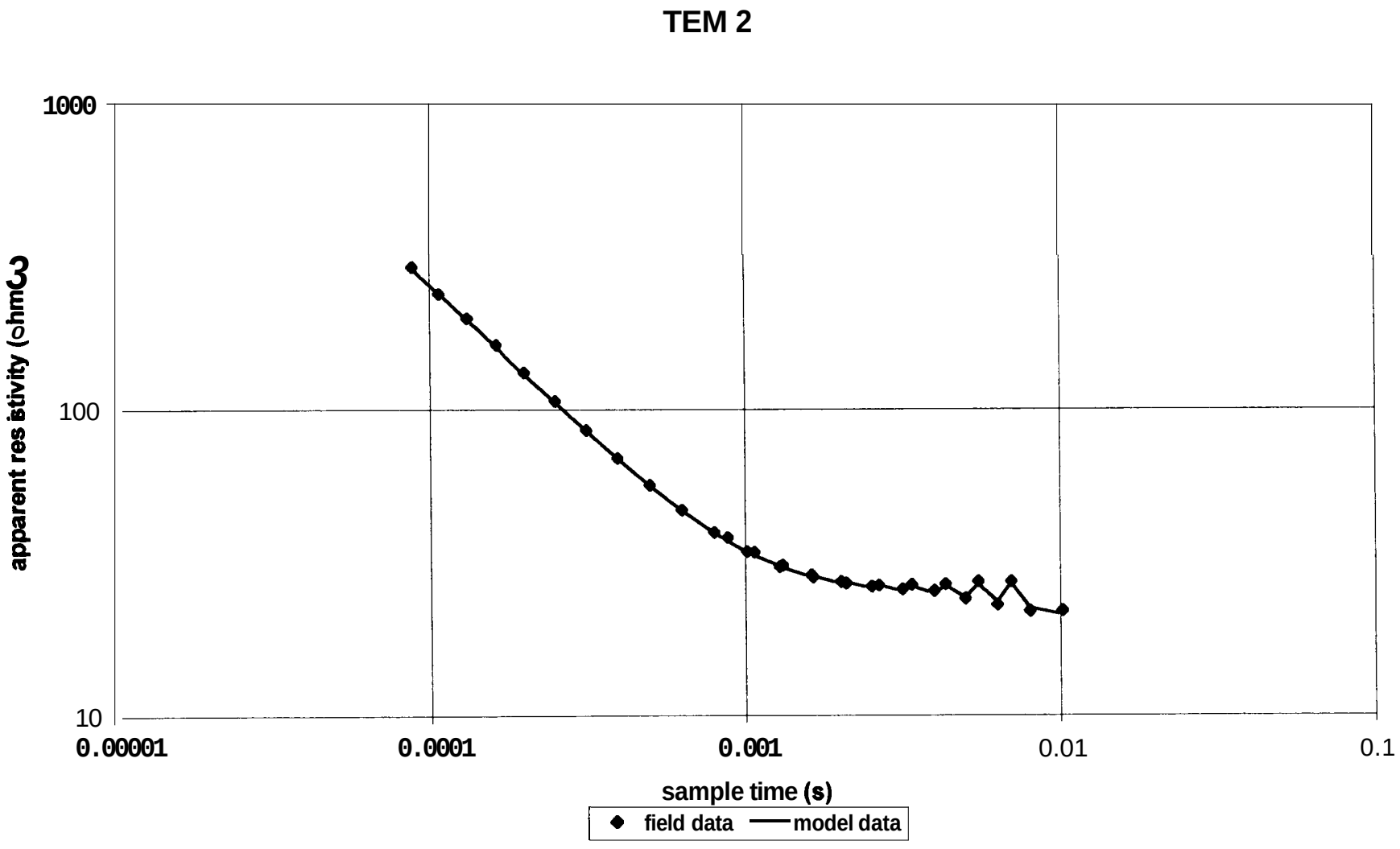

Figure 8. TEM 2 field data versus model data showing data fit. Values shown are late-time asymptotic apparent resistivities. Model is derived from TEM data only.

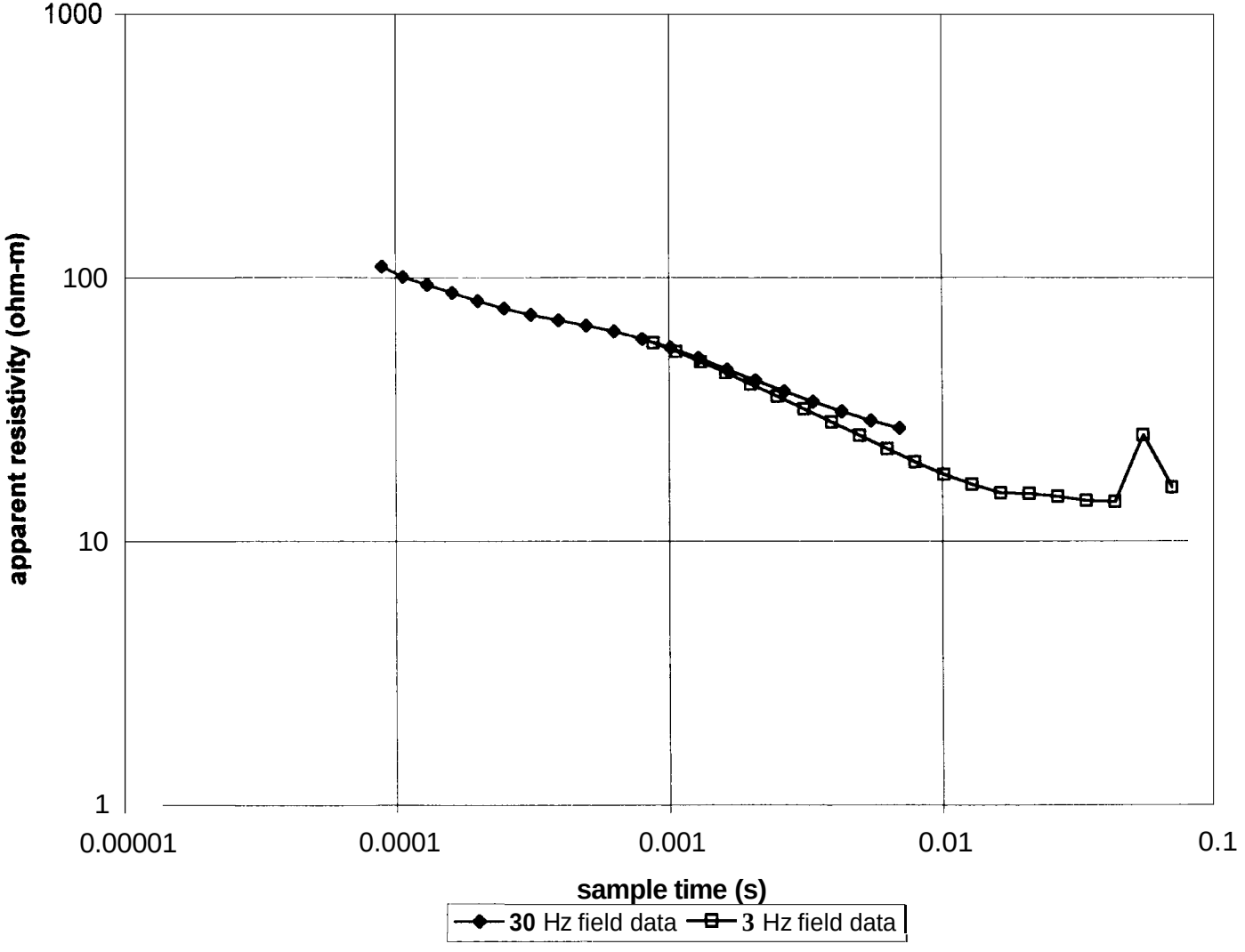

Figure 9. **Ramp-corrected TEM apparent resistivity curves for** TEM *3*.

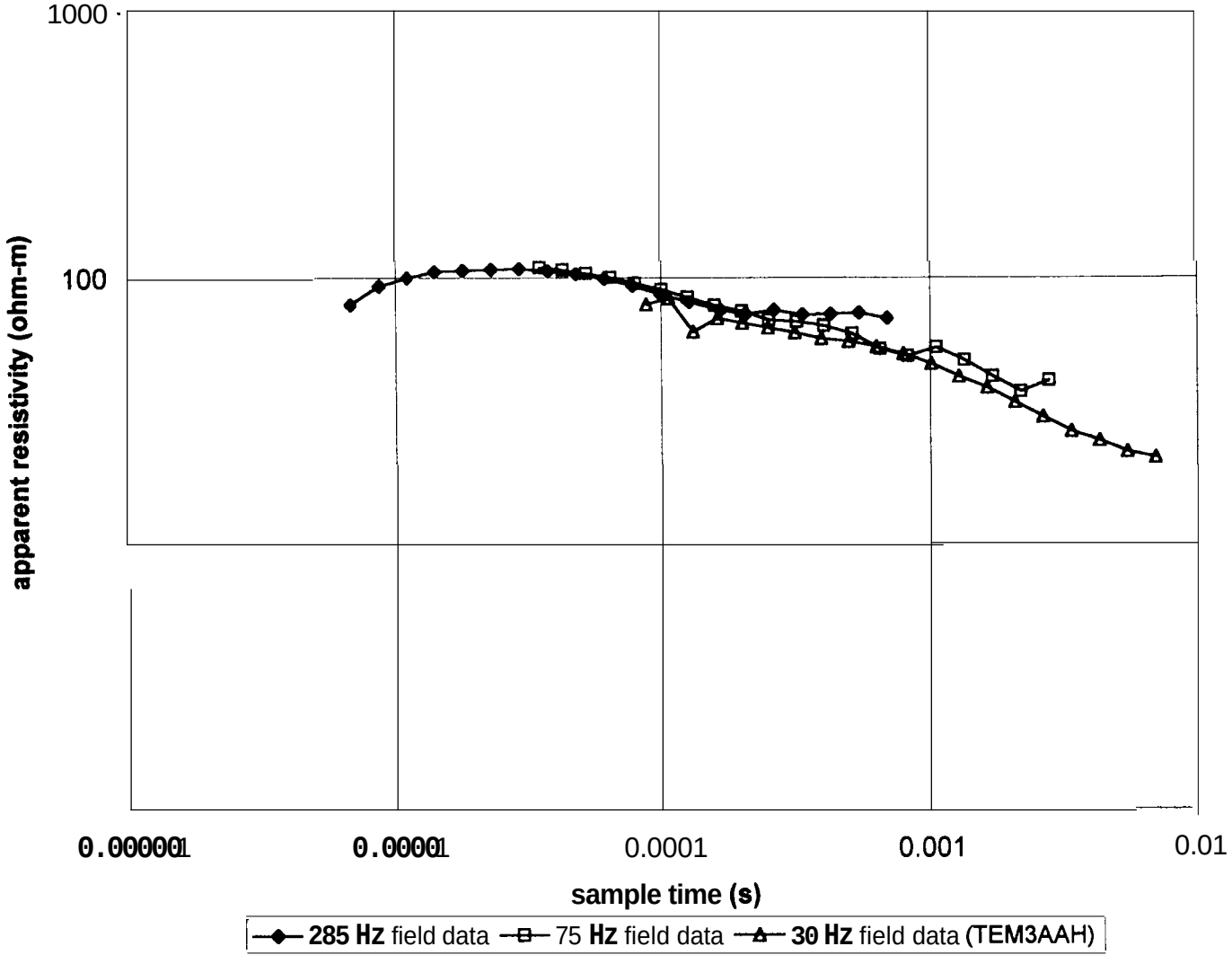

Figure 10. Ramp-corrected TEM apparent resistivity curves for TEM **3A.**

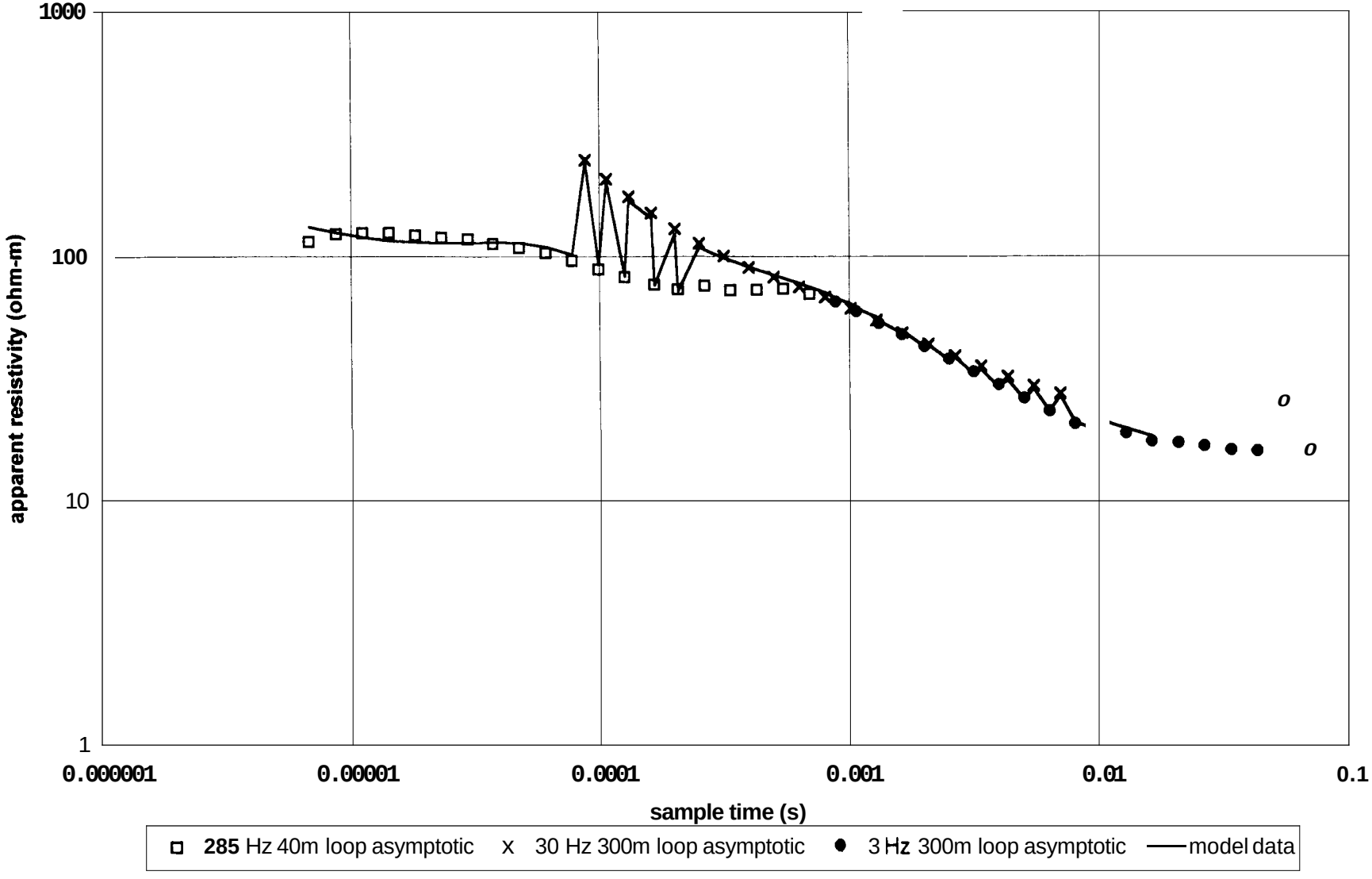

Figure 11. TEM **3** and TEM **3A** field data plotted with model data showing data fit.

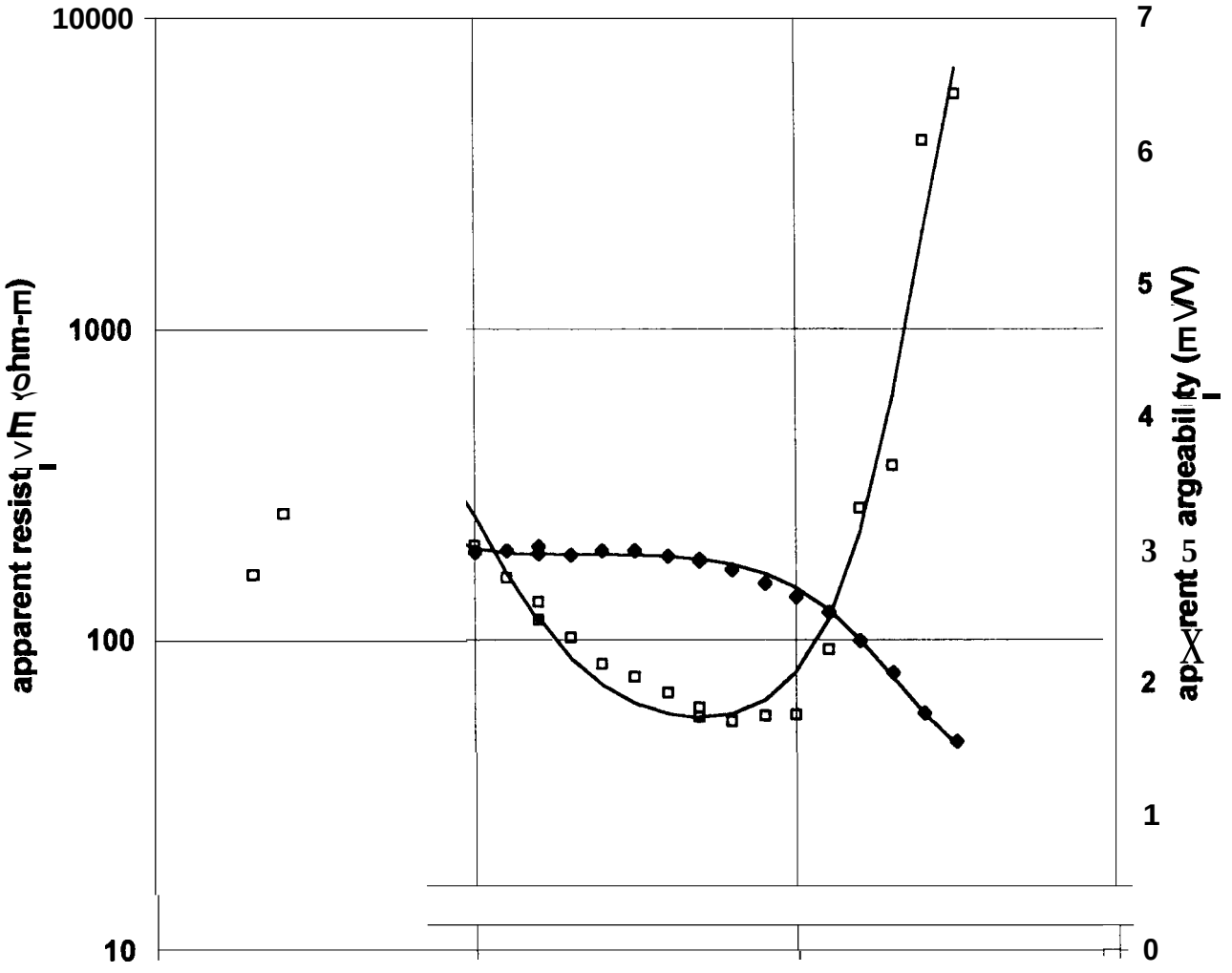
10000
1000
100
10
7
6
5
4
3
2
1
0
apparent resistivity (ohm-m)
apparent chargeability (mV/V)

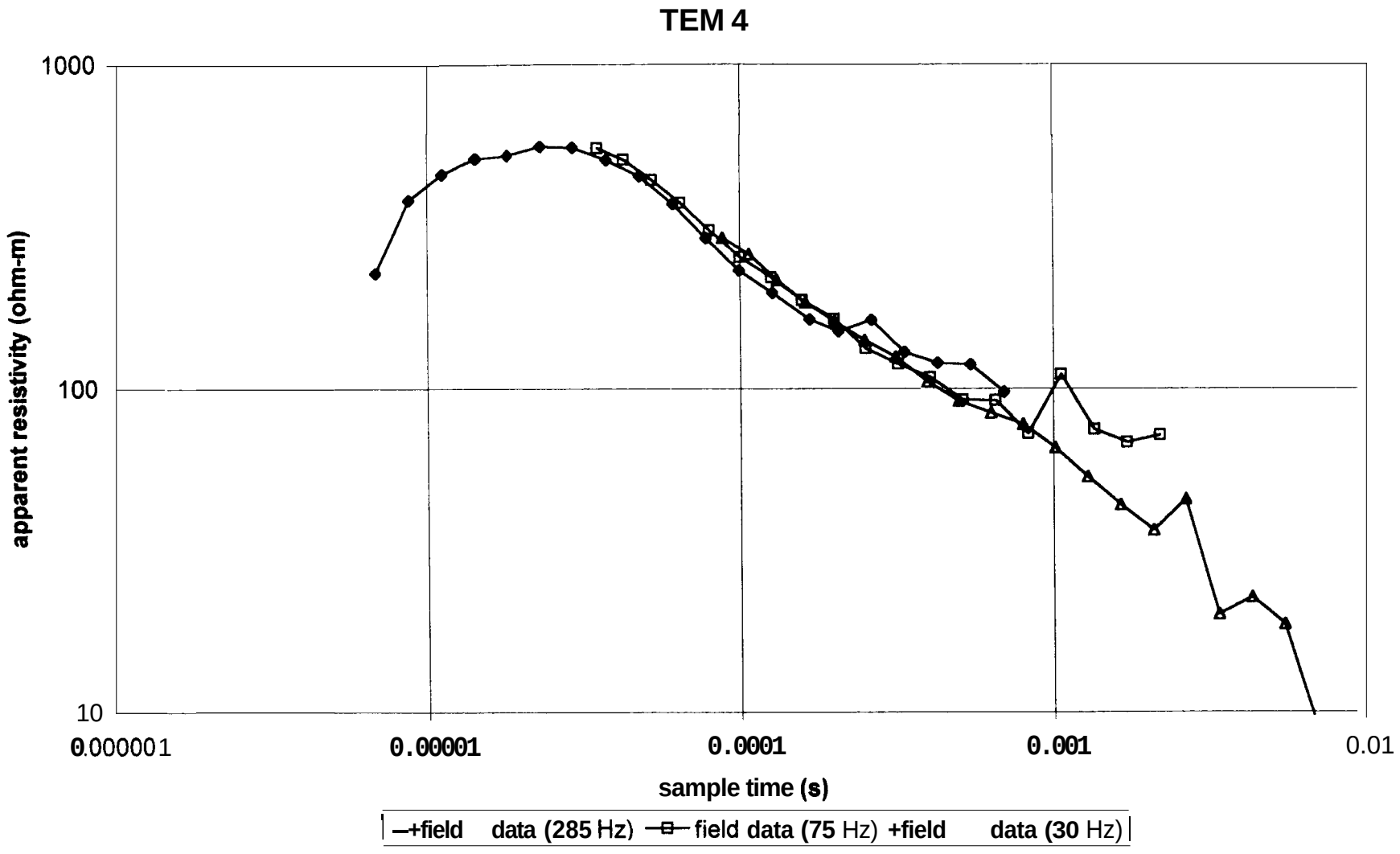

Figure 13. Ramp-corrected TEM apparent resistivity curves for TEM 4.

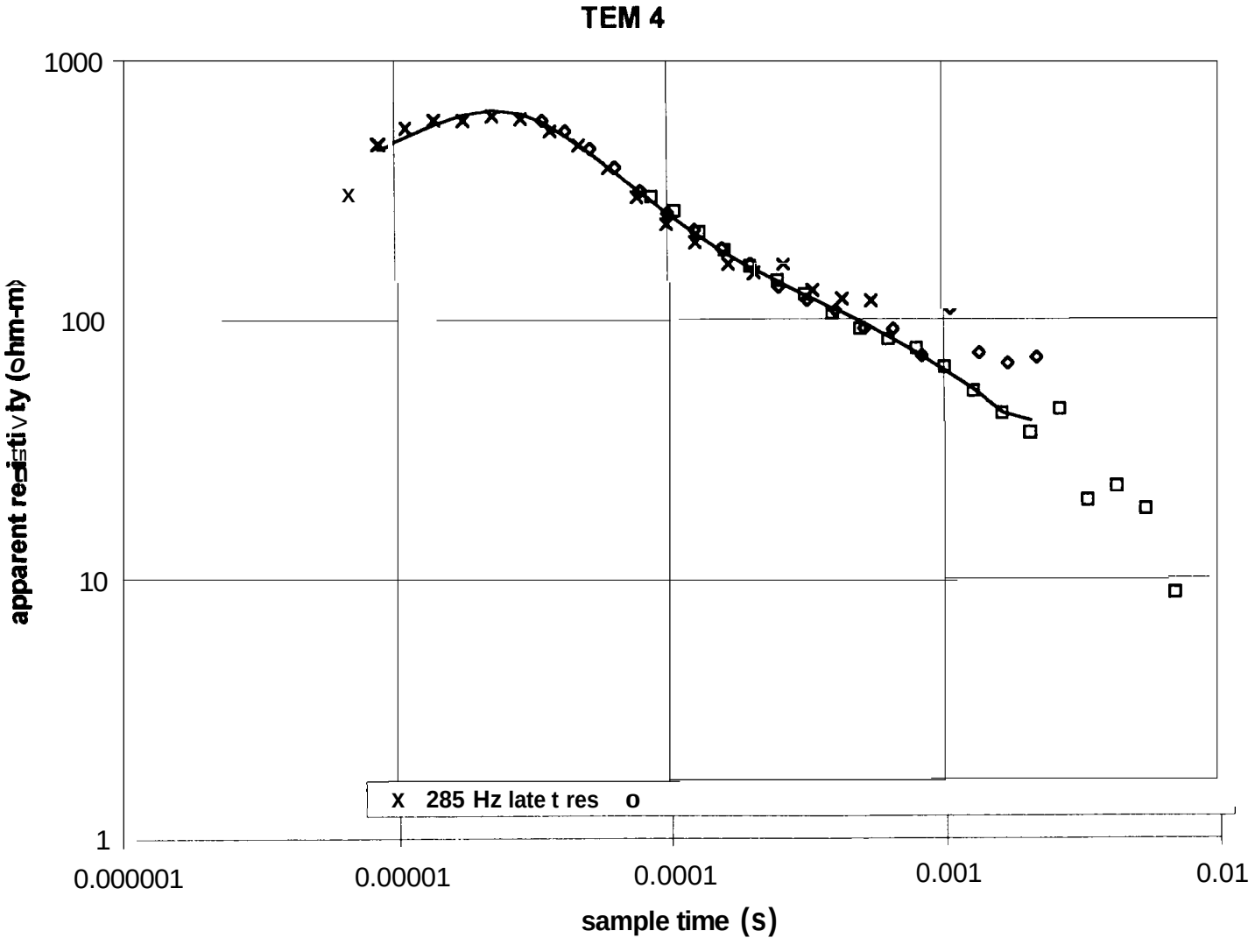

Figure **14.** TEM 4 field data versus model data showing data fit. Values shown are late-time asymptotic apparent resistivities.

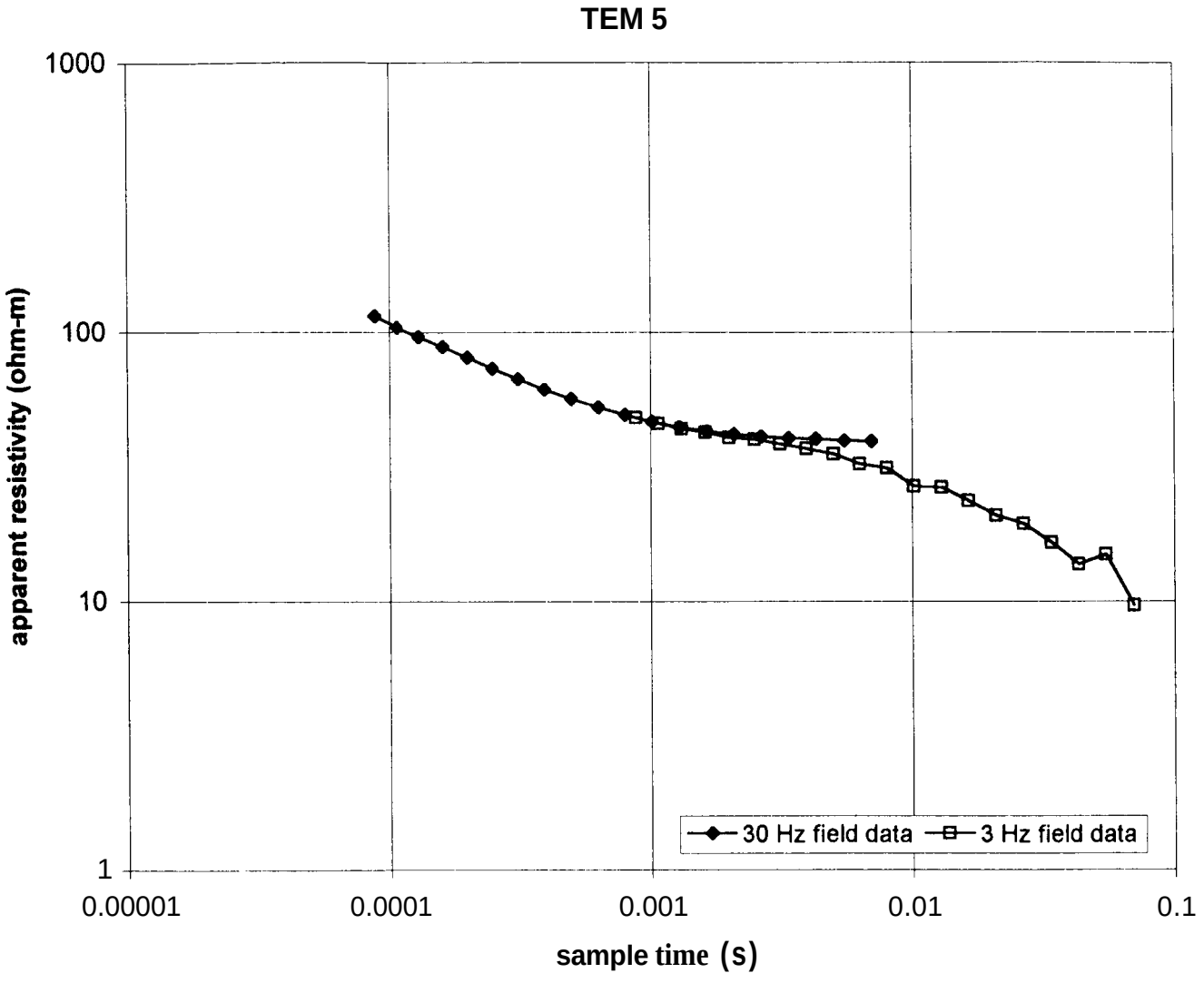

Figure 15. Ramp-corrected TEM apparent resistivity curves for TEM 5.

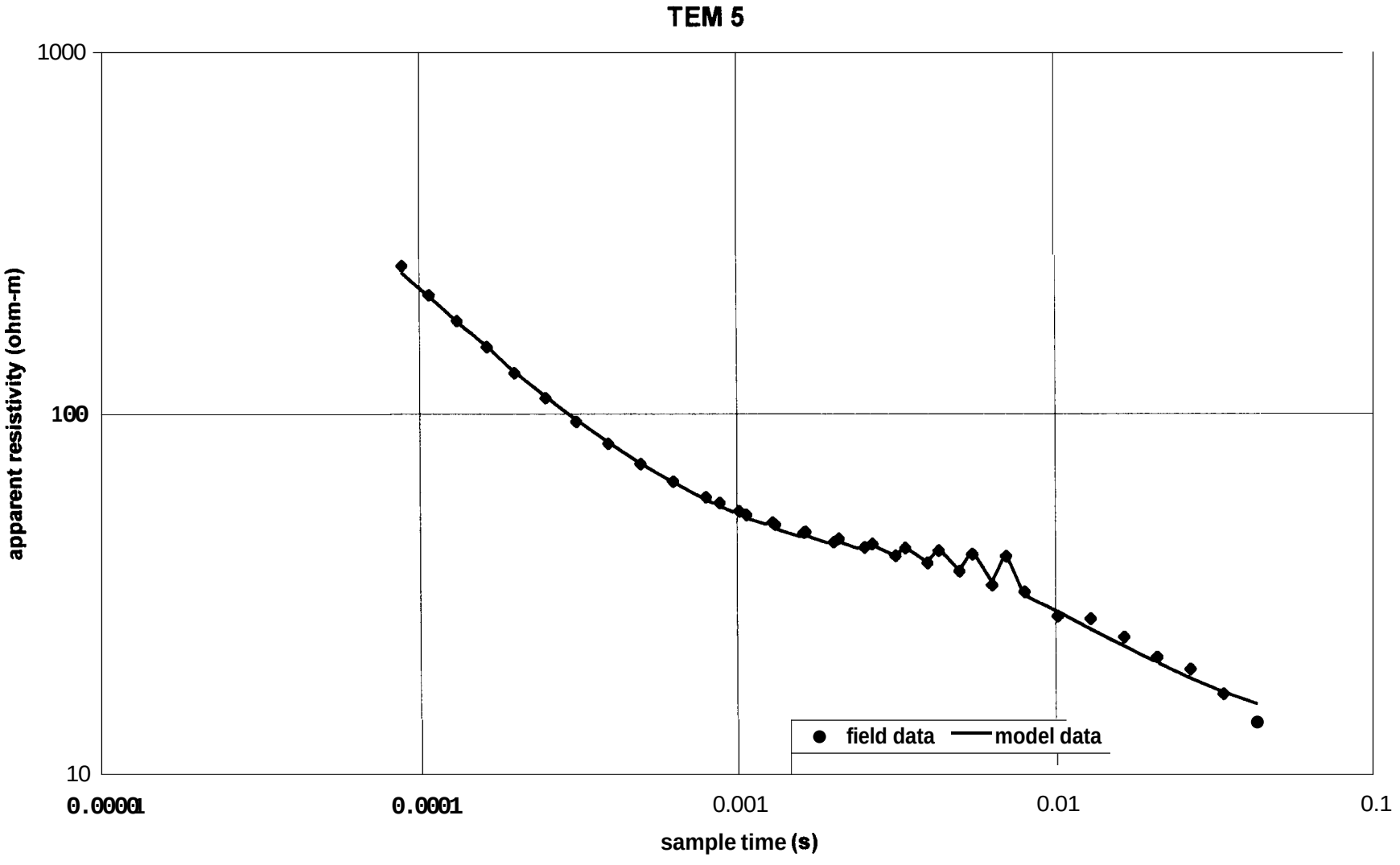

Figure 16. TEM 5 field data versus model data showing data fit. Values shown are late-time asymptotic apparent resistivities.

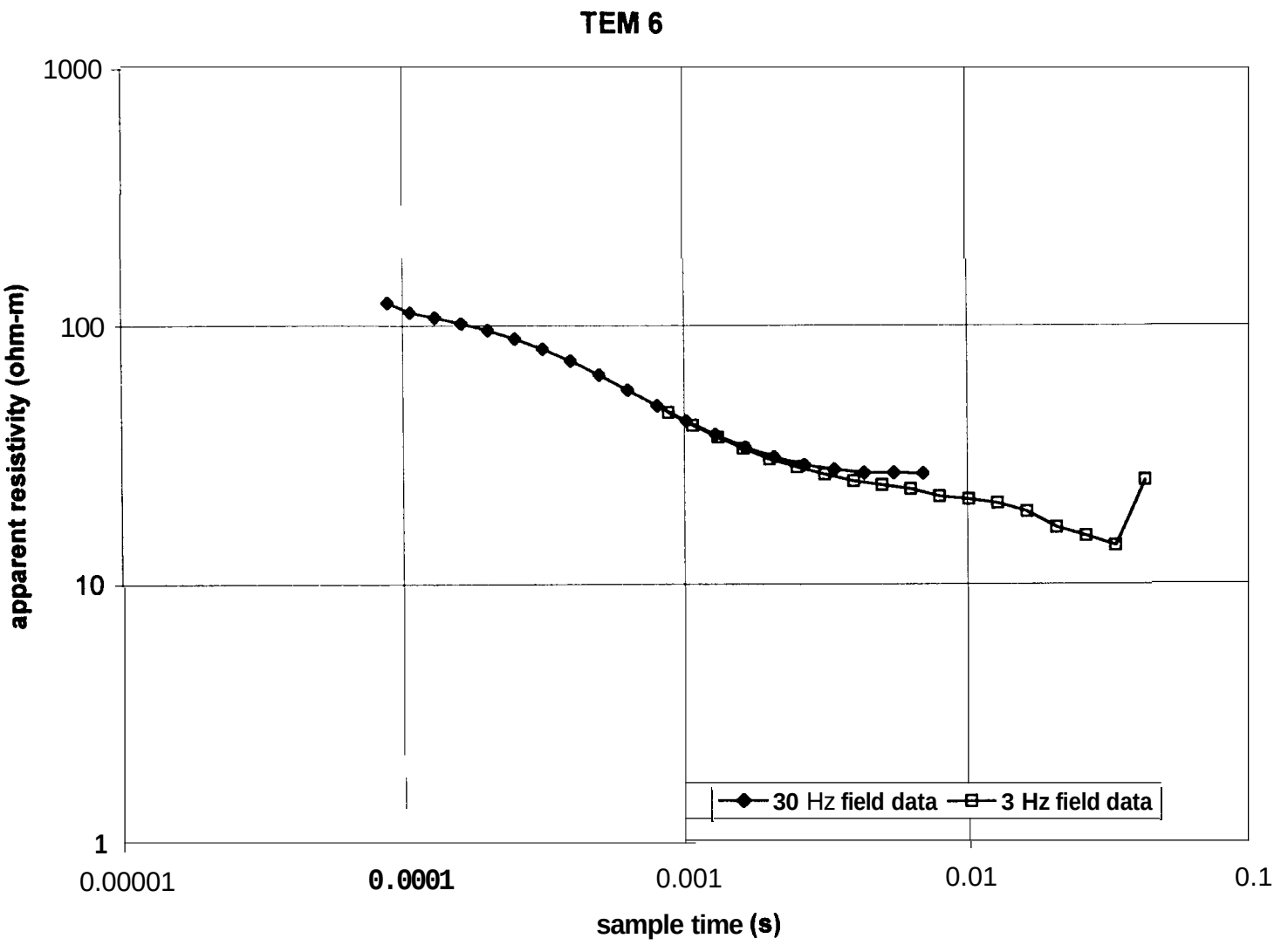

Figure 17. Ramp-corrected TEM apparent resistivity curves for TEM 6.

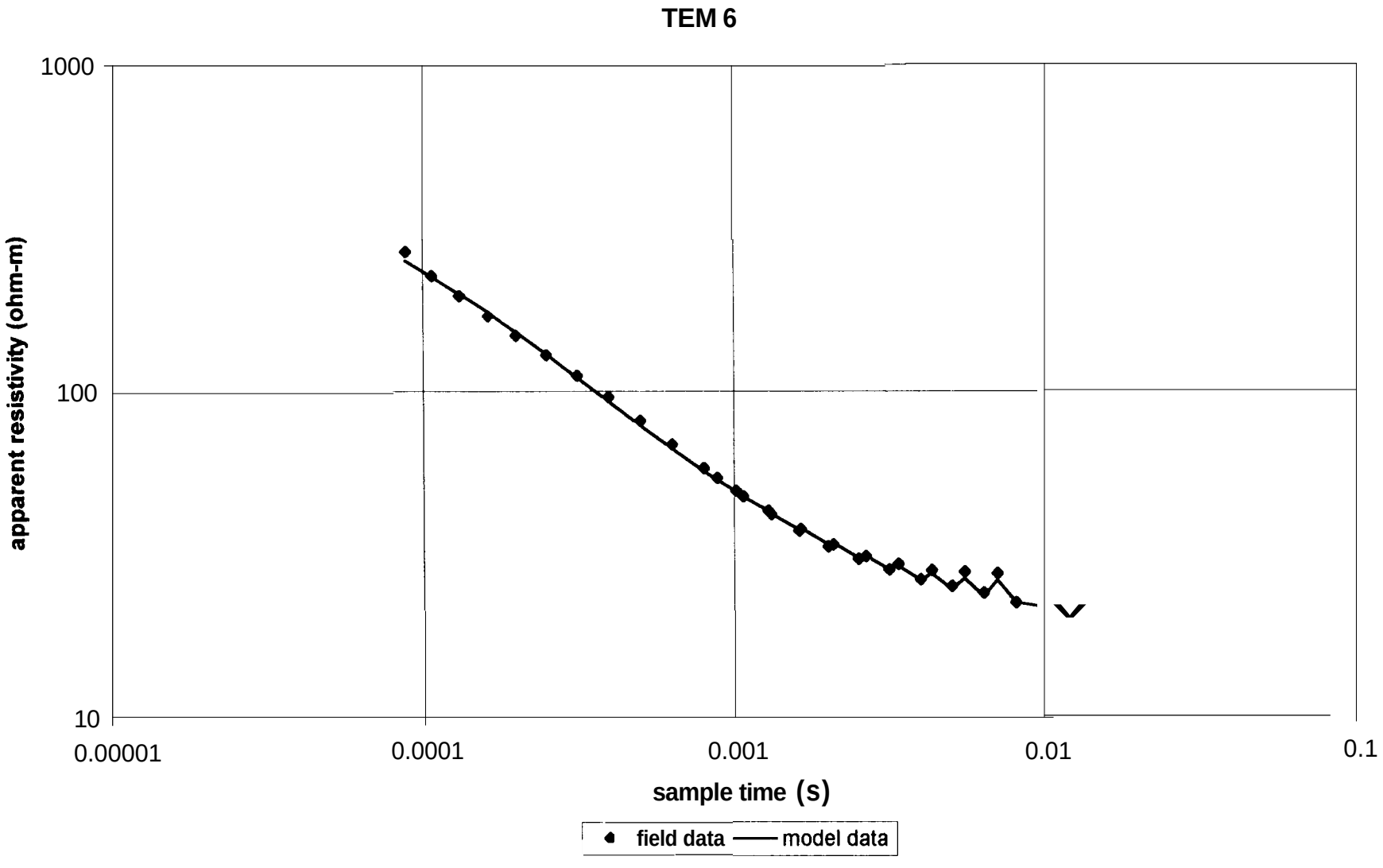

Figure **18.** TEM **6** field data versus model data showing data **fit.** Values shown are late-time asymptotic apparent resistivites.

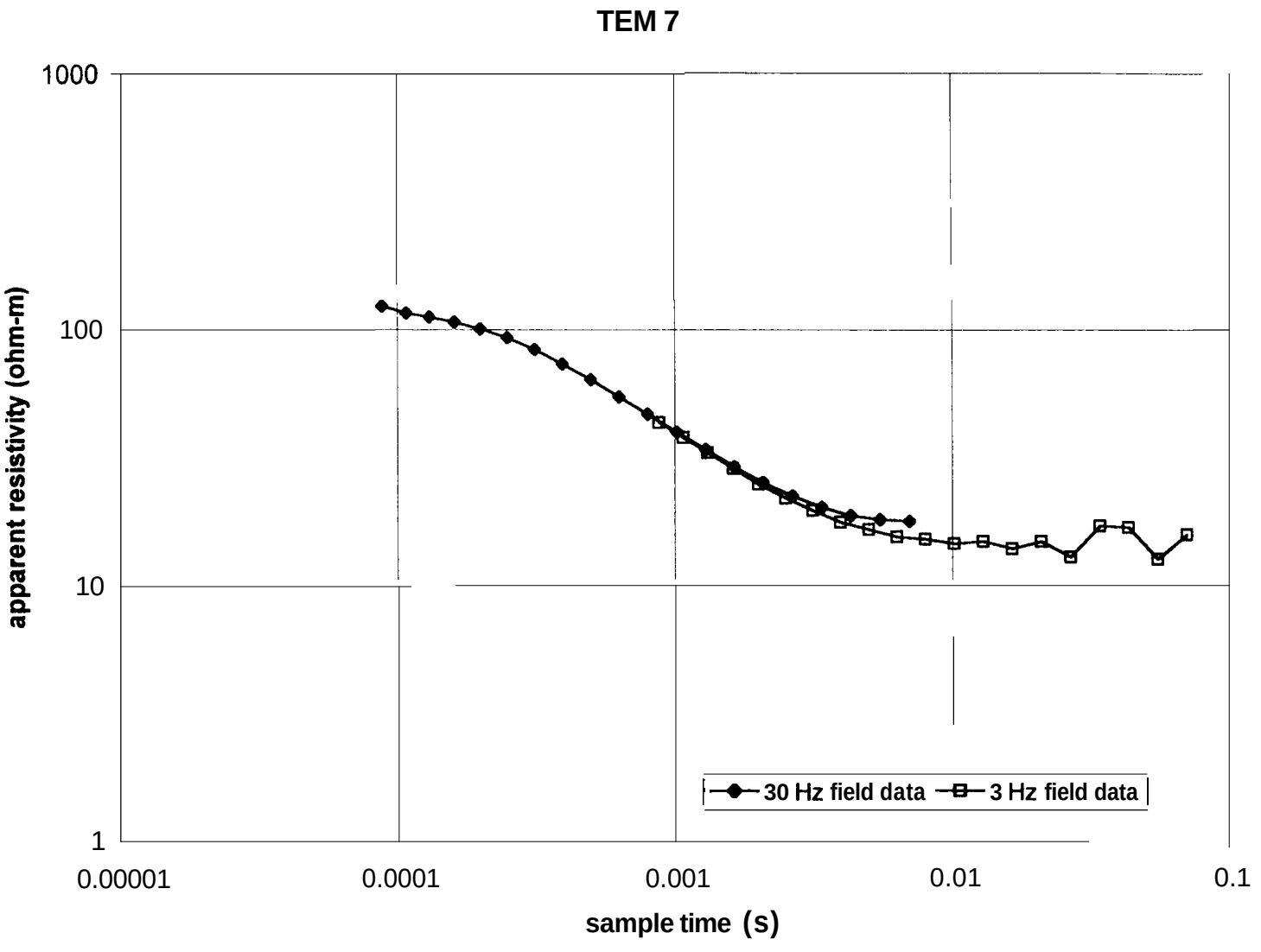

Figure 19. Ramp-corrected TEM apparent resistivity curves for TEM 7.

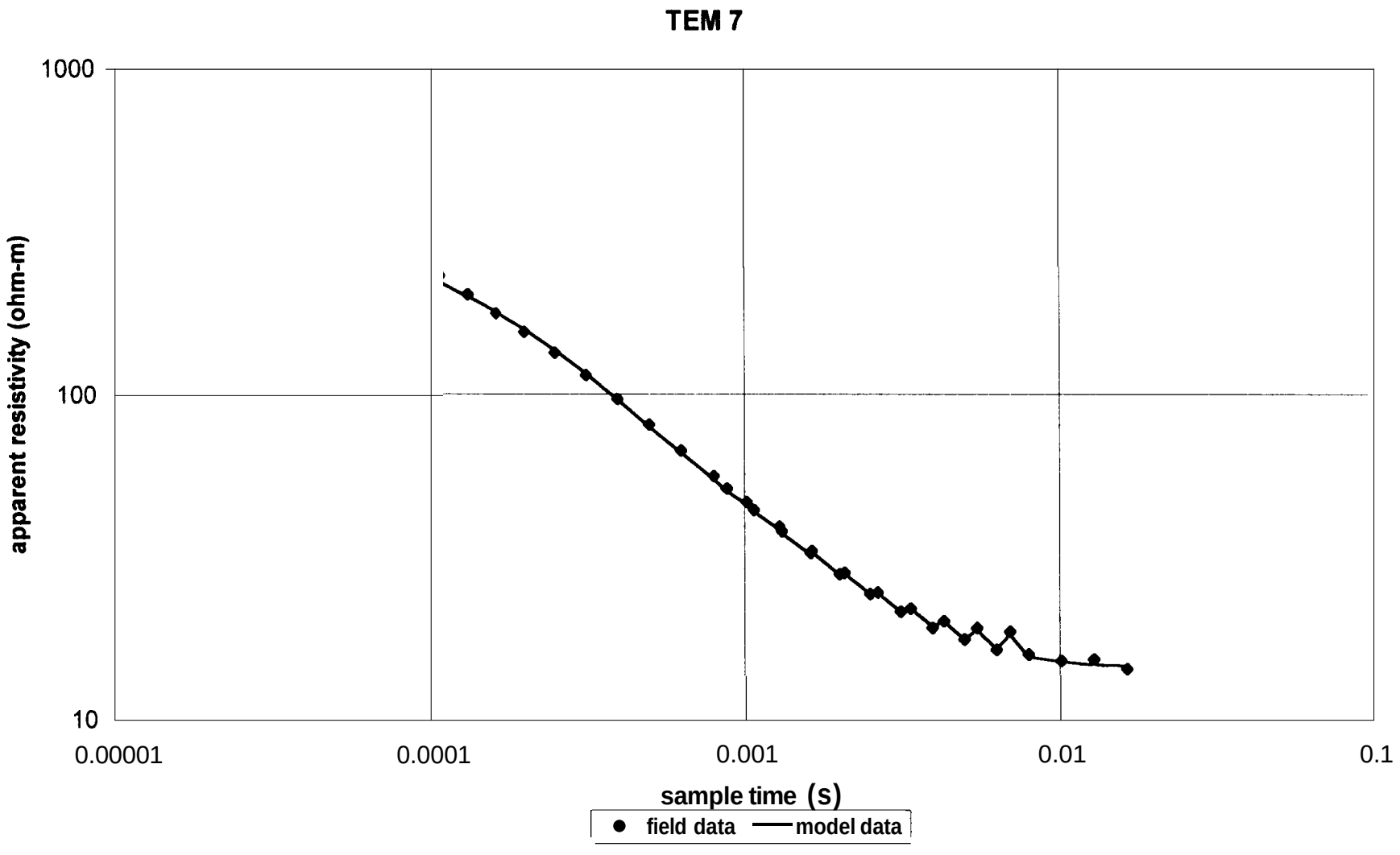

Figure 20. TEM 7 field data versus model data showing data fit. Values shown are late-time asymptotic apparent resistivites.

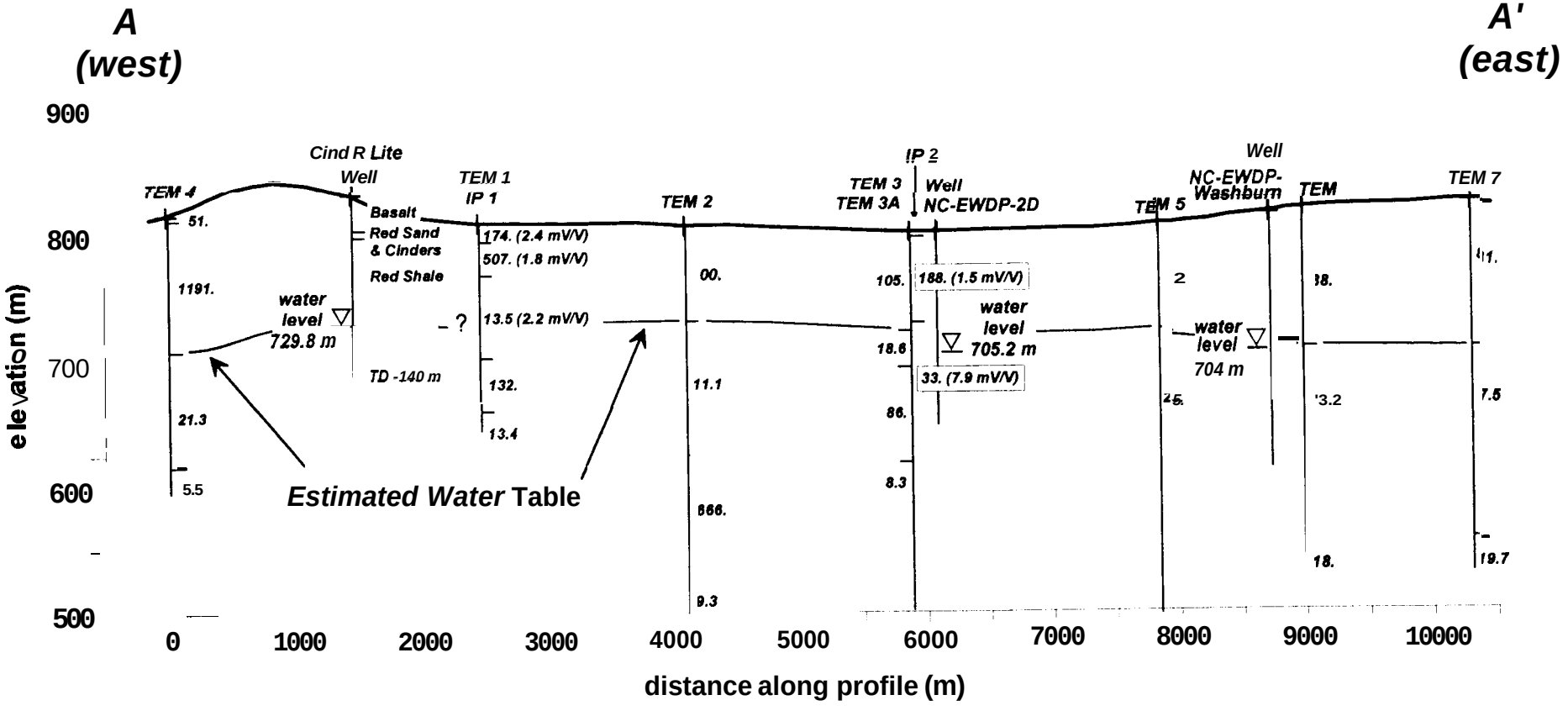

Figure 21. Interpreted cross-section A-A' showing resistivity structure versus depth. Modeled resistivities in ohm-m are shown at depth next to vertical line at the sounding position. Tick marks on the line represent breaks between layers. Modeled IP data is shown in parentheses as chargeability in mV/V.

Center for Nuclear Waste Regulatory Analyses
(210) 522-5208

From: **David A. Farrell** Date: 10/24/99

To: Bruce Mabrito

As promised here is my electronic note book.

Figure which were included in the earlier note book were not reproduced.

David Farrell

Figures 5 + 6 are in color but are reproduced here in black and white.

SCIENTIFIC NOTE BOOK # 317
Subsurface Electrical Conductivity Mapping of Fortymile Wash and the Amargosa Desert

by

David A. Farrell

Southwest Research Institute
Center for Nuclear Waste Regulatory Analyses
San Antonio, Texas

Date of Issue: March 18, 1999
Valid Dates: March 18, 1999 to October 24, 1999

Table of Contents **Page #**

List of Figures **Page #**

List of Tables **Page #**

1. INITIAL ENTRIES

Scientific Note Book: # 317

Issued to: David A. Farrell

Issue Date: March 18, 1999

Printing Period:

Project Title: **Subsurface Electrical Conductivity Mapping of Fortymile Wash and the Amargosa Desert**

(USFIC KTI)

Project Staff: David A. Farrell and Peter La Femina (CNWRA, SWRI), Stewart Sandberg and Noel Rogers (Geophysical Solutions)

By agreement with the CNWRA QA, this notebook is to be printed at approximate quarterly intervals. This computerized Scientific Notebook is intended to address the criteria of CNWRA QAP-001.

[David A. Farrell, June 6, 19991

1.1. Objectives

Within the Amargosa Desert and Fortymile Wash regions adjacent to Yucca Mountain, Nevada, vast areas exist along the projected radionuclide flow path for which little hydrogeologic and geologic data are unavailable. As a result groundwater flow and mass transport models are poorly constrained within this region. One cost effective, non-invasive approach for improving our knowledge of the hydrogeology and geology of this region involves the use of surface geophysics. Several non-invasive geophysical methods are available for inferring subsurface structure, e.g., gravity methods, seismic methods, magnetic methods, electromagnetic methods and electrical methods. Of these methods, electromagnetic and electric methods are commonly used in hydrogeological studies aimed at identification of watertables and plume delineation due in part to the sensitivity of subsurface electrical conductivity to soil moisture content and pore-water chemistry.

The objectives of this study are to use electromagnetic, induced polarization and standard depth sounding resistivity methods to map subsurface resistivity distributions within the Amargosa Desert and Fortymile Wash with the ultimate goals being identification of the watertable, the tuff-alluvium contact and the zone where the watertable transitions from the tuff units into the alluvial valley fill deposits of Fortymile Wash. In addition to collecting and interpreting the data sets independently, a joint inversion of the data sets will be performed.

This notebook documents aspects of the work performed by CNWRA staff and consultants on this project. Some of the details regarding the field work are not described in this notebook. A detailed description of field procedures an experiences are included in the field notebooks of Stewart Sandberg and Noel Rogers (Geophysical Solutions) and Peter La Femina. (CNWRA). Sandberg's notebook deals specifically with geophysical data collection, while La Femina's notebook deals with aspects of geolocation. Copies of these notebooks are currently being acquired and will be attached as appendices to hard copies of this electronic notebook.

1.2. Computers, Computer Codes, and Data Files

The computer codes used in the data analyses were based on a suite of codes developed by Stewart Sandberg and purchased by CNWRA. Version 6 of this suite dated August 7, 1998, includes ZONGE, READZONG, T47INPUT, READ, SLUMBER, RAMPRES3 and EINVRT6. These codes are discussed in the software users manual "Inverse Modeling Software for Resistivity, Induced Polarization (IP), and Transient Electromagnetic (TEM, TDEM) Soundings" written by Stewart Sandberg and dated August 7, 1998 (Appendix 1). The data analyses were carried out using computer systems running either DOS 6.0, or Windows 95 or higher (Geophysical Solutions). Processed and unprocessed data files will be included on floppy disk with the hard copy of this report.

2. Introduction

The geophysical survey which this report discusses was an extension of the May 1998 geophysical survey performed by Charles Connor in Fortymile Wash and the northern portion of the Amargosa Desert, southern Nevada. Connor's work may be best described as a scoping exercise designed to investigate whether electromagnetic geophysical methods could be used to map geological structure and watertable elevation along the projected groundwater flow path from Yucca Mountain **(YM)** to regions located further south. At the time of Connor's survey, limited hydrogeological data existed within the survey area.

The geophysical survey discussed in this report was performed during the period January 13-24, 1999. The survey differed from the that performed **by** Connor in several aspects. First, in addition to the time-domain electromagnetic (TEM) technique which was used by Connor, time-domain induced polarization (TDIP) and Schlumberger resistivity depth profiling (SR) were also applied. The joint inversion of these data sets is expected to improve the resolution of subsurface features. Second, changes to the design of the TEM technique employed by Connor have been made. The changes relate to the dimensions of the survey loop and the current frequencies used. These changes should improve the method's depth of penetration and resolution. Third, wherever possible, survey lines started and ended at borehole elevations where hydrogeologic and geologic information were available. This design provides constraints for the proposed models.

3. **Theory** (May 24, 1999)

The TEM, TDIP and **SR** techniques were employed during the January, 1999 field survey. The following provides a brief summary of these methods.

3.1 Time-Domain IP (TDIP) Method

The theory behind the time-domain IP method is documented in Telford et al. (1976), Sharma (1997) and Parasnis (1986). The following provides a cursory discussion of the technique. Consider an electrode spread along the ground surface shown in Figure 1, where **A** and B represent current electrodes, and N and M represent voltage or potential electrodes. Further, assume that the subsurface has a finite resistivity. If the current applied across **A** and B is interrupted, the voltage across M and N will decrease to zero in a finite amount of time as shown in Figure 2. This relaxation in voltage, starts from some initial value less than the applied voltage, and may last from seconds to minutes. This decay in voltage is due to the process of induced polarization and essentially represents the time it takes for the system to return to its original state. When the voltage decay is measured as a function of time following application of a DC pulse, the technique is termed "time-domain IP".

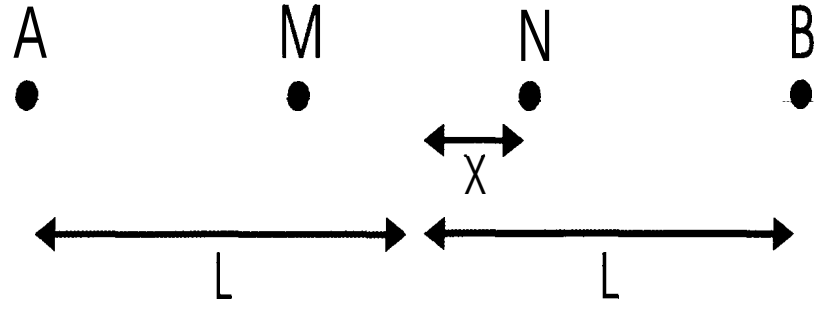

Figure 1: Schematic of TDIP electrode array

IP effects may due to either membrane polarization or electrode polarization. Membrane polarization results from ion flow in pore fluids under an induced voltage. This process **is** enhanced by the presence charged mineral and soil grains such as clay particles. When an electric current is forced through such a system, the motion of negative ions may be inhibited by the presence of the negatively charged particles within the porous medium. This results in localized regions of negative ion accumulation. Interruption of the applied voltage produces an observed voltage decay as the ions diffuse back to an equilibrium state. Membrane polarization is generally enhanced by the presence of clay minerals scattered throughout the matrix.

Electrode polarization is due to the presence of metallic minerals in the subsurface. Where this occurs, subsurface current flow results from the combination of electronic and electrolytic processes. This may be demonstrated by considering a metallic mineral in the subsurface. Under an applied voltage, the opposite faces of the mineral grain will develop opposite charges and a localized electrolysis cell will develop. This

results in a pile up of ions along the faces of the mineral grain. When the applied voltage is interrupted, the residual voltage decays as the ions diffuse back to their equilibrium state.

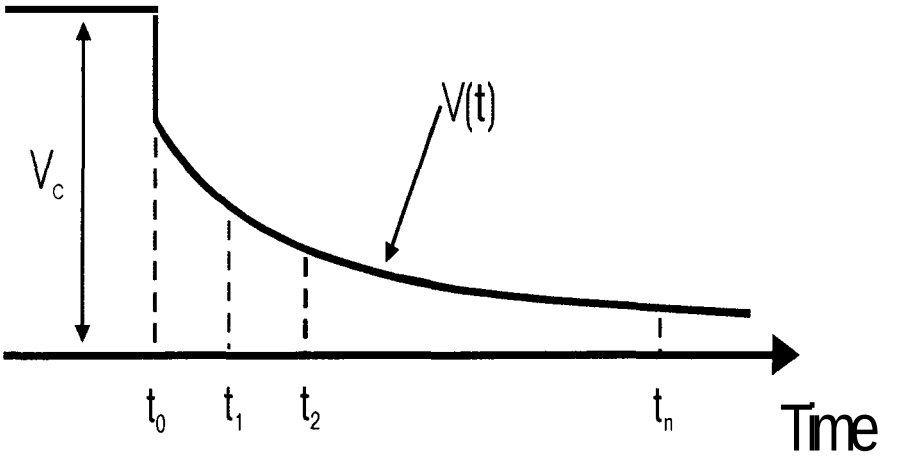

Figure 2: Observed voltage decay due to IP effects.

Induced polarization is frequently measured in terms of chargeability *(M)*,

$$M = \frac{1}{V_c}\int_{t_1}^{t_n} V(t)\,dt$$

where *V(t)* represents the residual voltage after the current is interrupted, V_c represents the steady voltage measured at the potential electrodes (Figure 2), and t_1 and t_n represent the first and last measuring times. The units of chargeability are mVs/V (millivoltsecond per volt).

An advantage of **IP** is that it provides **a** means **for** distinguishing between clay layers and other low resistivity strata.

3.2 Schlumberger Resistivity **(SR)** Method

The theory behind the **SR** method is well documented in Telford et **al.** (1976), Sharma (1997) and Parasnis (1986). Subsurface electrical resistivities may be determined by passing a current through the subsurface and measuring the voltage difference across **a** pair of electrodes inserted into the subsurface. The resisitivity measured in this way, the apparent resistivity, is a function of the combined resistivities of the subsurface porous medium and pore fluids present. **A** shortcoming of electrical methods such as the Schlumberger method, is their sensitivity to minor variations in electrical conductivity near the surface (Telford et al., 1976).

The SR approach is one of the more commonly applied resistivity surveying methods. The electrode array used is identical to that described in Figure 1. Here the current electrodes are **A** and B while the potential

electrodes are represented by M and **N.** Apparent resistivities (ρ_a)for this array are computed using the following expression:

$$\rho_a = \frac{\pi L^2}{2x}\frac{\Delta v}{I}$$

where *I* represents the applied current, ***L*** represents the distance from the mid-point of the array to the current electrodes, *x* represents the distance from the mid-point of the array to the potential electrodes, and Δv represents the measured voltage across the voltage electrodes. In depth sounding mode, the voltage electrodes are ideally kept fixed while the current electrodes are expanded symmetrically about the mid-point of the array.

The equipment and field procedures used for the **SR** soundings are quite similar to those used for the TDIP with the exception that a direct current is applied to the current electrodes and voltages across the potential electrodes are measured during the current on-time.

3.3 Time-Domain Electromagnetic (TEM) Methods

TEM methods are based on electromagnetic induction theory, whereby a changing magnetic field, which may be due to an electromagnetic source, induces an electromotive force (emf) in a nearby conductor. Associated with these induced or secondary emfs, is a magnetic field, the secondary magnetic field. This secondary magnetic field may then induce emfs in nearby conductors which may be recorded. This approach is commonly applied in geophysics to map subsurface resistivities.

TEM methods in geophysics generally involve laying out a large square wire loop on the ground surface which is connected to a transmitter. The dimensions of the transmitter loop can vary from tens of meters to hundreds of meters depending on the depth of penetration required. At the center of the transmitter loop is placed **a** smaller circular receiver loop. This configuration **is** termed the central loop configuration. Application of symmetrical square wave current to the transmitter coil produces a constant magnetic flux in the subsurface. When the applied current rapidly falls to zero during the off-cycle, the changing magnetic flux in the subsurface induces secondary time varying emf in conductive layers. The vertical component of the changing secondary magnetic field associated with these emfs induce emfs in the receiver coil present at the surface. The induced emf in the receiver is recorded and later analyzed. Corrections to the raw field data may be applied to account for the finite turn-off time of commonly used transmitters (Sandberg, 1998).

In the central loop configuration, measurement of the decaying field at the loop center is equivalent to measurement of resistivity as a function of depth (Sharma, 1997). Sharma (1997) describes the depth of investigation as a function of delay time of the decaying secondary field which is independent of the transmitter-receiver separation.

Advantages of the time-domain system over frequency-domain systems include greater depth of penetration (Sharma, 1997). The data scatter frequently observed in d.c. resistivity and magnetotelluric soundings are

often due to lateral variations in resistivity and measurement of the electric field. The scatter is reduced in central loop TDEM soundings mainly because of short source-receiver separation and measurement of time derivatives of the magnetic field.

4. Equipment and Field Procedures

As pointed out earlier, the field survey was conducted between January 13-24, 1999 and utilized the techniques described above. The following provides a summary of the equipment used.

4.1 Time-Domain IP (TDIP) Method

Equipment:
Time-domain IP soundings were performed using the PHOENIX V-5 multipurpose receiver and the PHOENIX T-3 transmitter. The instruments were on temporary loan from the University of Southern Maine. The transmitter was used to supply current to the current electrodes **A** and **B** while the receiver was used to record the potential difference across the potential electrodes M and N. The transmitter was powered by a portable generator. Steel stakes were used for the current electrodes while porous cups containing a copper sulphate solution were used for the potential electrodes.

Field Procedures:
Data acquisition procedures used during this survey conformed to standard operating procedures as outlined in the operations manuals of the equipment, and standard field procedures described in literature. In addition, Dr. Sandberg gave all members of the survey team a brief demonstration of the safe operation of the equipment. Note that Dr. Sandberg and Noel Rogers operated the IP instruments in all cases, and used their professional judgement to suggest modifications to the survey, i.e., array design etc.

The field procedures used may be summarized as follows:

(i) Figure 1 shows a schematic of the field layout. The separation of the potential electrodes was generally kept fixed while the separation of the current electrodes was expanded outward in a symmetric manner about the center point of the array. Note that for the cases where the measured potential at the potential electrodes were low and undiscernable from background noise, the potential electrodes were expanded outward from the center point. **(S.** Sandberg and N. Rogers)

(ii) The electrode grid was mapped using both **GPS** and a measuring tape.(D. Farrell and P. La Femina)

(iii) The transmitter is connected to the portable generator and the transmitter is powered up and tested. During this phase, output from the transmitter to the current electrodes was turned off. **(S.** Sandberg and N. Rogers, monitored by D. Farrell)

(iv) Next, the current electrodes are inserted into the ground surface and the area around them is saturated with a saltwater solution to ensure good electrical coupling. Porous cups containing a copper sulphate solution are used for the potential electrodes. The area beneath these electrodes is also saturated with saltwater to ensure good electrical coupling. Note that current to the electrodes is turned off while the electrodes are moved. (R. Klar and B. Strye under the supervision of **S.** Sandberg, monitored by D. Farrell)

(v) Next, the receiver is connected to the potential electrodes. **(S.** Sandberg and N. Rogers, monitored by D. Farrell)

(vi) The transmitter is then connected to the current electrodes and a periodic square wave of known frequency and amplitude (see Figure 3) is passed through the system. **(S.** Sandberg and N. Rogers, monitored by D. Farrell)

(vii) The current in the system is adjusted until the observed IP response (the voltage recorded at the receiver) is above background. Data for the different time gates at the receiver are then stacked. The stacked voltage at each time gate is then recorded along with the applied current, current electrode spacing and potential electrode spacing. The current in the system is verified using a voltmeter. **(S.** Sandberg and N. Rogers, monitored by D. Farrell **...** data stored in the field notebooks of **S.** Sandberg and N. Rogers Appendix 2)

(viii) Current to the system is then switched off **(S.** Sandberg) and the current electrode spacing expanded (R. Klar and **B.** Strye, monitored by D. Farrell).

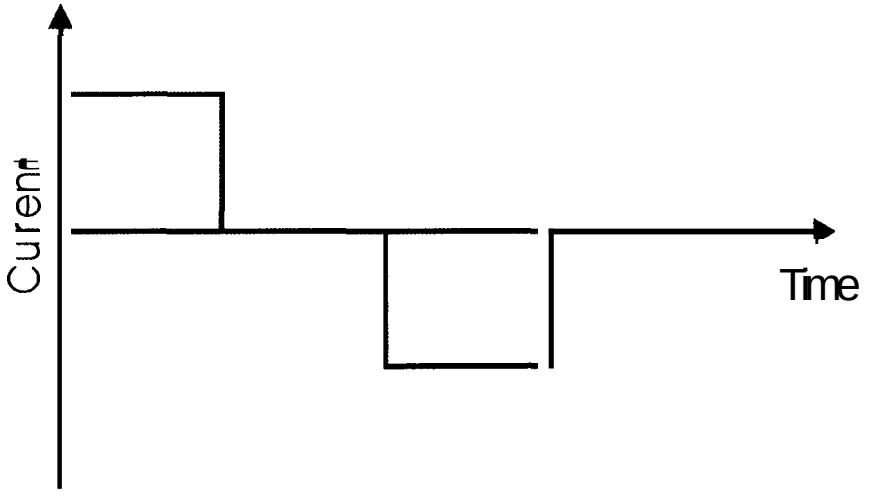

Figure 3: Input signal to current electrodes.

4.2 Schlumberger Resistivity (SR) Method

The equipment and field procedures used for the SR soundings were quite similar to those used for the TDIP with the exception that adirect current was applied to the current electrodes and voltages across the potential electrodes were measured during the current on-time. These measurements were performed simultaneously with the TDIP.

4.1 Time-Domain Electromagnetic (TEM) Method

Equipment:

The equipment used for the TEM survey was the GEONICS PROTEM TEM system. This system consists of a transmitter and a receiver. Two transmitters were used in this survey: the PROTEM 57-MK2 transmitter and the PROTEM 47/S transmitter. The PROTEM 57-MK2 transmitter was rented from TerraPlus in Littleton, Colorado while the PROTEM 47/S transmitter was obtained on a temporary loan from the University of Southern Maine. The former is used for large loops *(> 100m x 100m)* and is powered by a battery pack or **a** portable motor generator, while the latter is used for loop sizes on the order of *(≤ 100m x 100m)*. In the field survey, the PROTEM 57-MK2 transmitter was used with a portable generator. A PROTEM Digital receiver was used to store the received signal. Two receivers coils were also employed with this receiver. For the larger transmitter loop dimensions, a low frequency (bandwidth 60 kHz) air-cored coil 1.Om in diameter was employed whereas for the smaller transmitter loop dimensions, a higher frequency (bandwidth 850 kHz) air-cored coil 0.63 m was employed. The smaller loop was obtained on a temporary loan from the University of Southern Maine while the larger was rented from TerraPlus in Littleton, Colorado.

Field Procedures:
Data acquisition procedures used during this survey conformed to the Center for Nuclear Waste Regulatory Analyses Quality Assurance Procedures, standard operating procedures as outlined in the operations manuals of the equipment, and standard field procedures described in literature. Note that Dr. Sandberg and Noel Rogers operated the IP instruments in all cases, and used their professional judgement to modifying aspects of the survey approach.

The general field procedures used may be summarized as follows:

(i) For the TEM soundings the circular receiver coil was located at the center of the larger square transmitter loop. In most cases, the transmitter loop was oriented N-S and E-W. The comers of the loop were established using GPS (D. Farrell and **P.** La Femina). In addition to the UTM coordinates of the comers of the transmitter loop, the UTM coordinates and the elevation of the center of the loop were also recorded in most cases. (Note that elevation data was not initially collected due to some initial confusion regarding its use ... some of this data was later collected ... some elevation data could not be collected due to logistic problems, e.g., rover packs unable to see the base station)

(ii) The transmitter loop was laid out and an electric current passed through the loop to test its integrity. This was particularly important for the large loop which was constructed by splicing, three 400 m cables (loop layout and integrity were supervised by **S.** Sandberg, monitored by **D.** Farrell).

(iii) Receiver set up: Several steps were required to set up the receiver prior to data acquisition. These included (i) auto-testing and auto-calibration of the receive; (ii) crystal clock synchronization between the transmitter and the receiver when the two instruments were not physically connected during the sounding; (iii) selection of the appropriate receiver coil; (iv) selection of the desired component of the magnetic field to be read; (v) selection of the appropriate "turn-on/turn-off times"; (vi) selection of the transmitter instrument type and the transmitter loop dimensions; (vii) selection of the transmission frequency; (viii) creation of a new data file; (ix) assessment of background noise; (x) gain adjustment. (Receiver setup, synchronization and internal calibration performed by **S.** Sandberg, monitored by D. Farrell)

(iv) On completion of the steps listed in (3.) the receiver and the receiver coil are both moved to the center of the transmitter loop and connected together **(S.** Sandberg). The transmitter is then connected to the transmitter loop (N. Rogers). Note that for small loops a physical connection is maintained between the transmitter and the receiver.

(v) The system is power-up and data recorder at several frequencies, currents and gains **(S.** Sandberg and N. Rogers (under the supervision of **S.** Sandberg, monitored by D. Farrell)).

(vi) At the end of the recording session, the data is stored on a data logger in the receiver, the systems is powered-down, and the equipment collected **(S.** Sandberg).

5. **Field Work** (June 7, 1999)

This section summarizes various field aspects of this work. Field work began on January 14, 1999 and terminated on January 24, 1999. Parameter values used at each measuring station during this period were recorded in the field notebooks of Stewart Sandberg, Noel Rogers and Peter La Femina and are not reproduced here. However, copies of, or excerpts from, these notebooks will be placed in appendices at the end of this report.

Day 1 (Thursday, Junuury 14, 1999):

Equipment collection in Las Vegas, NV. Rolls of cable necessary to perform the TEM survey did not arrive but are expected to arrive on Friday. Visited the Badging Office at Mercury to make sure that the badges were available. Site familiarization.

*Day 2 (Friday,January **15,** 1999):*

TDIP survey at station TEM 1 (IP 1). Located east of the Lathrop Wells Cinder Cone (Cind-R-Lite). At this location two TDIP surveys were performed perpendicular to each other as a means of estimating any subsurface dip. TDIP data reported in **S.** Sandberg's notebook (Appendix 2). La Femina and Connor returned to Las Vegas to collect the rolls of wire for the TEM.

Day 3 (Saturday, Junuury 16, 1999):

TEM survey at the site of the previous TDIP. Recorded as TEM **1 ...** large loop used (300 m x 300 m). Second TEM survey performed further east **...** recorded as TEM 2. TEM instrument settings recorded in **S.** Sandberg's notebook (Appendix 2).

Day 4 (Sunday, January 17,1999):

TEM and TDIP survey performed adjacent to Nye County well NC-EWDP-2D. Two transmitter loop sizes used for the TEM survey **...** TEM 3 (300 m x 300 m) and TEM 3A (40 m x 40 m). North trending IP survey performed (recorded at TDIP 2) along the western edge of the large loop. TEM instrument settings recorded in **S.** Sandberg's notebook (Appendix 2). TDIP data reported in **S.** Sandberg's notebook (Appendix 2).

Connor returned to San Antonio.

Day 5 (Monday,January IN, 1999):

Small loop TEM survey performed immediately west of the Lathrop Wells Cinder Cone. Recorded as (TEM 4 (40 m **x** 40 m)). Aim of this survey was to investigate the possible characteristic signal of the tuff-alluvium

contact. A short distance away from this site, the tuff can be observed dipping beneath the alluvium. TEM instrument settings recorded in **S.** Sandberg's notebook (Appendix 2).

Large loop surveys (300 **m** x 300 m) performed east of TEM 3 location. Recorded as TEM *5*, TEM 6 and TEM 7. Note that TEM *5* is located adjacent to an excavated area. TEM 7 is the farthest east. TEM instrument settings recorded in **S.** Sandberg's notebook (Appendix 2).

Day 6 (Tuesday, January 19, 1999):
Survey moved to the NTS. Daily check-in at the Mercury gate and FOC.

Small loop TEM survey (40 m x 40 m) performed on the eastside of the Fortymile Wash, south of Busted Butte and JF-3, near gravel road ... recorded **as** TEM 8. Small cables located further to the east following the survey ... these could cause some problems with the interpretation ... note these cable were located more than 75 m from the closest edge of the survey line. Recognizance located additional cables in the region making it difficult to find suitable survey stations. TEM instrument settings recorded in **S.** Sandberg's notebook (Appendix 2).

Large loop TEM survey (300 m x 300 m) performed southwest of TEM 8 adjacent to the Fortymile Wash. Recognizance indicates no cables present. Sounding recorded as TEM 9. Small loop (40 m x 40 m) also recorded at this site ... recorded as TEM 10. Additional small loop (40 **m** x 40 m) also nearby in Fortymile Wash ... recorded as TEM 11. TEM instrument settings recorded in **S.** Sandberg's notebook (Appendix 2).

Recognizance performed on the west side of the wash revealed no cables. Decision made to perform the surveys on the west side of the wash to avoid complications related to the presence of cables.

Day 7 (Wednesday, January 20, 1999):
Returned to NTS. Daily check-in at the Mercury gate and **FOC.**

New site located on the west side **of** Fortymile Wash, along the east-west gravel road located south of Busted Butte. Tuff can be seen dipping beneath the alluvium about 500 to 1000 m further west. Large loop TEM survey performed (300 m x 300 **m) ...** recorded as TEM 12. Small loop survey (40 m x 40 m) was also performed at this location ... recorded as TEM 13. Stewart was surprised by the TEM 13 data so an additional small loop TEM survey (40 m x 40 m) was performed further south. This is reported as TEM **14.** An IP survey was also performed parallel to the road at this location. Recorded as TDIP 3. TEM instrument settings recorded in **S.** Sandberg's notebook (Appendix 2). TDIP data reported in **S.** Sandberg's notebook (Appendix 2).

Large loop TEM survey (300 m x 300 m) performed east of TEM 12 adjacent to Fortymile Wash. Recorded as TEM **15.** TEM instrument settings recorded in *S.* Sandberg's notebook (Appendix 2).

Day 8 (Thursday, January 21, 1999):
Returned to NTS. Daily check-in at the Mercury gate and FOC.

Large loop TEM survey (300 m x 300 m) performed south of TEM 15 along the west side of Fortymile Wash. Recorded as TEM 16. At the same site a small loop TEM survey (40 m x 40 m) was also performed ... recorded as TEM 17. TEM instrument settings recorded in **S.** Sandberg's notebook (Appendix 2).

Large loop TEM survey (300 m x 300 m) performed further south. Recorded as TEM 18. Small loop TEM survey (40 m x 40 m) also performed ... recorded as TEM 19. TEM instrument settings recorded in **S.** Sandberg's notebook (Appendix 2).

Day 9 (Friday, January 22, 1999):
Returned to NTS. Daily check-in at the Mercury gate and FOC.

Large loop TEM survey (300 m x 300 m) performed further south of TEM 18. Recorded as TEM 20. Small loop survey also performed at this location ... recorded as TEM 21. TEM instrument settings recorded in **S.** Sandberg's notebook (Appendix 2).

To map the tuff-alluvium contact beneath the west side of Fortymile Wash, an east-west, small loop (40 m x 40 m) survey was performed. The western end of the survey approached the tuff out-crops along the southern margins of the wash. The station locations for this survey are recorded as TEM 22 through TEM 26. TEM instrument settings recorded in **S.** Sandberg's notebook (Appendix 2).

Surveys on the NTS now complete.

Day 10 (Saturday, January 23, 1999):
Surveys on this day performed in the Amargosa Desert south of Lathrop Wells cinder cone. Survey designed to map both deep and shallow structures beneath Fortymile Wash. Survey line projects southeast from well at Lathrop Wells cinder cone to the Amargosa Town ***C*** well.

Large loop TEM survey (300 m x 300 m) performed ... recorded as TEM 27. Small loop survey (40 m x 40 m) survey also performed at this location ... recorded as TEM 28. South-east of this location an additional large loop (300 m x 300 m) and small loop survey (40 m x 40 m) performed ... recorded **as** TEM 29 and 30. TEM instrument settings recorded in **S.** Sandberg's notebook (Appendix 2). At the second location, a TDIP survey was performed ... data for this survey recorded in **S.** Sandberg's field note book. Note that the TDIP survey was terminated prematurely due to declining weather conditions (sand-storm).

Day 11 (Sunday, January 24, 1999):
Surveys on this day performed in the Amargosa Desert southeast of the previous day's locations. Large loop TEM survey (300 m x 300 m) performed ... recorded as TEM 31. Small loop survey (40 m x 40 m) survey also performed at this location ... recorded as TEM 32. South-east of this location an additional large loop (300 m x 300 m) and small loop survey (40 m x 40 m) performed ... recorded as TEM 33 and 34. TEM instrument settings recorded in **S.** Sandberg's notebook (Appendix 2). Note that the field work ended early due to **S.** Sandberg's declining health.

Day 12 (Monday, January 25, 1999):

Equipment shipped from Las Vegas back to rental companies. Returned to San Antonio.

6. Analyses and Results: (June 8, 1999)

The survey can be broken up into three zones. Zone 1 occupies the lower section of Fortymile Wash, and extends from the Lathrop Wells Cinder Cone to the town of Amargosa Valley; Zone 2 occupies the Fortymile Wash region of the NTS; and Zone 3 occupies the Amargosa Desert region between the Lathrop Wells Cinder Cone and the town of Amargosa Farms. The following provides a summary of the data collected within each zone.

Table 1: Sounding Locations and Survey Type

Station Number	UTM_East (m)	UTM_North (m)	Zone	Sounding Type
1	544736	4059006	1	TDIP; SR; TEM 1
2	546700	4058850	1	TEM 1
3	548050	4057600	1	TEM 1; TEM 2; TDIP; SR
4	543130	4060860	1	TEM 2
5	550075	4057275	1	TEM 1
6	551189	4057024	1	TEM 1
7	1552500	4056750	1	TEM 1
8	554820	4065605	2	TEM 2
9	553218	4064962	2	TEM 1
10	553068	4065112	2	TEM 2
11	552868	4065324	2	TEM 2
12	552910	4068390	2	TEM 1
13	552769	4068528	2	TDIP; SR; TEM 2
14	1552790	4068239	2	TEM 2
15	1553650	4068400	2	TEM 1
16	1553500	4067360	2	TEM 1

17	553390	4067470	2	TEM 2
18	552690	4066 170	2	TEM 2
19	552580	4066280	2	TEM 1
20	552130	14064850	2	TEM 1
21	55 1980	4065000	2	TEM 2
22	55 1680	4065000	2	TEM 2
23	55 1380	4065000	2	TEM 2
24	55 1080	4065000	2	TEM 2
25	552346	4064956	2	TEM2
26	552504	4064927	2	TEM 2
27	544753	4056625	3	TEM I
28	544623	4056746	3	TEM 2
29	545100	4055732	3	TEM 1
30	544977	4055862	3	TDIP; SR; TEM 2
31	547220	4052850	3	TEM 1
32	547175	4052666	3	TEM 2
33	547446	4050363	3	TEM 1
34	547316	4050233	3	TEM 2

TEM 1: 300m **x** 300m TEM transmitter loop
TEM 2: 40m x 40m TEM transmitter loop
SR: Schlumberger resistivity sounding
TDIP: Time-domain IP

Interim reports have been received from Geophysical Solutions.

Interim Report I: The first of these reports is dated February 10, 1999. This report presented the results of analyses on the data collected at station TEM 1. The data included the TEM survey data, the IP data and the SR data. Simultaneous inversion of these data was performed and a model of the results presented. **A** possible watertable at elevation 770 m was identified. A copy of the interim report is attached as Appendix 3.

Interim Report 2: The second interim report is dated March 25, 1999 and contained in Appendix 4. This report presented a more extensive discussion of the results of analyses on data collected at stations within Zone 1. Included in the report are plots of the processed data and models fitted to the data. Where relevant (e.g., TEM 1 and TEM 3) simultaneous inversion results are presented. An important aspect of this report in the resistivity cross-section model presented for the data in Zone 1. The watertable as indicated by the cross-section model shows reasonably good agreement with observed waterlevel data recorded at Nye County wells NC-EWDP-2D and NC-EWDP-Washburn 1X. Discrepencies observed appeared to be due to poor surface elevation control ... elevations were inferred and not measured at some of the stations located in Zone 1. Elevations will be recorded for these locations in the near future. A correlation of the modeled resistivities to well bore data from NC-EWDP-2D will also be performed in the near future.

Entries into Scientific Notebook No. 371 for the period March 18, 1999 to July 28, 1999 have been made by David A. Farrell David A Farrell July 28, 1999.

No original text entered into this Scientific Notebook has been removed.

Data Analysis Update (October 13, 1999)

Stewart Sandberg forwarded a contour map of a processed cross-section for an east-west line (BB') located on the NTS, south of Busted Butte. This line include sounding locations TEM-24, TEM-23, TEM-22, TEM-21, TEM-25, TEM-26, TEM-I1, TEM-10, and TEM-8 (Figure 4). The line shows a high resistivity anomaly at depth along the western edge of the profile. This high resistivity is believed to be an expression of the tuff units which can be observed (visually) dipping beneath the alluvium west of TEM-24. The fault located along the western section of the line requires further investigation since it has not been identified in any of the previous literature (personal communication, D. Sims). The low resistivity zone beneath Fortymile Wash is interesting and requires further investigation since it may represent infiltration water (note this is speculation at this point in time).

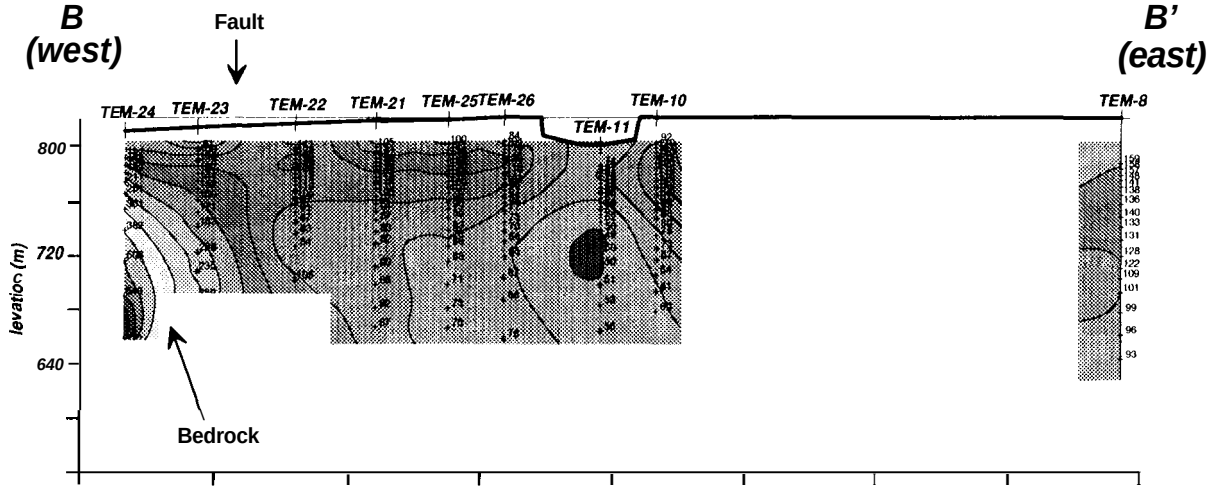

Data Analysis Update (October 21, 1999)

Resistivity depth section forwarded from Stewart Sandberg for work performed on the NTS along the northeast trending line DD'. This includes sounding locations TEM-20, TEM-18, TEM-16, and TEM-15. I've forwarded a comment to Stewart Sandberg concerning the low resistivities at TEM-20. Figure 5 shows the depth section.

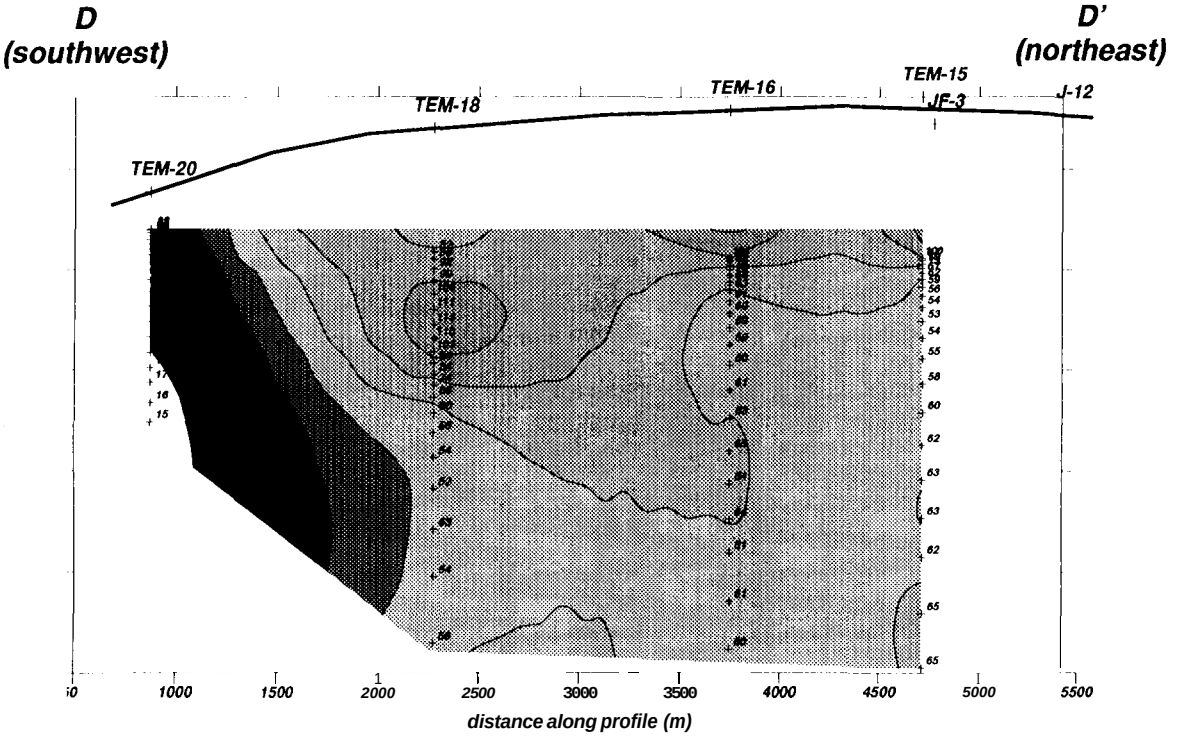

Figure 6: Approximate depth section for line DD'showing resistivity versus depth.

Data Analysis Update (October 22, 1999)
Depth section for line DD' forwarded from Stewart Sandberg. The section shows the interpreted water table based on observed data at wells JF-3 and J-12.

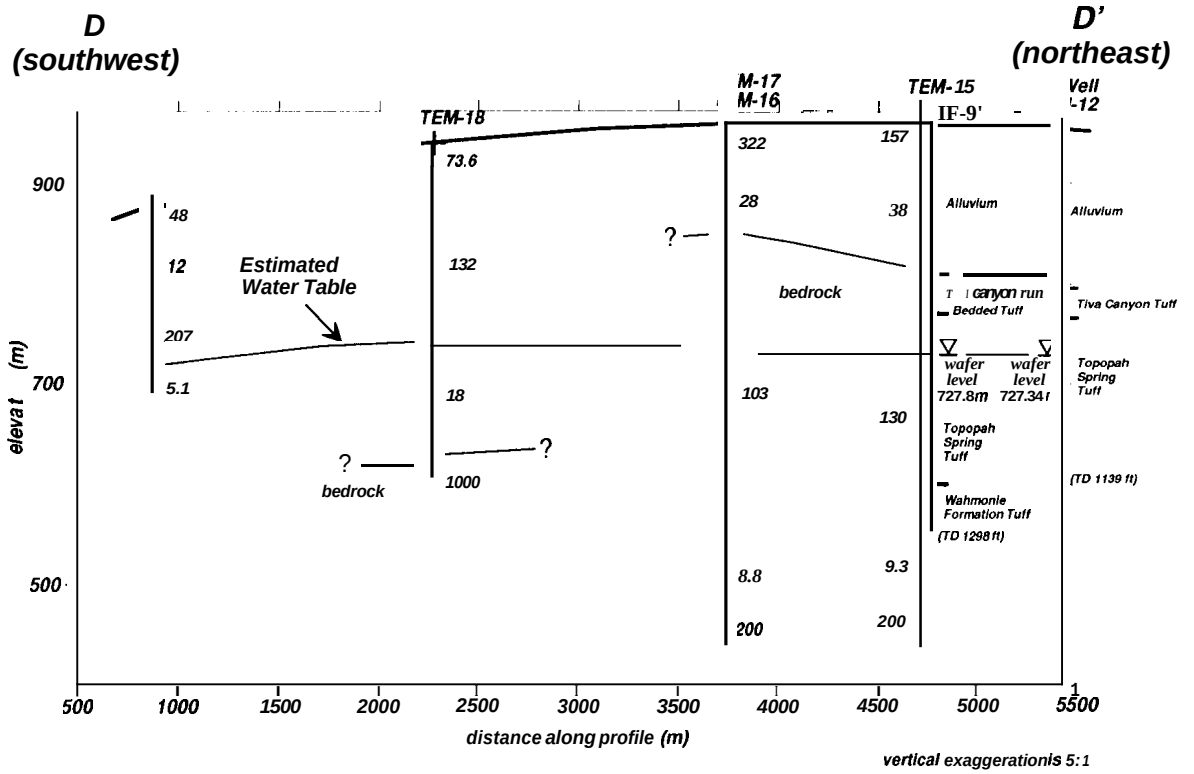

Figure 7: Interpreted cross-section for line DD' showing resistivity structure versus depth. Modeled resistivities are in ohm-m are shown at depth next to vertical line at **the** sounding position. Tick marks on the line represent breaks between layers.

Entries into Scientific Notebook No. 317 for the period July 29, 1999 to October **24.** 1999 have been made by David **A.** Farrell David A. Farrell Oct. 24, 1999

No original text entered into this Scientific Notebook has been removed.

References

Parasnis, D.S. 1986. Principles of Applied Geophysics. 4th Edition. New **York:** Chapman and Hall.

Sandberg, **S.K.** 1998. Inverse Modeling Software for Resistivity, Induced Polarization (IP), and Transient Electromagnetic (TEM) Soundings.

Sharma, P.V. 1997. Environmental and Engineering Geophysics. Cambridge University Press, UK.

Telford, W.M., L.P. Geldart, R.E. Sheriff, and D.A. Keys. 1976. Applied Geophysics. Cambridge University Press, USA.

ADDITIONAL INFORMATION FOR SCIENTIFIC NOTEBOOK #: 317E

Document Date:	03/18/1999
Availability:	Southwest Research Institute® Center for Nuclear Waste Regulatory Analyses 6220 Culebra Road San Antonio, Texas 78228
Contact:	Southwest Research Institute® Center for Nuclear Waste Regulatory Analyses 6220 Culebra Road San Antonio, TX 78228-5166 Attn.: Director of Administration 210.522.5054
Data Sensitivity:	■"Non-Sensitive" ☐ Sensitive ☐"Non-Sensitive - Copyright" ☐ Sensitive - Copyright
Date Generated:	01/20/2000
Operating System: (including version number)	Windows
Application Used: (including version number)	Surfer; Excel
Media Type: (CDs, 3 1/2, 5 1/4 disks, etc.)	1 zip drive
File Types: (.exe, .bat, .zip, etc.)	Various
Remarks: (computer runs, etc.)	Media contains: Geophysical solutions-geophysical survey at Fortymile Wash, Yucca Mountain, Nevada